Master's thesis

NTNU
Norwegian University of Science and Technology
Faculty of Natural Sciences
Department of Chemistry

Martin Andreas Wiken

Releases of oily produced water from offshore installations

A combined laboratory and modelling study comparing resulting surface oil slicks and oil slicks detected by satellite

Master's thesis in Environmental Chemistry
Supervisor: Per Johan Brandvik
Co-supervisor: Janne Lise Myrhaug
June 2021

NTNU
Kunnskap for en bedre verden

Martin Andreas Wiken

Releases of oily produced water from offshore installations

A combined laboratory and modelling study comparing resulting surface oil slicks and oil slicks detected by satellite

Master's thesis in Environmental Chemistry
Supervisor: Per Johan Brandvik
Co-supervisor: Janne Lise Myrhaug
June 2021

Norwegian University of Science and Technology
Faculty of Natural Sciences
Department of Chemistry

NTNU
Norwegian University of
Science and Technology

Abstract

Produced water is a liquid waste byproduct from the petroleum industry and is brought up to the surface along with the extraction of oil and gas. After the produced water has gone through cleaning treatments to meet environmental regulations, discharge to sea is the most common practice used on offshore installations to handle the oily water. Several petroleum fields have a continuous release of produced water and can under certain conditions lead to the formation of oil sheens on the sea surface that are detected by satellite radar. There is raised a concern regarding the potential harm for seabirds and other marine life that resides on or near the sea surface. The aim of this study was to contribute to a better understanding of the behavior of produced water once it is discharged at sea, satellite radar detection, droplet size and discharge conditions.

Experiments and simulations were carried out to meet the aim of the study. The experiments were conducted indoor in a wave basin under varying conditions and focused on release angle, velocity, temperature and salinity. It was also conducted produced water releases that included a gas flow or oil droplets. Additionally, simulations were carried out in the OSCAR model to comprehend how winds, currents, tide and waves might affect the plume behavior. Five simulations were conducted with a varying oil droplet size in the produced water.

The observed trend from the conducted experiments in the wave basin were that the denser produced water plumes sank deeper. It was shown that the outlet angle influences how deep the plume sinks, as releases with a downward outlet angle sank deeper compared to releases with a horizontal outlet angle. Also, the temperature played an important factor to the produce waters density, which was seen to influence its behavior. The inclusion of gas in the produced water release affected the plume to rise towards the surface. The oil droplet size did not affect the plume behavior, but bigger droplets were observed to favor the formation of oil sheens if the plume surfaced. This thesis also helps fill some of the knowledge gaps regarding PW releases and its behavior once let out in the ocean.

Sammendrag

Produsertvann er et biprodukt fra petroleumsindustrien som blir sett på som avfall, og blir ført opp til overflaten sammen med olje og gass. Etter at produsertvannet har gått gjennom nødvendige renseprosesser på oljeplattformen for å imøtekomme dagens miljøkrav, er den vanligste håndteringen å slippe produsertvannet ut i havet. Flere oljeplattformer på norsk sokkel har kontinuerlige produsertvann-utslipp som under visse forhold kan føre til oljeflak på havoverflaten som kan detekteres av satellittradar. Det er knyttet bekymring til den mulige skaden oljeflakene har på fugleliv og annet marint dyreliv som oppholder seg på eller nært havoverflaten. Målet med denne studien har vært å bidra til en økt forståelse knyttet til hvordan produsertvann oppfører seg når det slippes ut i havet, i tillegg til økt kunnskap om deteksjon med satellittradar, dråpestørrelse og utslippsforhold.

Eksperimenter og simuleringer ble gjennomført for å imøtekomme målet med studien. Eksperimentene ble gjort innendørs i en bølgerenne under en rekke varierte forhold og fokuserte på utslippsvinkel, hastighet, temperatur og salinitet. Det ble også gjennomført produsertvann-utslipp hvor gasstrøm eller oljedråper ble tilført. I tillegg ble det gjort simuleringer i programmet OSCAR for å bedre forstå hvordan vind, strøm, tidevann og bølger påvirker oppførselen til produsertvann-plumen. Fem simuleringer ble gjennomført med en varierende størrelse på oljedråpene i produsertvannet.

Den observerte trenden fra eksperimentene gjort i bølgerennen var jo større tetthet produsertvannet hadde, jo dypere sank det. Det ble vist at utslippsvinkelen påvirket hvor dypt produsertvannet sank, ettersom utslipp med en nedovervendt utslippsvinkel sank dypere sammenlignet med utslipp som hadde en horisontal utslippsvinkel. Temperaturen spilte også en viktig faktor for tettheten til produsertvannet, som igjen påvirket oppførselen til produsertvannet i havet. Tilførselen av gass i produsertvann-utslippet førte til at plumen steg nærmere vannoverflaten. Størrelsen på oljedråpene påvirket ikke oppførselen til plumen, men om produsertvannet steg til havoverflaten ble det observert at større oljedråper var en favoriserende faktor for dannelse av oljeflak. I tillegg kan denne oppgaven bidra med kunnskap om produsertvann-utslipp og dens oppførsel i havet.

Acknowledgements

This master thesis is the end-product of my two-year journey at NTNU. I am very humble and grateful for being a part of the Environmental Toxicology and Chemistry program. I would like to express my gratitude towards all the dedicated people making this thesis possible.

First, I would like to thank my main supervisor Per Johan Brandvik (SINTEF/NTNU) for being of great guidance throughout this project. I am grateful for the help, knowledge and experience you have brought into this project, it has been very instructive. It is also of importance to mention that I appreciate your efforts of getting me going in this project in a challenging year.

A thank you to my co-supervisor Janne Lise Myrhaug (Equinor) for the opportunity to write a thesis with Equinor. Your contribution with information and data has been of great importance for this project.

I would also like to acknowledge the following people. A thank you is given to Frode Leirvik (SINTEF) for the support and help in the Sealab and for always being available on such short notice. You made the experimental work in the wave basin easier with all your practical solutions. Also, a thank you to Kristin Bonaunet (SINTEF) for the tour at SINTEF Brattøra and for the necessary HSE training I needed before my experimental work. Thank you, Jørgen Skancke (SINTEF), for giving me advise and important hacks in the OSCAR simulation program, it was very helpful. A big thank you to Regina Hamre for the assistance in the finalization of this thesis.

To my fellow master students at the ENVITOX program, it has been a pleasure to meet all of you. Thank you for the good memories, especially our trips to Dovrefjell and Mausund. Even though our exchange semester got shortened by the pandemic, it was a blast being there with some of you and exploring Longyearbyen, Svalbard. An extra thanks to Anna for being a very good friend and for the important hikes in between studying. Also, a thank you to Maja for the good collaboration and help with SPSS.

To my family, thank you for believing in me and for showing interest in my studies. My mom especially, for her support and encouragement when it comes to my education. A thank you to my friends, with a special thanks to Celine and Thea. Last, but not least, thank you Henning for lifting me up whenever needed, you always keep me going forward.

Table of contents

List of figures

List of tables

List of abbreviations

Abbreviation	Meaning
AP	Alkyl phenol
DREAM	Dose related Risk and Effects Assessment Model
etc	Latin for “and so on”
IR	Infrared
LabVIEW	Laboratory Virtual Instrument Engineering Workbench
LISST	Laser In-Situ Scattering and Transmissometer
MEMW	Marine Environmental Modelling Workbench
Metno	Norwegian Metrological Institute
NaCl	Sodium chloride
NCS	Norwegian continental shelf
NIR	Near-infrared
OSCAR	Oil Spill Contingency And Response
OSPAR Convention	Convention for the Protection of the Marine Environment of the North-East Atlantic
PAH	Polycyclic aromatic hydrocarbon
ParTrack	Particle tracking for drilling discharges
PFD	Process flow diagram
PW	Produced water
ROI	Region of interest
SAR	Synthetic aperture radar
UV	Ultraviolet
WAF	Water accommodated fraction

1. Introduction

Produced water (PW) is a liquid waste byproduct from oil and gas production processes. It is saline water from subsurface formations that is brought up to the surface along with extraction of oil and gas [9]. When the oil/water fraction reaches the platform, it goes through a processing system where as much as possible of the water is removed from the oil. The removed oily water goes further through a cleaning process before it is either discharged to sea or re-injected into a suitable reservoir. Discharge to sea is the most used practice and these discharges of produced water are the largest waste stream generated by the petroleum industry. On a global scale, several billion cubic meters of PW is let out into the oceans yearly. The oily produced water that is let out into the seas on the Norwegian continental shelf (NCS) constitute of a yearly release of more than 100 million cubic meters [35]. These regular discharges can under certain conditions lead to observations of oil slicks on the sea surface by satellite radar detection. This raises concern regarding the potential harm for sea birds and other marine life that resides on or near the sea surface. Additionally, oil droplets in the water column resulting from PW releases may also cause harm to marine organisms [29, 36].

Research has been carried out with a focus on treating oily saline PW in order to meet environmental regulations as well as to find solutions for reuse and recycling of this liquid waste [9, 18, 59]. Various methods are used to reduce the oil content and salinity of produced water. At offshore platforms, because of limited space, compact treatment technologies are preferred [9]. Even with several treatment processes, regular continuous releases of PW can lead to the formation of oil sheens on the sea surface. The Norne platform is one of the northernmost fields in the Norwegian Sea and is located 200 km west of the Norwegian coast. Thin surface oil sheens are regularly detected by SAR satellite at Norne, and the field has been further studied in the present project [34].

To better understand when these regular PW discharges are likely to be observed by satellite radar, the understanding of oil droplet size, plume behavior, weather conditions and detection limit for the satellite radar is needed. The aim of this study was to fill some of the knowledge gap regarding satellite detection, droplet size, plume behavior and discharge conditions.

Experiments and simulations were carried out under various conditions in order to better understand the behavior of produced water once let out into the marine environment.

2. Theoretical background

Continuous regular releases of PW can under certain conditions lead to the formation of oil sheens on the sea surface that are detected by satellite radar. To better understand the behavior of the PW once let out into the sea knowledge in several disciplines is needed. In the following sections in this chapter, an overview of the main theoretical perspectives guiding this thesis will be presented.

2.1 Produced water (PW)

PW is brought to the surface along with hydrocarbons (oil and gas) and its composition can vary by order of magnitude between different sources. Its characteristics depend on the geographical location of the field, the natural geological formation, the operational conditions, as well as the reservoir lifetime [9,17]. In the oil and gas reservoirs there are naturally occurring rocks that are saturated with fluids such as oil, gas and saline water [10, 18]. The reservoir rocks can appear in different forms, from loose sands to dense and tight rocks, and contains pores and throats. This creates flow paths and work as an accumulating system for hydrocarbons and also consists of a sealing mechanism for prohibiting hydrocarbon penetration to surface layers [11]. Since the density of water is higher than the density of hydrocarbons, the water is located in vast layers below the hydrocarbons in the reservoir rocks [10]. The sources of this water are flow from above or below the hydrocarbon zone, flow from within the hydrocarbon zone or flow from injected fluids and additives resulting from production activities [9,18]. Water that occurs naturally within the reservoir is called formation water, but all water is referred to as PW when it is mixed with hydrocarbons and brought to the surface [9,12,18].

PW is not a single product, but a simple to complex mixture consisting of formation water and injected water, but also dissolved organics, gases, traces of heavy metals, dissolved minerals, suspended oil, solids like sand and silt and production chemicals [10,18]. Its composition may vary continuously when production is initiated due to injection of seawater, reinjection of PW, bacterial activity and introduction to chemicals such as biocides and corrosion inhibitors that are used during drilling, fracturing and operating processes [10,18]. The main dissolved

organics in PW constitutes of benzene, toluene, ethyl benzene, xylene, polycyclic aromatic hydrocarbons (PAH) and alkylphenols (AP) [9,10].

As stated in the Introduction, PW can be treated two ways, either re-injected into a suitable reservoir or discharged to sea. The most environmentally friendly solution is re-injection because the PW is stored away where it is not bioavailable for marine organisms [62]. Re-injection is an expensive practice and not always applicable in every field, but where it is possible the re-injection is done to both maintain the pressure in the reservoir and for disposal of the PW. The industry wants to get as much of the oil out of a reservoir as possible and uses a technique for that called waterflooding. This technique entails that water is injected into the reservoir to help force the oil to the production wells. The injected water eventually reaches the production wells and in the later stages of waterflooding the PW proportion of the total production increases [9]. The most common way to deal with the PW is to discharge it to sea. This method affects the environment the most and it is therefore important to minimize the water pollution before letting it out into the environment [9,10].

2.1.1 Produced water behavior

There is little research about PW behavior and the size distribution of oil droplets in the release. Information about oil droplet behavior and plume behavior has therefore been gathered from some of the available literature on subsea releases/leaks of oil. As mentioned, produced water releases may contain gas. A report by Brandvik et al. [1] suggests that if the gas in a PW release is sufficient, the buoyancy from the released gas could bring the plume towards or to the water surface. Contrastingly, with little to no presence of gas in a PW release, the plume could become trapped in the water column because of the lack of buoyancy from the gas to lift the plume. In addition to the lack of gas in a PW release, certain other conditions can lead to the PW plume being trapped in the water column but does not imply that the oil droplets in the plume also are trapped. It implies that the main volume of the plume does not have a net transport or movement to the surface. The oil droplets fate is further determined by their own rise velocity towards the surface as individual oil droplets. The droplets rise velocity is determined by their diameter/volume. When the oil droplets reach the sea surface, its fate depends on the sea conditions. The formation of oil sheens on the sea surface are also reliant on the amount of oil droplets rising to the surface in the area. If the

amount of oil droplets is sufficiently high, individual smaller sheens could start to emerge. This could be the start phase for the generation of a continuous thin oil slick [1, 60, 61, 63, 64].

2.1.2 Produced water treatment

There are different techniques to treat PW due to its composition that include physical, chemical and biological methods [9]. Numerous treatment technologies have been proposed as PW contains several different contaminants with varying concentration. Contaminants might not all be removed through one single process and therefore the treatment system require a series of individual unit processes for contaminant removal [18]. There are some considerations which must be taken into account regarding PW treatment offshore. That includes space and weight limitations on the platform, capacity, performance and reliability of maintenance. In research done by Nature Technology Group [19], it is expected that PW production will increase because of an increase in age of the wells and a decline in oil and gas production. It is therefore important that the PW production system is designed to receive a continuously increasing quantity of water as the fields mature [10]. PW production is thus driven up by maturing old fields and driven down by new and better technologies and the introduction of new oil fields [9]. The PW that is discharged into the marine environment are regulated by discharge permits. Based on the Convention for the Protection of the Marine Environment for the North-East Atlantic (the OSPAR Convention), the annual average limit for discharge of dispersed oil for PW into the sea is 40 mg/L [13].

2.1.3 Compounds of concern found in produced water

Compounds like PAHs and APs, among others, are both found in PW and make up a small fraction in the oil-droplets that are present in the PW [15]. PAHs are a group of organic compounds that are composed of multiple aromatic rings, only containing carbon and hydrogen. Naphthalene is a simple example of a PAH, containing two aromatic rings. These compounds are hydrophilic and lipophilic, and therefore tend to bioaccumulate in the environment. PAHs come from both natural and anthropogenic sources and can result from incomplete combustion of organic matter. Anthropogenic sources of PAHs can be fossil fuel and natural sources can be volcanic eruption. [15, 29]. Alkylphenols are stable, persistent and

hydrophobic which leads to a concern for the effects it causes in the marine environment [46]. Both PAHs and APs are abundant in the environment and together they comprise hundreds of different compounds exhibiting variable levels of carcinogenicity, genotoxicity and physiological impairment [15, 29, 46]. PAHs and APs are also naturally found in formation water, are both toxic and bio-accumulative and together with heavy metals considered the most harmful contaminants in PW [10, 15]. PW is let out continuously and a concern is therefore raised for the possible chronic effects in the marine environment through long term exposure.

2.2 Composition of crude oil

The oil in the PW is present as suspended oil droplets and as dissolved components [9]. The crude oils composition can mainly be divided into two groups: hydrocarbons and non-hydrocarbons [52]. The majority of the compounds present in crude oil are hydrocarbons, but small amounts of organic compounds are also found. The organic compounds in crude oil consist of nitrogen, oxygen, sulfur and also metallic constituents as vanadium, nickel, iron and copper [10, 44]. Table 1 present an overview of the elemental composition of crude oil.

Table 1. Elemental composition of crude oil [10].

Element	**Content in crude oil (weight, %)**
Carbon	80 – 87
Hydrogen	10 – 14
Nitrogen	0.2 – 3
Oxygen	0.05 – 1.5
Sulfur	0.05 – 6

2.2.1 Hydrocarbons

Hydrocarbons consist of hydrogens and carbons, and these vary in complexity from light volatile compounds to heavier compounds [47, 52]. Hydrocarbons can be further classified into saturates and aromatics. Saturates are a non-polar group of hydrocarbons and are the lightest compounds in crude oil. They may be straight-chained, branched, or cyclic but are

without double or triple bonds [10, 52]. Straight chained alkanes up to 4 carbon atoms are in gaseous form, and straight chained alkanes with 5-17 carbon atoms are liquid [47]. The lighter saturates make up the components of an oil most prone to weathering and the larger saturates (< 18 carbon atoms or more) are termed waxes [44]. Aromatics contain one or more aromatic rings and are slightly more polarizable than the saturates. Aromatics are cyclic unsaturated hydrocarbons and can make up 40-50 % of the crude oil [10]. Table 2 gives an overview of the crude oil fractions and some example compounds.

Table 2. Chemical compounds in crude oil [45, 47].

Classification	**Example classes, names, and compounds**			
	Chemical class	**Alternate name**	**Description**	**Example compound**
Saturates	Alkanes Cycloalkanes Waxes	Paraffins Naphthene's		Methane Propane
Aromatics	BTEX Polycyclic aromatic hydrocarbons Naphthene aromatics		Benzene, toluene, ethylbenzene, xylenes Combination of aromatics and cycloalkanes	Naphthalene Benzo(a)-pyrene
Resins	Class of mostly anomalous polar compounds sometimes containing oxygen, nitrogen, sulfur, or metals			
Asphaltenes	Class of large anomalous compounds sometimes containing oxygen, nitrogen, sulfur, or metals			Structure's unknown

2.2.2 Non-hydrocarbons

Resins and asphaltenes are both classified as non-hydrocarbons [47]. Resins consist of polar molecules which predominantly contain heteroatoms (N, O and S). This may lead to a larger density of functional groups in the resin and makes them capable of having strong intermolecular interactions with other polar molecules like asphaltenes. The resins are structural similar to asphaltenes but have lower molecular weights and higher H/C ratio than the asphaltenes [10, 44, 45, 52]. Asphaltenes have polar molecules with very high molecular weights and have the highest amount of heteroatoms. Its chemical properties are not well known and asphaltenes are in general a complex mix of organic matter. The asphaltene molecules consist of polycyclic aromatic clusters with 6-20 rings, varying side chains, heteroatoms (N, O and S) and metals [10, 44, 45, 47].

2.3 Weathering of oil at sea

There are various natural processes that alter the physical and chemical properties of the oil once it is discharged at sea [47, 48, 51]. A common term for these natural processes is weathering [48, 51] and the degree of weathering is dependent on the oils original physical and chemical properties [47]. The weather conditions (wind, waves, air temperature etc) and the properties of the sea (temperature, salinity, density, oxygen, currents, bacteria etc) also affect the weathering processes [48, 51]. In Figure 1, the weathering processes of oil at sea is shown.

Oil is present as dispersed droplets in the PW plume [9] and when these droplets are released with the PW into the water column, small hetero compounds and low substituted aromatic hydrocarbons are prone to dissolution. This natural process removes the most soluble components in the oil [47, 51]. Further, evaporation is a process that occur early on when oil is present at the sea surface, and it takes an important part in removing the lightest components in oil from the water [47]. The rate of evaporation is dependent on the vapor pressure, but also wind, sea temperature and thickness of the slick. During higher wind speeds, the lighter components in oil will evaporate faster because the gas that is present above the slick will diffuse and be removed from the equilibrium above the oil sheen. In total there will not evaporate more oil, it will just happen faster [49].

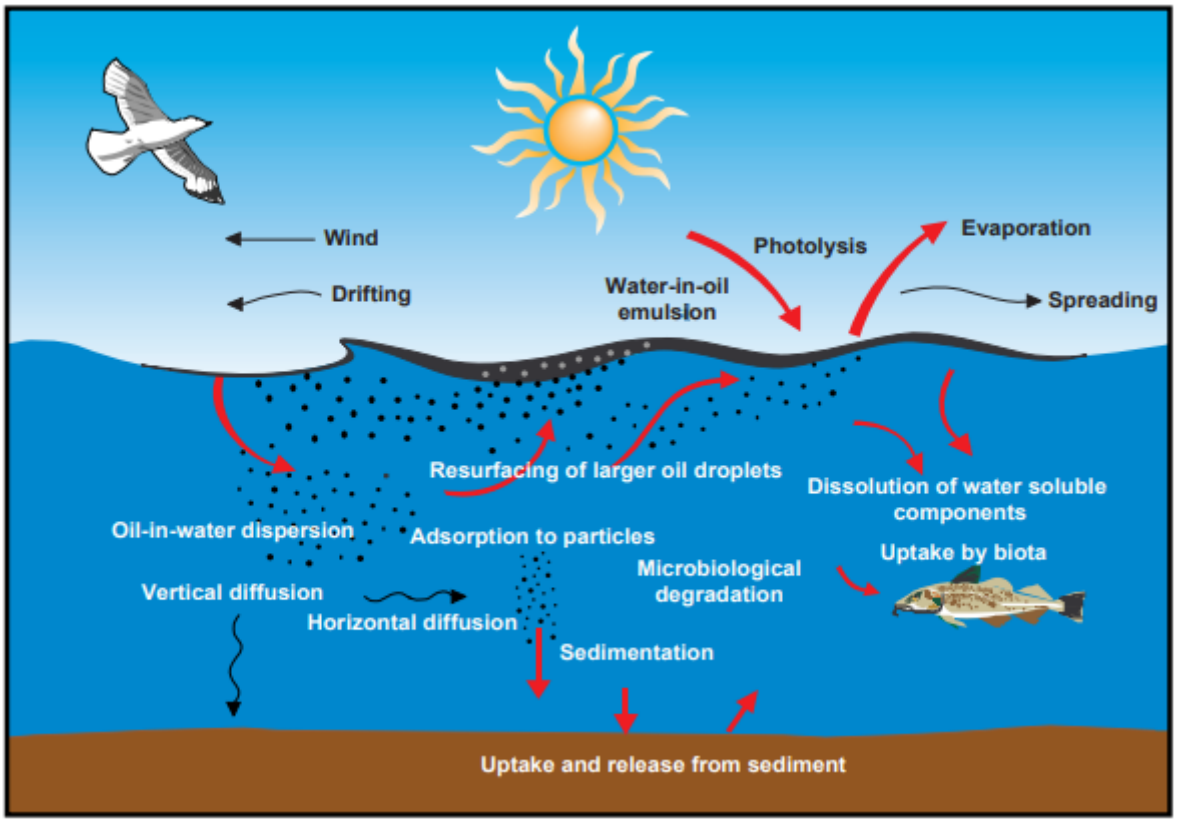

Figure 1. The weathering processes of oil on the sea surface [51].

If oil is present at the sea surface, components in the oil may also be oxidized under the influence of sunlight [49] and affects strongest during summer. This process favors the formation of a stable water-in-oil emulsion and increases the oils persistence at sea. Microorganisms are present in seawater and some of these use the oil components as an energy source. The biodegradation is not prominent before about two weeks after the oil is discharged to the sea [47, 51] and takes place on the interface between oil and water. Most of the oil can be degraded by microorganisms except for asphaltene [49].

2.4 The Norwegian Sea

The Norwegian Sea covers an area of about 1,383,000 km^2 and is less thoroughly explored than the North Sea. The Norne field is located in the Norwegian Sea along with 21 other petroleum production fields. The Norwegian Sea has an average depth of 2,000 m and holds a maximum depth of 3,970 m. There has been petroleum activity in the Norwegian Sea since the opening of the Draugen field in 1993.

2.4.1 Current, tide, wind and waves

The upper layer (average depth of 500 m) in the Norwegian Sea is mainly influenced by the Norway Current which enters north of the United Kingdom. This current is a continuation of the Gulf Stream that flows from the Gulf of Mexico. The Norway Current flows northeastward along the Norwegian coast before flowing into other northern waters. When the current enters Europe's warmer climate, this causes an increased evaporation. This gives the Norwegian sea an elevated salinity of 35.0-30.2 psu [57]. The Norway Current influence the climate of Norway and northern Europe and holds temperatures ranging from 8 °C in the south to about 4 °C in the north [40, 41, 42].

The drifting and spreading of oil sheens on the sea surface is under the influence of winds and currents [51]. Tides affect the currents in the Norwegian Sea and is a natural phenomenon. All of Earth's oceans are influenced by the gravitational force from the moon and the sun. The tide moves through the oceans like a current in response to the forces exerted by the moon and the sun. Tides are very long-period waves that originate in the oceans and move towards the coastlines. At the shore, the tide appears as the regular rise and fall of the sea surface, also called high- and low tide. The incoming tide along the coast is called a flood current, and the outgoing tide is called an ebb current. Periods with weaker currents, called slack tides, occur in the period when the tide move from the ebbing to the flooding stage and vice versa. After a period of slack tides, which can vary from seconds to minutes, the current switches direction and increases in velocity [43]. If the currents in the ocean are greater than the velocity of the PW release, the PW plume can get trapped in the water column. The trapping of the plume is influenced by several other factors like the density of the PW, the buoyancy from the gas and the momentum from the release. If the PW terminates after being in the water column for a period, the oil droplets can possibly rise to the sea surface by their own terminal velocity during slack tides when the currents are weaker, as they no longer are trapped in the plume or currents [1].

Winds and sea currents have a strong influence on the presence of surface oil slicks from regular PW releases. A high wind speed will increase upper ocean turbulence as speeds above a certain threshold will result in a wave formation that breaks up the surface oil slick. The surface slick may not reform again as the ocean turbulence cause the oil droplets to disperse

over a large water area. The oil concentration in the surface slick is a result of a balance between the diluting effect of the ocean current speed and the release rate of PW, which affects the thickness of the film. Weather conditions like weak currents and no wind will facilitate formation of a thicker oil film, while stronger currents and high wind speed will dilute and break the slick apart [2, 3, 4].

It is known that the wind speed is in general higher in the period from September to April. This seasonal weather difference can be observed in Figure *2*, where the mean wind speed for the weeks of 2020 is shown at the Norne field. During the period from April to September 2020, the mean wind speed varied between 4-7 m/s, as opposed to the period from September to April, where the mean wind speed varied from 6-13 m/s. In the first week of 2020, Figure *2* also show that the mean wind speed was as high as 15 m/s. The lower mean wind speed during summer can result in a higher number of oil spill detections in the months from April to September. The data in Figure *2* is from the Norwegian Meteorological Institute.

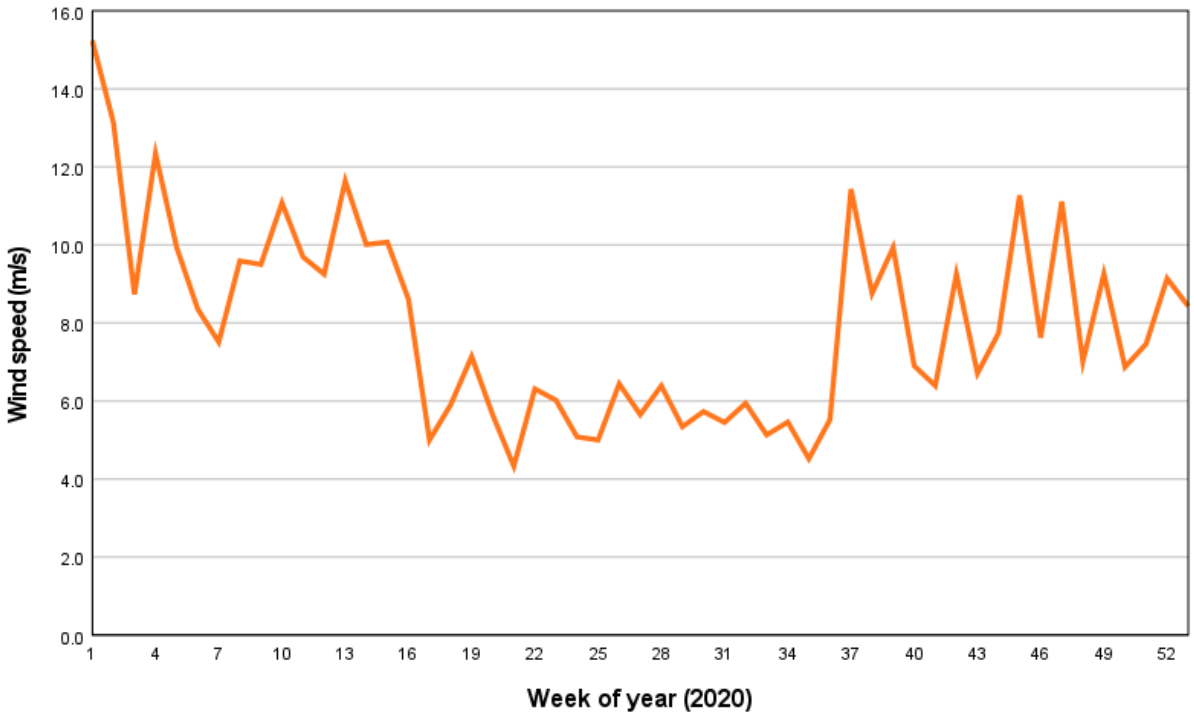

Figure 2. Wind speed at the Norne field for each week in 2020. Data is from the Norwegian Metrological Institute and 8 wind speed measurements were available for each day. This figure shows a mean value for each week during the period 01.01.2020-01.01.2021.

2.4.2 Produced water effects on life in the Norwegian Sea

The coastal zone in the Norwegian Sea holds important areas for both marine life and birds. Numbers from 2019 estimate that about 1,270,000 pairs of seabirds use the Norwegian parts of the Norwegian Sea as their breeding grounds. Out of these, 870,000 pairs were breeding along the mainland coast and 400,000 on Jan Mayen [42]. In research by O'Hara et al. [61] it was found that seabirds may be impacted by the sheens forming around offshore installations from discharged produced water containing currently admissible concentrations of hydrocarbons. Another report by the International Council for the Exploration of the Sea [42] showed that many of the bird species that use the Norwegian Sea as their breeding grounds have decreased since the monitoring of the population started three to five decades ago. There is no single culprit to these trends, and the long-term breeding failure for species feeding in pelagic waters indicate that much of the problem along the mainland coast is related to drastic changes in the availability of fish, and variations in the ocean climate [42]. Further studies are needed in the field to fully understand the impact of thin oil sheens on seabirds.

The Norwegian Sea is also important for the marine life. Fish rely on locations in the Norwegian Sea for spawning and migrate to the area from the North Atlantic and the Barents Sea during their spawning season [42]. Water-accommodated fractions (WAFs) are a preparation method commonly used in the available literature [29] where oil is mixed with a volume of seawater. This method is used to reflect environmental behavior and petroleum-water mixtures for laboratory toxicity testing. It is found that WAFs is dependent on oil type, mixing time and exposure temperature in the environment. It is also to be considered that the WAFs contain the highest possible concentrations of dissolved hydrocarbons expected from an oil spill [28]. Early life stages of polar cod (*boreogadus saida*) have shown high sensitivity to very low levels of a crude oil WAF [29], while adult specimen is considered more robust when exposed to low environmentally relevant concentrations of dietary crude oil [30]. In a study by Nahrgang et al. [31], effects of crude oil on energy homeostasis and associated physiological processes in polar cod was conducted. Crude oil and related contaminants, such as PAHs have previously been shown to affect growth and metabolism in fish in a study by Christiansen et al. [32]. Polar cod invest high amounts of energy into reproduction [33] and may be vulnerable to stressors such as dietary crude oil during gonadal maturation. In Nahrgang et al. [31] crude oil had a negative impact on growth performance on adult polar cod in early spring. Furthermore, with different physiological states between sexes, mortality

was only observed in male polar cod, while females showed an increase in their routine metabolic rate. These findings show that the species might not be as robust to additional stressors such as pollution during sensitive periods of development as previously thought [29, 31, 32].

2.5 The Norne field

The Norne field is a part of the present study and is located 66°0’49.35’N and 8°4’26.48’E on the Norwegian Continental Shelf (NCS) about 200 km west of the Norwegian coast. As shown in Figure 2, the platform is among the northernmost fields, embracing block 6608/10 and 6608/11 and was officially opened in November 1997. The Norne field consists of a production and storage ship which is tied to subsea templates [34]. The ship contains a processing plant on deck and has storage tanks for stabilized oil. The ship rotates around a cylindrical turret that is moored to the seabed, making it able to face the direction of the shifting weather. The area has a water depth of 380 meters and the reservoir is found 2,500 meters below the sea level. The oil and gas enter the ship from flexible risers that carry the well-stream to the surface. The nearby fields Urd and Alve are connected into Norne for processing and transport [35].

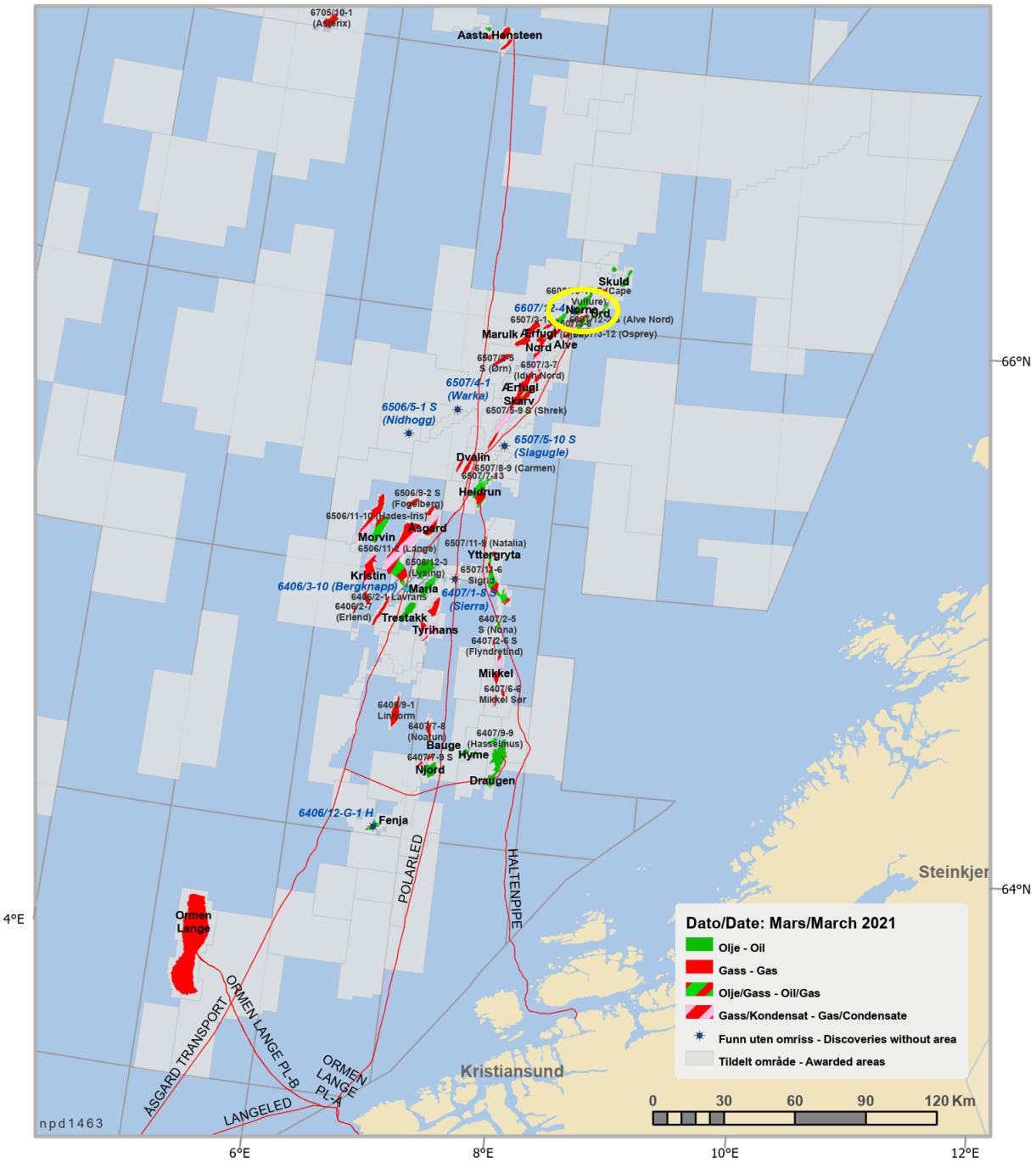

Figure 3. Map over the petroleum activity in the Norwegian Sea. The Norne field is located north in the map and is marked with a yellow circle. This figure is used with permission to reuse from the Norwegian Petroleum Directorate [40].

PW is let out into the Norwegian Sea and the Norwegian part of the North Sea every day. Data provided from Equinor show that the Norne field has a PW discharge between 12,000 to 20,000 m^3day^{-1}. This adds up to a total yearly discharge of 4.38 to 7.30 million m^3 of PW. With an increasing amount of PW discharges the production at a global level is as much as 39.5 million m^3day^{-1} (2019) [18], which is about 14.4 billion m^3 a year. Figure 3 show that Norway contributed with a total of 125.1 million m^3 of PW discharges in 2019 [35], and that the projections for the years to come are not decreasing. The daily release (2007) of PW corresponds to over 70 tons of PAHs and 350 tons of APs from oil drilling activities [2].

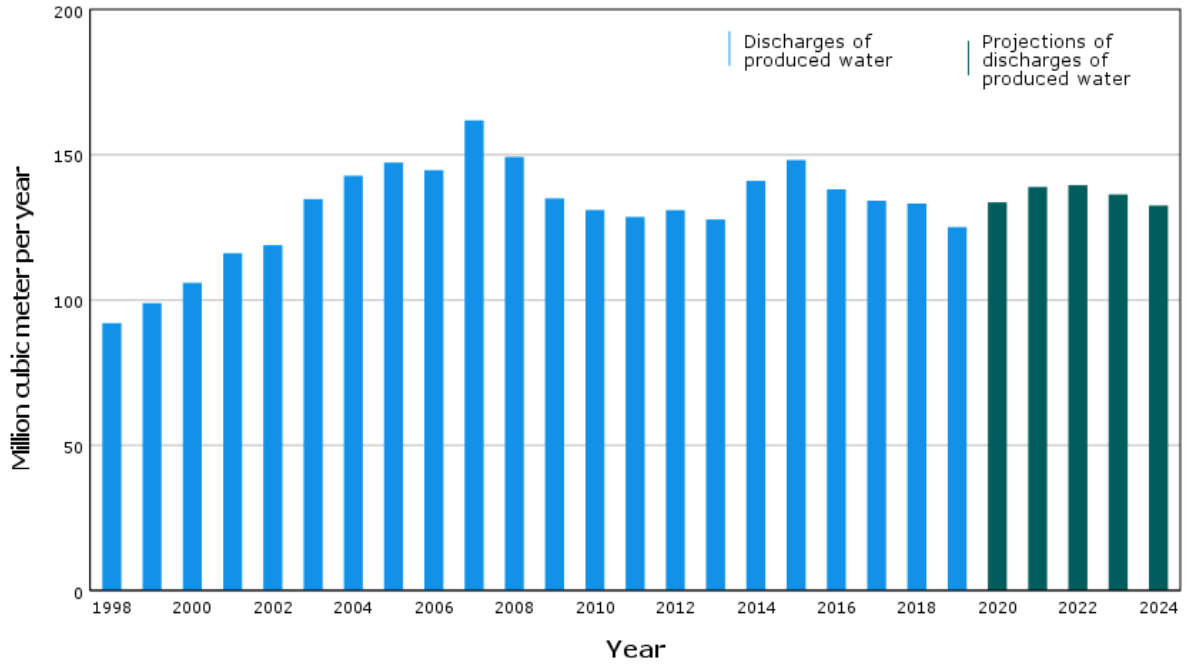

Figure 4. Yearly discharges of produced water into the Norwegian Sea and the Norwegian part of the North Sea. Historical numbers for 1998-2019 and projections for 2020-2024. The numbers given in this figure are used with permission to reuse from the Norwegian Petroleum Directorate [35].

2.5.1 Produced water at the Norne platform

The oil that is produced at the Norne platform has a high content of waxes, as shown in Figure *5*. This waxy oil is present as dispersed oil droplets in the produced water that is released from Norne. The PW that is released from the platform leaves from one single outlet point, which has a horizontal release angle and is located 12 m below the sea surface. The release constitutes of regular PW from oil extraction processes, but also jetting water. Jetting water is the leftover water from cleaning of separators, sand-cyclones, coalescers, storage tanks and

pipes at the processing plant on the platform [50]. The cleaning process of the systems is not a daily routine and is done irregularly, which means that it occurs jetting water discharges only on some days. Data for both PW releases and jetting water was provided by Equinor. Data for PW was given for the period 01.12.20-28.02.2021, held a mean oil index of 12.7 ppm and is presented in Appendix A.4. PW samples are taken 3 times a day on the Norne platform and the final data that was provided is a mean value of these 3 samples. Each sample contains information about oil index (ppm), volume of water (m^3) and weight of oil (kg) released on that day. Data for jetting water was given for the period 04.12.20-25.02.21 and had 10 days of jetting water releases. These data show that several releases of jetting water could be done in one day from cleaning of different systems. The mean oil index for the 10 days of jetting water releases was 122.8 ppm. The oil index varied from 15-644 ppm for these days and the data for jetting water releases is presented in Appendix A.3.

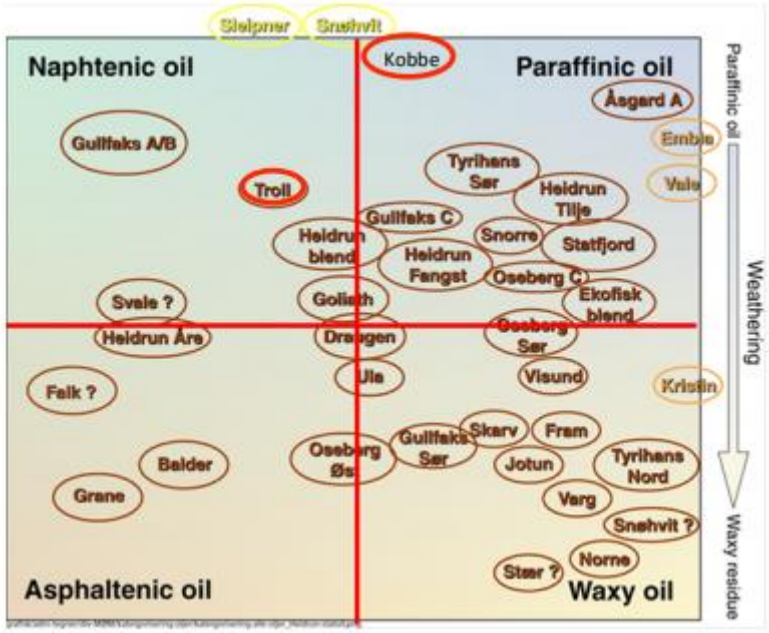

Figure 5. Overview of the characterization of the oils extracted from offshore fields on the Norwegian Continental Shelf. The Norne oil is located in the bottom right corner and has a high content of waxes [65].

2.5.2 Temperature of produced water

The oil/water fraction that is extracted from a reservoir can hold temperatures between 100-200 °C [51]. As previously mentioned in section 2.1, produced water is brought up along with the extraction of oil and is thereafter separated from it before further processing [9]. The PW holds high temperatures, and it is probable that the PW suffers some heat loss during the

cleaning treatment(s) before re-injection or disposal to the sea. It is known that PW composition differs between platforms because of unique conditions in each reservoir and the in-flow of water [10, 18]. Various treatment system may influence the PW differently and an individual outlet temperature for each field is therefore possible. With data provided by Equinor, it is known that the PW holds an outlet temperature at 63 °C at the Norne field and 68 °C at the Grane field [37].

2.5.3 Salinity of produced water

Salinity is the amount of salt that is dissolved in a volume of water and is measured in psu (practical salinity unit) [9]. PW contains a high number of salts, mostly dissolved sodium and chloride, and can in some cases contain salt concentrations all the way up to 300 psu (saturated brine) [18]. Seawater has a salinity of about 35 psu, which means that it contains 35 g salt in 1 kg water [57]. The salinity of the PW varies between reservoirs since it is a result of the naturally occurring minerals in the reservoir rocks and is also affected by the in-flow of water [10, 18]. Numbers provided by Equinor show that the PW has a salinity at about 48 psu when discharged to sea after going through the treatment system on the platform [36].

2.5.4 Density of produced water

Temperature, along with salinity and pressure, is an important factor for the waters behavior and governs physical characteristics like density [53]. The density of seawater at the surface is about 1.0270 kg/L. What makes seawater more or less dense than 1.0270 kg/L is temperature and salinity. Temperature has a greater effect on the density of water than salinity and is indirectly proportional to density, meaning that when the temperature of the water increase, the density decrease. Salinity on the other hand makes the water more dense, so increasing salinity will increase its density [58].

PW is generally denser than seawater because of its high content of dissolved salts [18]. As a complex mix, PW also contain other components that do as well affect its density. As previously mentioned, PW contains formation water and injected water, but also dissolved organics, gases, heavy metals, dissolved minerals, suspended oil, solids and production

chemicals [10, 18]. It is the combined factor of these parameters, especially the temperature and salinity, that influence the PW density and affects its behavior when it is let out into the sea [54].

The density-temperature relationship is non-linear. It can only be linearized for temperature ranges from 2-35 °C and for salinity ranges from 2-42 psu. Since the experiments in this project exceed that area, a non-linear density equation was used. Sharqawy et al. [37] derived a non-linear density relationship based on experimentally derived datasets for both salinity and temperature at 1 atm pressure from Isdale and Morris [38] and Millero and Poisson [39]:

$$\rho(T,S) = (999.9 + 2.034 * 10^{-2}T - 6.162 * 10^{-3}T^2 + 2.261 * 10^{-5}T^3 - 4.657 * 10^{-8}T^4) + (\frac{802.0S}{1000} - 2.001\frac{S}{1000}T + 1.677 * 10^{-2}\frac{S}{1000}T^2 - 3.060 * 10^{-5}\frac{S}{1000}T^3 - 1.613 * 10^{-5}\left(\frac{S}{1000}\right)^2 T^2 \quad (1)$$

where S is the salinity (psu), and T is the temperature (°C). This density relationship is valid for a temperature range of 0-180°C and a salinity of 0-160 psu with an accuracy of ± 0.1% [22].

2.5.5 Rate of the produced water discharge

The PW outlet opening has a diameter of 0.4826 m at the Norne platform. Data provided by Equinor measured a varying outgoing rate between 16,354-24,526 m^3day^{-1} for the period 01.12.2020 – 28.02.2021. The mean rate per day for the same period was 20,011 m^3 and the data is presented in Appendix A.4. Equinor do experience rates as low as 10,000 m^3day^{-1}, and a rate range of 10,000-22,000 m^3day^{-1} was therefore chosen for this project. The rate was converted into m^3s^{-1} by multiplying with the following:

$$Q = \frac{m^3}{day} * \frac{day}{24h} * \frac{h}{60min} * \frac{min}{60s} = 0.12 - 0.26\frac{m^3}{s}$$

Equation 2 was then further used to calculate the velocity of the PW release from the Norne platform:

$$Q = v * \pi * \left(\frac{D}{2}\right)^2 \quad \leftrightarrow \quad v = \frac{Q}{\pi * \left(\frac{D}{2}\right)^2} \tag{2}$$

where Q is the rate of the PW (m^3s^{-1}), and D is the diameter of the outlet opening (m). This gave an outlet velocity range of 0.63-1.40 m/s of PW from Norne.

2.5.6 Oil droplet size in produced water

As previously mentioned in section 2.1.1, there is little research on the size distribution of oil droplet in a produce water release. In one study by Judd et al. [60] small oil droplets were reported to be around 10-20 µm in size after hydrocyclone separation. In work done by Skancke, J. and Daling, P. [36] the mean volume droplet size from the samples conducted of the PW releases at the Grane field was 5 µm. From the same report, in a discussion with Equinor, it was noted that bigger droplets could occur in the PW release at Grane due to the possibility that one of the oil separation process steps was out of function part of the time [36]. No in situ samples were taken of the PW at the Norne platform for this project.

2.6 The importance of remote sensing

Oil spills are relatively often observed on the sea surface. These spills correlate well with the major shipping routes and commonly appear in connection with offshore installations [2]. To monitor the surrounding waters of offshore platforms and shipping routes for potential oil slicks, remote sensing is used to detect and map oil on the sea surface [4, 14]. Remote sensing is the ability to provide information about objects at or near the surface of the earth based on radiation reflected or emitted from those objects [6]. The foundation of remote sensing is the measurement and interpretation of emitted and reflected electromagnetic radiation from Earth's surface. Physical principles are used in remote sensing to determine characteristics about an object emitting or radiating at a specific wavelength. Radiation is normally measured and categorized based on wavelength using a logarithmic scale, known as the electromagnetic spectrum [6].

Visible detection of oil spills at sea is highly dependent of favorable lightning and sea conditions. The visible part of the electromagnetic spectrum ranges from 400 to 700 nm. Given the natural situations of night-time and fog, where oil on the surface may not be seen with the visible eye, there are other circumstances where it may not be visible. Floating objects like seaweed, ice and debris can mask the oils presence on the surface and in situations with big amounts of leaked oil, the area might be too big to be mapped visually. On the other hand, at times with no oil, natural conditions like surface wind patterns on the sea could appear as oil. Sun glitter, which can be confused for oil sheens, is also a problematic phenomenon in visible remote sensing. The use of human vision is a common technique for oil spill surveillance but is not considered remote sensing alone. Visual detection has been used in the past with varying degrees of success. With these known difficulties in visual detection, remote sensing systems are a god asset to be used in the task of mapping and identifying oil at sea [3, 4].

The practice of remote sensing has evolved since the early 1900s. Remote sensing evolved further in the following decades and by the end of the century satellites were able to capture data from the entire surface of the Earth with much finer detail than previously available. It started off being aircraft-based, capturing small areas of Earth's surface and only accessible to a few specialists, to becoming space-based, with coverage of the entire Earth's surface and available to most people with a computer. Technology has contributed to the evolution of remote sensing sensor design and electronics are becoming increasingly sophisticated and much less expensive [6].

Products from the petroleum industry, large oil spills and PW are found to have substantial environmental impacts [15]. With an increasing public understanding of these environmental consequences of oily discharges, the public expectation is that oil spill extent and location is precisely mapped. Remote sensing from satellites is now an increasingly common practice with the benefit of enabling 24-hour monitoring of the ocean. To generally improve clean-up processes and response time, remote sensing plays an increasingly important role in these efforts [3].

2.6.1 Satellite sensors for oil spill detection

There are different sensors that are being used for oil spill detection at sea. Remote sensing can be divided into different categories because the utility of the sensors is used for different situations. Remote sensing systems used to detect oil on shorelines and land differ from those used for routine surveillance. One tool does not serve all functions. There may be necessary with many types of systems for a given function. Additionally, it is needed to consider the end use of the data gathered from remote sensing. Dependent on the end use, this might dictate the needed resolution or character of the data [3]. In the coming section there will be given an overview of the sensors available today. Since the satellite data that is provided by Equinor for this project is from a SAR satellite, SAR will be the main focus sensor.

2.6.2 Optical sensors

Optical sensors can mainly be divided into three categories: infrared (IR), near-infrared (NIR) and ultraviolet (UV). Oil is optically thick, meaning it absorbs solar electromagnetic energy and re-emits some of that radiation as thermal energy. Emissions from the oil is measured when using IR sensors and these long waves are usually found in the region of 8-14 μm. IR sensor technology is reasonably inexpensive and is today a common and available asset [2, 3, 19]. Near infrared (NIR) sensors operates in the wavelength range of 0.75-1.4 μm and has recently been taken into use. Its time in oil spill monitoring is thus short and further research is needed for effective application to oil spills [4,19]. Ultraviolet (UV) technology can be used to detect oil spills as oil shows a high reflectance of sunlight in the UV range (100-400 nm), even in thin layers (<0.1 μm). Because of other factors that can cause false alarms in the conducted data, it is often the combination of UV and IR that is used to provide more reliable indications of oil on the sea surface and can also be used to estimate the oil thickness [2-4, 19].

2.6.3 Laser Fluorosensors

Laser fluorosensors use a laser operating in the ultraviolet region of 308-355 nm. The sensors use the phenomenon that aromatic compounds in petroleum oils absorb UV light and release the extra energy as visible light. Few other compounds show the same tendencies, and the absorption and emission wavelengths are unique to oil. The technique provides a unique

method for oil identification and discriminates best between light, medium and heavy oil types. [3, 4].

2.6.4 Microwave Sensors

Microwave sensors are becoming the most used form of sensor in the field, the active sensors especially [3]. Microwave radiometers (MWR) is one type of microwave sensor that measure the microwave radiation that the ocean emits. MWR is a passive sensor and looks at the microwave radiation in the wavelength cm to mm range. The sensor has potential in all weather conditions and is commonly used for oil spill monitoring by remote sensing [2, 3].

Radar sensors detect emitted energy from the ocean. The capillary waves in the ocean reflect radar energy to the sensor which creates a “bright” data image known as sea clutter. The oil is differentiated from the water and detected because oil on the sea surface dampens the waves. The presence of oil in the data will be areas of “dark” sea or the absence of the sea clutter. There are found to be many false targets that are detected this way because of wave dampening [2, 3, 7]. Even though the sensor has its limitations, radar is an important asset for oil spill remote sensing because of its wide area coverage and detectability at night-time and through clouds and fog [3]. The two basic types of imaging radar that can be used to detect oil spills for environmental remote sensing are Synthetic Aperture Radar (SAR) and Side-Looking Airborne Radar (SLAR). The SAR will be presented in more detail.

2.7 Synthetic Aperture Radar (SAR)

Synthetic Aperture Radar (SAR) is an active microwave sensor capturing two-dimensional images. SAR is useful in oil spill monitoring because of its wide area coverage and night-time all-weather capabilities [2, 7]. From the available research, SAR is viewed as the most efficient and superior satellite sensor for oil spills detection, though it does not have capabilities for oil spill thickness estimation and oil type recognition [2, 3]. Even with its limitations, SAR is a very reliable satellite with its ability to collect imagery day or night, regardless of cloud cover, and with a large area coverage [26].

The SAR satellite works in the same way as radar sensors. Compared to other satellites that take reflectivity from the sun, SAR satellite sends out its own energy that is reflected back to its sensor from the surface of the earth. The sensor receives radio waves from various angles from the ocean. When slicks of oil are formed on the sea surface it dampens the waves, and the oil is seen as darker areas surrounded by sea clutter in the SAR images. As a contrast to the dark area of oil in the images, the surrounding spill-free sea appears relatively bright. The radio waves and angle differ when emitted from the ocean versus from an oil sheen. This difference in the imagery between the oil slick and the water is dependent on several parameters. These include wind speed, wave height, amount and type of oil spilled, and some parameters connected to the sensor [3, 5, 25]. Satellite radar sensors, especially SAR, has had an increased use in the field of surveillance and has been the focus in research for many years. This is in part because of the increased importance for the public to track and detect oil spills. It is of importance to improve the efficiency of maritime surveillance systems to decrease the impact of oil pollution on the marine environment [7].

The weathering processes are important to consider as they influence the oils physicochemical properties at sea and detectability in SAR images [2, 7]. Brekke et al. [2] presents the four stages in the processing of SAR data. These stages include image processing, selection of regions of interest (ROIs), parameter extraction, and classification. It is of interest to go through the radar image analysis since some of the images might not have the needed quality to proceed. After the second step, ROI selection, a pixel-based binary classification (either dark spot or ocean surface) identifies if the data features any dark areas. A new dataset is created in the third step from the extracted information from the ROIs and development of the parameter vector of the selected dark areas. Features of the parameter vector can in some cases also include additional external information such as wind speed, currents, oil spill movement, and the presence of ships or platforms in the vicinity of the spill. The last stage, classification, uses the parameter vector information to differentiate between oil spills from look-alikes [2, 3, 7, 8].

Equinor receives its SAR data from Kongsberg Satellite Services (KSAT) located in Tromsø, Norway. The operators working with the SAR images are experiencing a growing workload as the amount of SAR images are increasing. The algorithm for automatic detection is of great

benefit for the operators and help in screening the images and prioritizing the alarms [2]. Equinor experience that oil signatures on the sea surface gets classified mostly as PW, although in some cases they have accidental leaks of oil from the platform or from nearby shipping vessels. Thus, to identify the source of the oil slick is of great importance since it is necessary to perform countermeasures when it is not regular PW discharges.

2.7.1 SAR weaknesses

The SAR sensor sometimes detect false targets because of wave dampening. These natural phenomena include freshwater slicks, currents, wind slicks, shallow seaweed beds, glacial flour, biogenic oils, and whale and fish sperm. These are referred to as look-alikes and comprise the main issue for discrimination [2, 3, 7]. Besides from possible look-alikes on the sea surface, the SAR satellite is also dependent on the sea state. If the sea state is too low, the result can be insufficient sea clutter in the surrounding sea to contrast to the oil in the SAR images. On the other hand, if the sea state is too high, this will scatter radio waves enough to block detection because of the breaking waves. Sea state is dependent on wind and based on the available research the impression is that conditions that are optimal for SAR detection are wind speeds between 1.5-10 m/s. Wind below 1.5 m/s is too low for waves to form and for detection to happen. With wind in the region between 10-15 m/s it is somewhat possible to get detection of oil, but winds above 15 m/s hinders detection as the sea state is too high. The high wind speed results in turbulence in the upper sea layer causing the oil spill to break apart. This gives the radar a limit window of application for detecting oil slicks [3, 4, 19].

2.8 Instrument and program

Additional equipment like a velocimeter and the OSCAR model was utilized in this project and information about these is presented in the following section.

2.8.1 Vectrino field probe

The Vectrino field probe is a velocimeter used to measure the velocity of fluids and was used in this project. The instrument is typically used in difficult measurement situations such as turbulence measurements, very slow flow, and rapidly varying flows in the laboratory or the

ocean. The velocimeter use sound waves and the Doppler effect to measure the velocity in the water. Part of the sound wave reflects back to the instrument and the detected return-signal will be further processed by the instrument [23].

2.8.2 Oil spill modelling

Many models have been developed over the years for oil spill modelling. These have been developed for both surface and subsurface oil spills. The first blowout models were developed in 1980 by Fanneløp and Sjøen [66] and did not include models for deepwater blowouts. The oil plume behaves differently in deepwater compered to a plume in shallow to moderate waters [67]. The development of deepwater models and the inclusion of hydrate formation was first seen in the models by Topham [69]. Deepwater blowout models were further developed and later published in the work of Johansen et al. [70] and Yapa et al. [71]. In a study from 2018 by Dissanayake et al. [72] the development of bubble and droplet dynamics of multiphase plumes in the environment was presented. In the same study, it was presented new developed models that had added advantages like tracking the pathways of individual bubbles and droplets after they separate from the main plume or intrusion layer. The field of oil spill modelling is under constant development and the inclusion and discussion of all available models are not included in this thesis. The present study focused on the release of produced water from offshore installations into seawater. These regular releases are let out into the water column in closeness to the sea surface and the use of the OSCAR model by SINTEF was both available and suitable for the planned simulations.

2.8.3 OSCAR

The Marine Environmental Modelling Workbench (MEMW) is developed by SINTEF and consists of three numerical models:

1. DREAM – Dose related Risk and Effects Assessment Model
2. ParTrack – Particle tracking for drilling discharges
3. OSCAR – Oil Spill Contingency And Response

OSCAR is a model that is used for overall oil spill simulation and was used in this project to simulate releases of PW from offshore installations. It is a simulation tool that predicts the fate and effects of releases of oily produced water, oil and gas into the marine environment. It

is also used for planning and response actions for oil spilt at sea. The modules found in OSCAR have been developed through laboratory studies at SINTEF, in addition to field studies in temperate and Arctic areas. The OSCAR program models oil as particles that are influenced by currents, wind, and turbulent diffusion, and includes weathering processes like evaporation, dissolution and dispersion [55, 67, 68]. These program qualities were suitable features for the present study since it is known that oil is present as dissolved particles in produced water.

This theory chapter is the base for this project and has further been used to strengthen the experimental work, the simulations conducted in OSCAR and the Results and discussion chapter.

3. Experimental method

3.1 Produced water experiments

3.1.1 Experimental work in the SINTEF wave basin

The experiments took place at SINTEF Sealab in Trondheim, Norway. A wave basin, shown in Figure 6, was used for the PW release experiments. The basin is equipped with a climate simulator and holds good conditions for observation of plume behavior. It was important that the PW release experiments were exposed to the most realistic conditions possible. The basin has technologies that can be used to show the effects of temperature, ocean currents, winds, sunlight, waves and ice conditions on the behavior of oil and PW in the marine environment [21]. As presented in the theory chapter, there are many parameters affecting the discharges in the Norwegian Sea. This makes the basin a good fit with the intention to achieve as realistic environmental conditions as possible. The basin was also convenient to use because of its open roof solution that allowed easy access and use of additional equipment.

The wave basin is comprised of stainless steel and covered with tempered, laminated glass on both sides. It measures 14 meter in length, 2 meter in height and is 0.5 meter widthwise. Only a section of the basin was used for the PW release experiments. The basin has a "double bottom" to obtain circulation and was filled to 1.5 meter with seawater for the experiments (or about 1 meter above the "double bottom"). This corresponds to about 10.5 m^3 of seawater. Propellers are installed in the lower department of the basin to obtain wanted circulation within the basin and a piston type wave maker is installed at one end [22]. A weak current was necessary for the PW releases, but no waves were used for the experiments in this project.

A blue light was installed above the wave basin to bring forward the fluorescence used in the PW. The fluorescence made it possible to track the plume behavior because it stood out against the black background that had been attached to the glass on the opposite side.

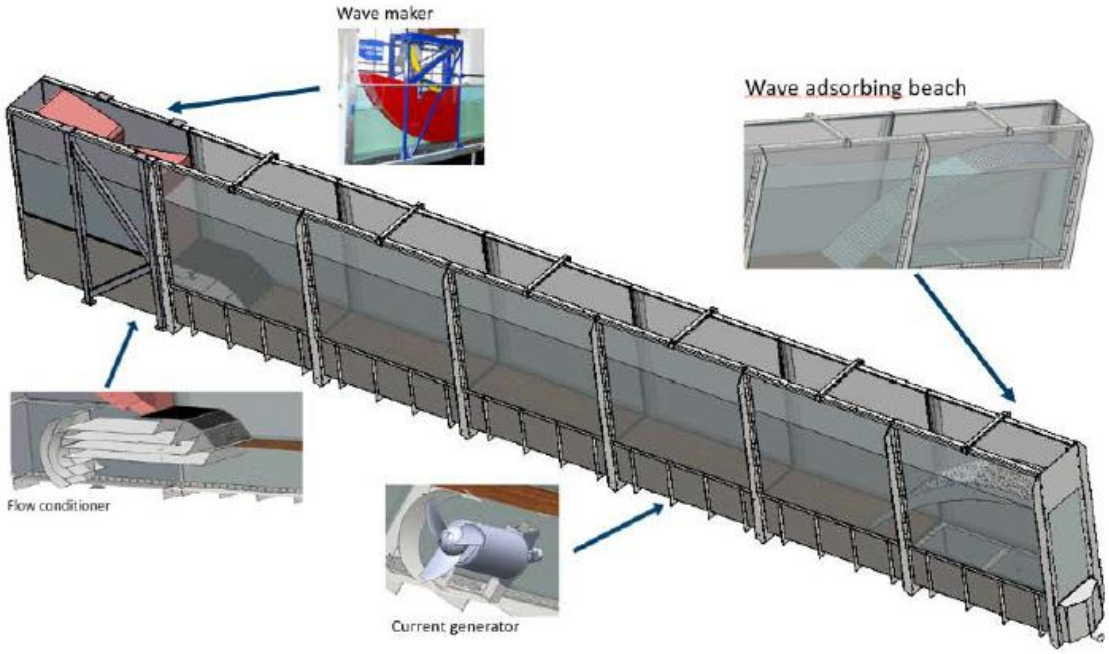

Figure 6. Sketch of the wave basin at SINTEF Sealab used for the produced water release experiments in this project. The sketch shows the main principles and architecture of the wave basin with a focus on the equipment installed inside the basin [22].

3.1.2 Experimental setup

A schematic representation of the setup used during the experiments for PW release in the wave basin is shown in a process flow diagram (PFD) in Figure *7*. The wave basin was connected to a supply of both seawater and freshwater and was filled with seawater each day of an experiment. Produced water was heated to a target temperature on a cooking stove and was manually controlled by the user. The setup provided two possibilities for temperature control, one in the PW tank and one at the outlet. It was necessary to control the outlet temperature because of some known heat loss in the pipelines. The setup also made it possible to adjust the angle and depth of the release outlet. A computer was connected to the pump, flowmeter, flow controller and current generator. The whole process was controlled in the program LabVIEW (Laboratory Virtual Instrument Engineering Workbench) from a computer. The already built setup in LabVIEW was produced by SINTEF staff and had previously been used for other experiments in the wave basin.

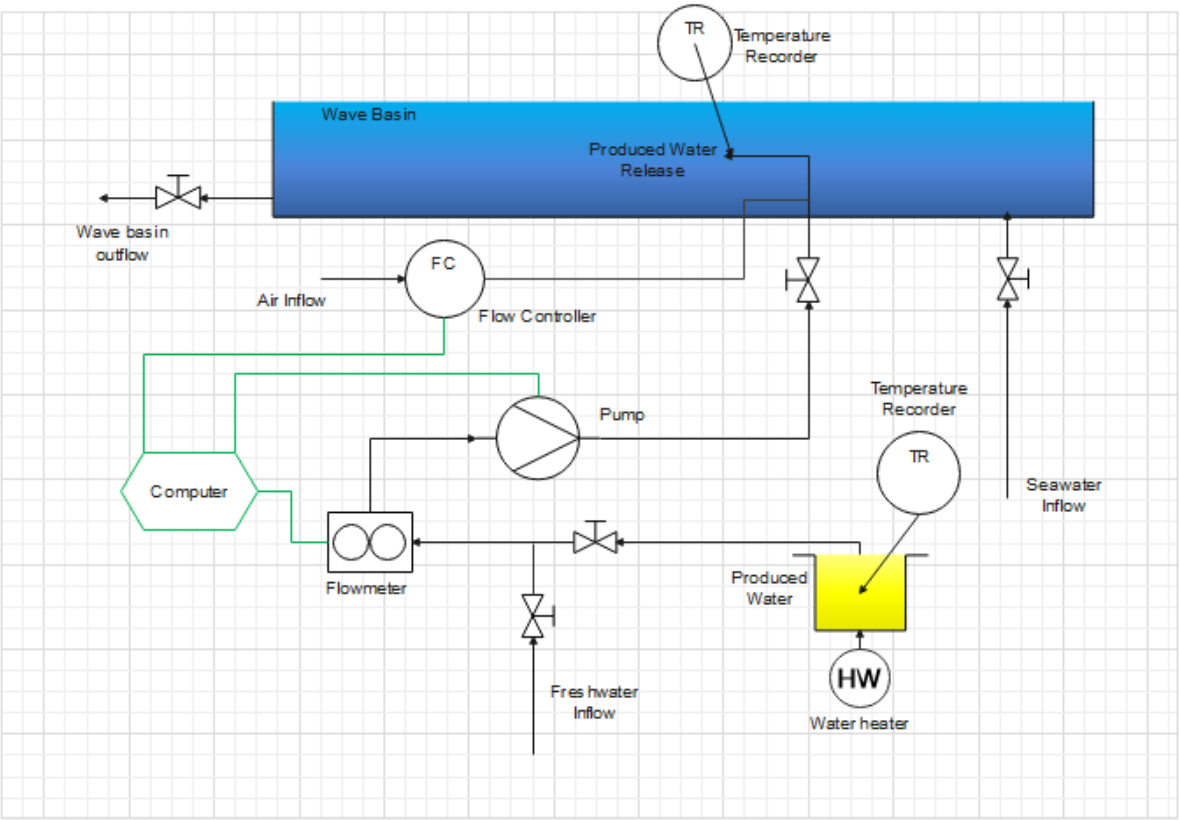

Figure 7. Process flow diagram (PFD) of the experimental setup for the produced water releases in the wave basin at SINTEF Sealab, Trondheim.

3.1.3 Experimental parameters

Data about the discharge condition at the Norne platform was provided by Equinor. The release parameters given in Table 1 are scaled down to fit the wave basin and are representative values to mimic the different conditions at Norne.

Table 1. Experimental values for the releases in the wave basin at SINTEF Sealab.

Nozzle diameter	0.004 m
Nozzle alignment	Horizontal or 45° down
PW temperature range	25 – 67 °C
PW salinity range	35 – 60 psu
PW flow rate	0.45 – 1.09 L/min
Gas (air) flow rate	5 - 25 % of PW flow rate
Oil concentration in PW	20 ppm
Oil type	Oseberg blend fresh (SINTEF-ID: 2013-0439)

3.1.4 Experimental procedure

From the test experiments with fluorescence, it was found that about 3-4 releases were the maximum amount of PW discharge the wave basin could take before all the seawater was colored light green. It was therefore planned to do this amount of releases each time the basin was filled with fresh seawater. The experiments were planned based on information provided by Equinor. The rate at the Norne platform is between 10,000-22,000 m^3day^{-1} and was used to calculate the rate for these experiments. The rate had to be between 0.45-1.05 L/min to match the outlet velocity for discharges at Norne. 0.45 L/min was used as the low rate, 0.75 L/min as the medium rate and 1.05 L/min as the high rate. The salinities and temperatures were also divided into low, medium and high. The salinity was either 35, 48 or 60 psu and the temperature was 30, 52 or 70 °C, respectively. The same salinity and outlet temperature was used for the releases conducted on the same day. A total of 25 experiments were done, with 3-4 releases per experiment.

Table 2. Overview of the low, medium and high levels for each parameter used during the experiments in the wave basin.

	Temperature (°C)	**Salinity (psu)**	**Rate (L/min)**
Low	30	35	0.45
Medium	52	48	0.75
High	70	60	1.05

3.1.5 Produced water preparation

A tank was filled with 12 L of seawater and heated to the target temperature. When the temperature was reached, 2 L of seawater was used to heat the pipe-system. With 10 L seawater remaining, 0, 130 or 250 g of Sodium Chloride (NaCl) was added to achieve the correct salinity. Further, 0.2 gram of fluorescence powder was measured and dissolved in 200 mL seawater. This was added in with the seawater to make the release visible in the wave basin and gave it a bright yellow/green color. The amount of fluorescence added was decided after some initial test-releases that clarified what amount was necessary to track the plume.

It is though that very small droplets of oil (< 50 µm) found in PW do not affect the rise of the plume, and for these experiments the focus was therefore to look at the salinity, temperature, rate and release angle. The PW made for these experiments did not contain any oil, except for the last 10 releases.

An Oseberg blend fresh (SINTEF-ID: 2013-0439) oil was used for the 10 last PW releases. For the first 9 of these, a concentration of 20 ppm was added per liter seawater. 20 mg/L was added to the tank, which gave a total of 200 mg for the 10 L of seawater. The oil was initially added to 200 mL of seawater where it was mixed with a stick blender (used in cooking) to break up the oil and create small oil droplets in the seawater (d_{50} approximately 20 µm). This oil-in-water mix was thereafter added to the tank and stirred to get a homogeneous mixture. During the releases, the PW was continuously stirred in the tank to avoid variations. For the last release, additional oil was added to the tank with a bigger droplet size (d_{50} approximately 100 µm). There was 3 L PW left for the last release and the oil added corresponds to 800 mg. This oil was not mixed with a stick blender, but some dispersant was added to it. The oil/dispersant mix was shaken before it was added to the PW tank.

3.1.6 Background current in the wave basin

During some of the test-releases, it was found that a weak background current was needed in the basin to avoid backflow of the PW plume. A weak background current made it possible for a stable plume trajectory to form and the same background current was used for all the releases. The background current in the wave basin was measured by taking samples with a Vectrino field probe. Measurements were taken from top to bottom, starting at the water surface. A sample was taken every 10 cm to get the whole depth-profile of the basin. The velocimeter measured the current in the area 0-10 cm below its nodes and the last sampling depth was therefore 90 cm below the surface in the 100 cm deep basin (upper level). The velocimeter took 25 samples every second and 20-25 seconds were spent on sampling at each depth level. Additional data for the background current is presented in Appendix A.5.

3.1.7 Conducting the data in the wave basin

Each release experiment was videorecorded with a camera from the same exact position for all releases. The recording time varied between 2-4 minutes per release depending on the time needed for a stable representative plume to form. Each recording was saved to a computer as an mts-file and later processed with a Phyton script in Jupyter Notebook. A total of 78 PW releases were conducted over a six-week period. Out of all the releases there was conducted 61 releases with only PW, 7 releases including airflow, 9 releases with small oil droplets in the PW and 1 release with both small and large oil droplets in the PW. A full overview of the experiments (date, release ID, temperature, salinity, rate, velocity and release angle) is presented in Appendix A.1.

3.1.8 Data processing with Phyton

The 78 PW releases conducted in the wave basin was processed with a Phyton script in Jupyter Notebook. In Jupyter Notebook, the code was put into eight separate cells to make each step in the process easier to use. The releases were originally saved as a video-format, and each processed separately. Release experiment 11c is further used to better describe the data processing. The first cell was used to import the fundamental packages for computing with Phyton. Experiment 11c was uploaded into Jupyter in the second cell and was manually given its experiment ID and date. Further, cell three iterated through the video for experiment 11c and made still-photos for every 30 seconds. The multiple still-photos were saved to the computer and a list of the completed photos were made available in cell four. The photo with a representative plume for experiment 11c was manually chosen for further processing and is shown in Figure 8.

Figure 8. Photo of experiment 11c with a representative stable plume chosen for further processing.

The wanted photo of experiment 11c was uploaded from the computer into Jupyter in cell five and the yellow color channel was shown, as seen in Figure 9. Further, in the same cell step, the picture was cut so it included the needed section of the photo.

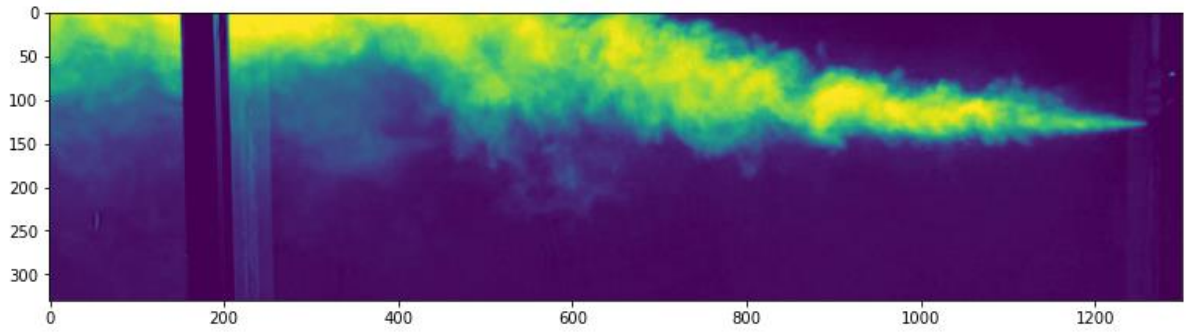

Figure 9. Photo of experiment 11c where the yellow channel is shown. This photo is also cut so it includes the needed section of the yellow plume.

The code in cell six iterated through the vertical lines in the experiment 11c photo (Figure 9) to calculate the argmax. Argmax is the y-position to the pixel with the highest intensity on each vertical line. Further, cell seven interpolated through all the argmax values by using a third-degree polynomial. Last, cell eight plotted the argmax values on top of the photo, shown as the red dots in Figure 10. The relative plume depth was also calculated in this step, which is the nozzle height subtracted from the average of the three values given by the intersection between the vertical lines and the polynomial. The nozzle heigh, which is given by the horizontal dotted line, was manually controlled in the last step. The final product is shown in

Figure 10 below and gives information about experiment ID, date, rate, relative nozzle height and relative plume depth. The relative plume depth was extrapolated to a 100 cm scale (the depth of the basin) and further used to present the behavior of each PW plume. The plume depth, as seen in Figure 10, was presented with a negative value for rising plumes and a positive value for sinking plumes relative to its nozzle height. When the values were used to present the data, the sign was swapped, giving the sinking plumes a negative value and the rising ones a positive value.

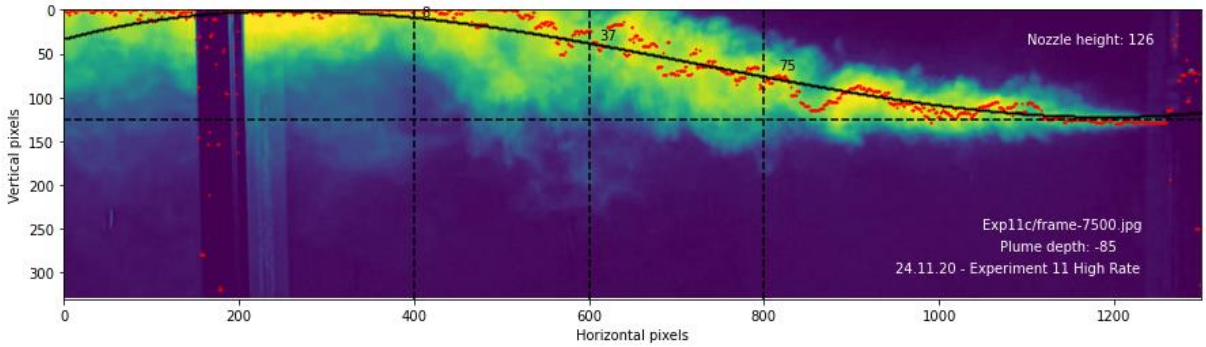

Figure 10. The final result after processing the video of experiment 11c with a Phyton script. The figure gives information about experiment ID, date, rate, nozzle height and plume depth.

3.2 Simulation in OSCAR

The OSCAR model was used in this project to simulate the discharge conditions at the Norne platform. Data was provided by Equinor for the period 01.12.20-28.02.21 and had detection of oil on the surface by SAR satellite on eleven of these days. The data for the period 13.01.21-18.01.21 was used further in this project and had detection of oil on five out of six days. The mean discharge rate for the chosen period was 20,011 m^3day^{-1} and a rate of 20,000 m^3day^{-1} was therefore used in the simulations. The simulations were conducted over a period of 8 days (12.01.21 including 19.01.21) since discharges from the previous day might surface later. Table 3 presents an overview of the conditions at the Norne platform that was used in the OSCAR simulation. There was in total done five simulations with different size on the oil droplets in the PW discharge. Table 4 show the mean volume droplet size used during the different simulations. Simulation 3 and 5 had the same mean volume droplet size, but the temperature was 63 °C and 68 °C, respectively. Each simulation generated an output file which contained extra information about the PW release (oil sheen surface area, wind direction, etc.). Due to time-limitations, the output files were not included in this project. For this project, it was chosen to focus on when the PW plume rose to the surface and made visible signatures of oil sheens for possible SAR detection.

Table 3. Release conditions at the Norne platform provided by Equinor and used in the PW discharge simulation in OSCAR.

Longitude	8.42648°N
Latitude	66.04935°E
Duration	8 days (12.01.21-19.01.21)
Depth	12 m
Rate	20,000 m^3day^{-1}
Salinity	48 psu
Temperature	63 °C and 68 °C
Diameter	0.4826 m
Angle	Horizontal
Direction of release	North
Liquid/ Solid particles	30,000
Mass fraction of oil	20 ppm
Oil type	Norne oil 2017

Table 4. Overview of the used droplet size in the OSCAR simulations.

	Mean volume droplet size (d_{50}, µm)
Simulation 1	20
Simulation 2	40
Simulation 3 & 5	60
Simulation 4	100

These five simulations were conducted in OSCAR to look at how tides, winds, currents, oil droplet size and temperature influence the plume once let out into the ocean. Data for currents, salinity, sea temperature and wind for the Norne area was provided by SINTEF for the simulation period. It was noted at what time the plume rose to the sea surface from the simulations and formed oil sheens on the surface. The collected data is presented in the Result and discussion chapter.

4. Results and discussion

The following section is divided into the experiments conducted in the wave basin and the simulations in OSCAR. There was conducted 78 PW releases in the wave basin and 5 simulations in OSCAR. The collected data was processed in SPSS and the section below is used to present and discuss the work from this project.

4.1 Wave basin experiments

4.1.1 Plume behavior with a downward release angle

Figure 11 show three PW releases all conducted with the same angle at 45° down, high temperature and medium velocity. Experiment 8b, 7b and 9b is shown from top to bottom, respectively. Experiment 8b was conducted with a salinity of 35 psu, 7b with a salinity of 48 psu and 9b with a salinity of 60 psu.

As mentioned in the Theoretical background, water density is influenced by both salinity and temperature [53, 54]. The PW in experiment 8b had a salinity of 35 psu and an outlet temperature of 56 °C and was released into cooler seawater at 8 °C. The temperature seemed to dominate the plume behavior in experiment 8b, and the plume had a density of 1.0111 kg/L compared to the seawater in the wave basin with a density of 1.0272 kg/L. The plume sank to a trapping depth of -26 cm and had an upward trend on the left side, moving towards the surface. The initial sinking of the 8b plume could be due to the influence of the release angle. Since the plume was released downwards with a velocity of 0.99 m/s, this force gave the plume momentum in that direction. The other conditions, like its density, seemed to not affect its behavior until that momentum was partly gone.

Experiment 7b had a salinity of 48 psu and an outlet temperature of 58 °C. With a higher temperature and a higher salinity compared to the seawater, the plume showed a sinking trend and stabilized at a trapping depth of -76 cm. With higher amounts of salts in the PW, making it denser, the increase in salinity took part in why the plume sank. It had a density of 1.0197 kg/L. This release was also affected by the downward release angle with a velocity of 0.99 m/s. Since release 7b had a high outlet temperature, making it less dense, that could have been

the reason why the plume was trapped mid depth and did not sink all the way to the bottom of the basin.

Last, experiment 9b had the highest salinity of 60 psu and an outlet temperature of 55 °C. This plume shows a sinking trend in Figure 11 and was greatly affected by the high salinity, giving the plume a density of 1.0301 kg/L. The high temperature did not seem to have had any effect on the plume behavior and was overridden by the high salinity and downward momentum. As with the other two releases (8b and 7b), this release also had a downward release angle with a velocity of 1.03 m/s.

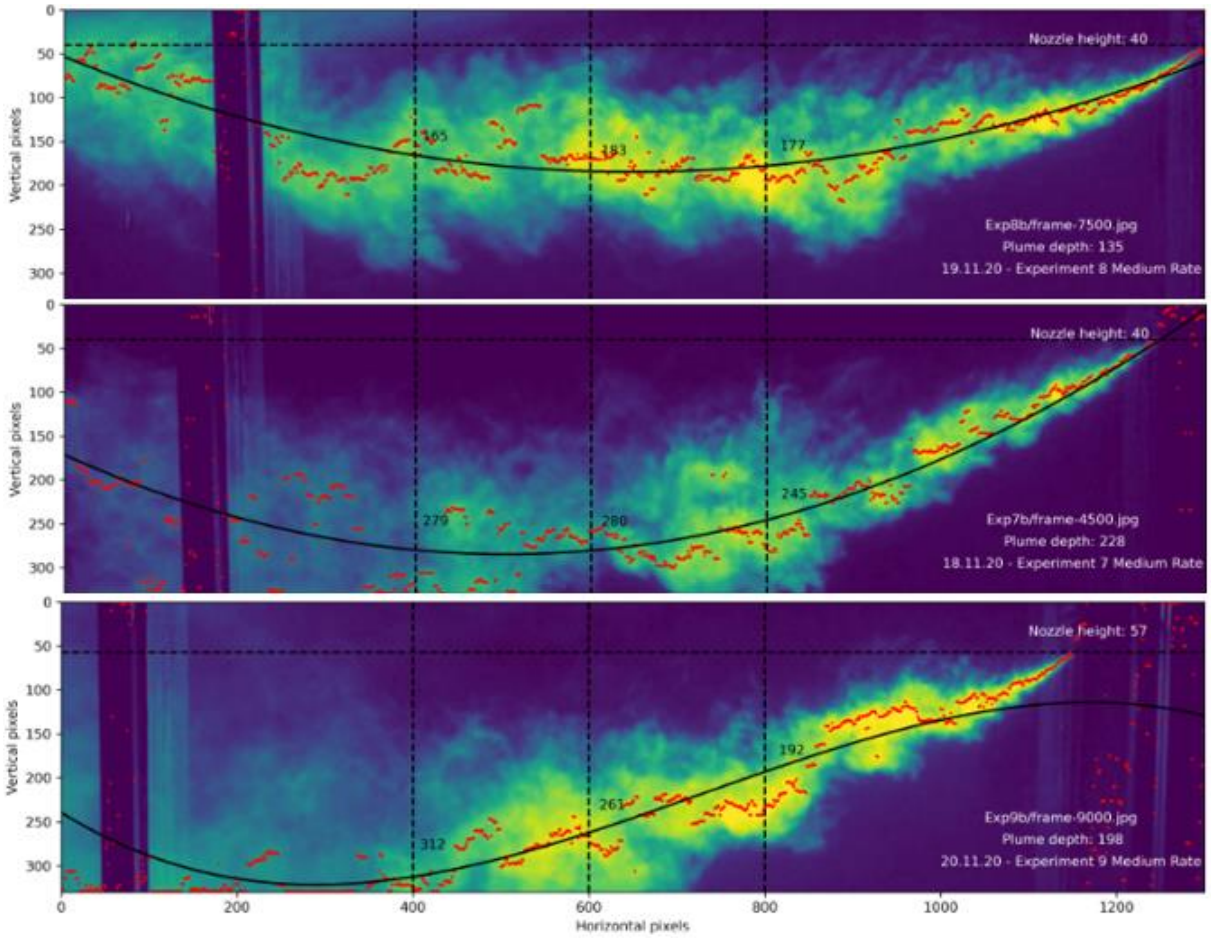

Figure 11. Example of three PW releases conducted in the wave basin. The shown releases were all conducted with the same angle (45° down), the same medium velocity and with a high temperature. The upper plume in the figure is conducted with a low salinity (35 psu), the middle plume with a medium salinity (48 psu) and the plume at the bottom with a high salinity (60 psu).

The plume trapping depth was -26, -76 and -62 cm for experiments 8b, 7b and 9b, respectively. The method that was used to quantify the trapping depth of the plume had its disadvantages. It could be reasonable to think that experiment 9b should have had a deeper plume trapping depth compared to 7b since it was denser. In this case, as seen in Figure 11, experiment 7b had the deepest plume trapping depth. The example shown in Figure 11 is unfortunate and shows a weakness in the chosen way to process the data. Experiment 9b most likely would have sank closer to the bottom of the basin giving it a deeper trapping depth compared to experiment 7b, but that was not taken into account at the time.

4.1.2 Plume behavior with a horizontal release angle

In Figure 12 on the next page, three PW release plumes are presented with a horizontal outlet angle. Figure 12 include, from top to bottom, experiment 17b, 16b and 18b, respectively. These experiments were all conducted with the same high temperature and medium outlet velocity. Experiment 17b has a low salinity, 16b a medium salinity and 18b a high salinity.

For experiment 17b, it had a salinity of 35 psu and an outlet temperature of 61 °C. This plume had a distinct behavior and rose immediately to the surface. It was released with a velocity of 1.01 m/s and had a low density of 1.0086 kg/L compared to the seawater with a density at 1.0272 kg/L. The plume behavior was affected by the temperature since the salinity was the same for the PW and the seawater. This release was also not affected by the outlet angle in the same way as those with a downward release angle, which made the density parameter to show instant affect.

Experiment 16b was released with a salinity of 48 psu and had a temperature of 60 °C. The plume sank to a trapping depth of -23 cm and had a density of 1.0160 kg/L. It was released with a velocity of 0.98 m/s and as seen in Figure 11 the overall trend for the plume was that it was slightly sinking. The plume had a lower density compared to the seawater and was given no momentum in the vertical direction.

For the last experiment in Figure 12, 18b, PW was released with a salinity of 60 psu and an outlet temperature of 54 °C. This plume had a sinking trend and sank deeper faster as compared to 16b. The release had a plume trapping depth of -74 cm and a density of 1.0306 kg/L. It was released with a velocity of 1.01 m/s. Even though the release had a higher temperature than the seawater, the high salt content affecting the density seems to have influenced the plume.

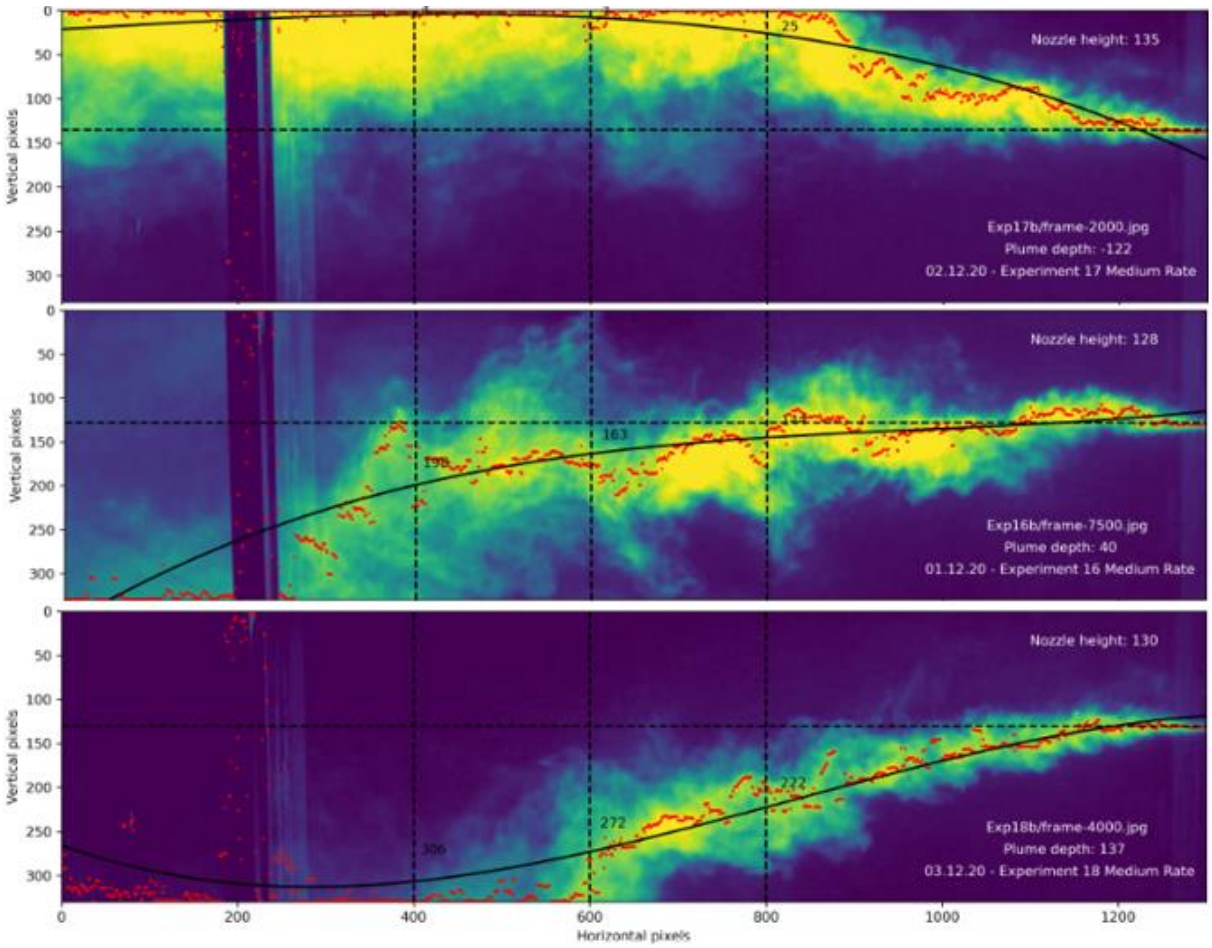

Figure 12. Example of three PW releases conducted in the wave basin. The shown releases were all conducted with the same horizontal angle, the same medium velocity and with a high temperature. The upper plume in the figure is conducted with a low salinity (35 psu), the middle plume with a medium salinity (48 psu) and the plume at the bottom with a high salinity (60 psu).

For experiment 18b, the plume had a downward trend somewhat exceeding the section shown in Figure 12, where the plume left halfway into the photo. More of the photo could have been included so that the plume behavior better could have been seen. Even though the plume trapping depth for experiment 18b might not be fully correct, the trend seen between the three releases is more fortunate in Figure 12 compared to the trend seen in Figure 11. The plume trapping depth was 24, -23 and -74 respectively for experiment 17b, 16b and 18b. These

results and the observed plume behavior were expected and show that the denser the PW, the deeper it sinks. It was also seen from Figure 11 and Figure 12 that releases with the same salinity as seawater rose to the surface. This was seen instantly for experiment 17b as it rose to the surface and later in the photo for experiment 8b which seemed to be instantly more influenced by the momentum from its release angle than its density. After the momentum had gradually disappeared, the density seemed to have had the largest effect on the plume behavior.

As a summary for Figure 11 and Figure 12, the key message is that the temperature and salinity of the PW influence the plume behavior. In cases were the PW and the seawater had the same salinity, the temperature had a higher influence on the PW plume compared to the cases were the PW had a higher salinity than the seawater. When the salinity was higher, the general behavior seen was a sinking plume due to the increased salt concentration in the PW. The three experiments shown in each figure are released with the same conditions from top to bottom, when it comes to temperature, salinity and velocity. Meaning that experiment 8b and 17b, 7b and 16b, and last 9b and 18b were released with the same conditions. The only difference was the angle. When comparing the two release angles, it gives indications that the plumes sank deeper with a downward release angle. This could be due to the momentum from the angle itself and is seen in the figures as the less dense PW (8b) stayed longer in the water column before it rose towards the surface as compared to 17b.

The method used to quantify the plume depth might not be the most descriptive for each plume. Experiment 9b sank over the course of the three vertical lines and gives 9b a less deep plume trapping depth. On the other hand, experiment 7b stabilized quicker in the basin, and its plume trapping depth quantified through this method seem to be descriptive enough for where it actually was trapped in the basin.

4.1.3 Experiments with a downward release angle

The experiments conducted with a 45° downward angle are shown in Figure 13. The colors of the dots represent the velocity of the release and the grey line represent the depth of the outlet opening in the 100 cm deep basin. An overview of the release parameters (temperature,

salinity, density, velocity, etc.) is available in Table A. 1 which is presented in Appendix. A.1. The data in Figure 13 show that the majority of the releases sank towards the bottom of the wave basin. Eight releases occurred as a stable plume between 0 and -45 cm and none of these releases rose to the surface neither higher than the nozzle outlet depth. The releases conducted seemed to have gotten a momentum from the release angle which influenced the plumes to sink towards or to the bottom of the basin. Furthermore, the trend in Figure 13 roughly show that the denser the release, the deeper it sinks.

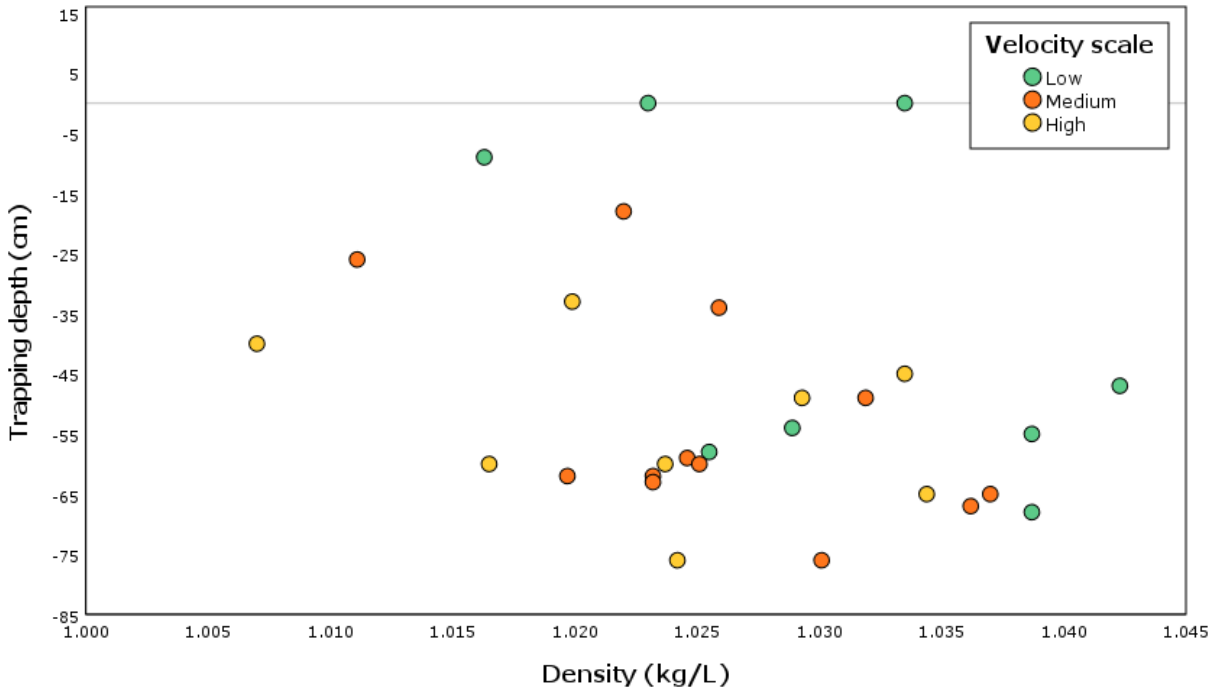

Figure 13. Trapping depth versus density of the produced water release. The release angle for these experiments were 45° down and the color of the circular dots represents the velocity of the PW release. The grey vertical line represents the depth of the release outlet in the 100 cm deep basin.

Unfortunately, experiment 2 was not included in the results and is not found in Figure 13, as the videorecording for those three releases contained an error. As a result, they could not be processed in Phyton and was therefore not included. 2a, 2b and 2c had a low salinity and a medium temperature, with a low, medium and high velocity, respectively.

4.1.4 Experiments with a horizontal release angle

The results conducted for the experiments with a horizontal outlet angle are shown in Figure 14. From these experiments, the releases had a varying plume trapping depth. The density of the plume seemed to be the most dominating factor for the horizontal outlet releases. There is a clear trend that the denser the release, the deeper it sank. For these experiments, the outlet angle did not give the plume a momentum in any vertical direction, which indicate that the density was the actual reason for this behavior. Nine releases with a low density rose to or close to the surface. The rest of the releases sank and had a plume trapping depth below the nozzle outlet.

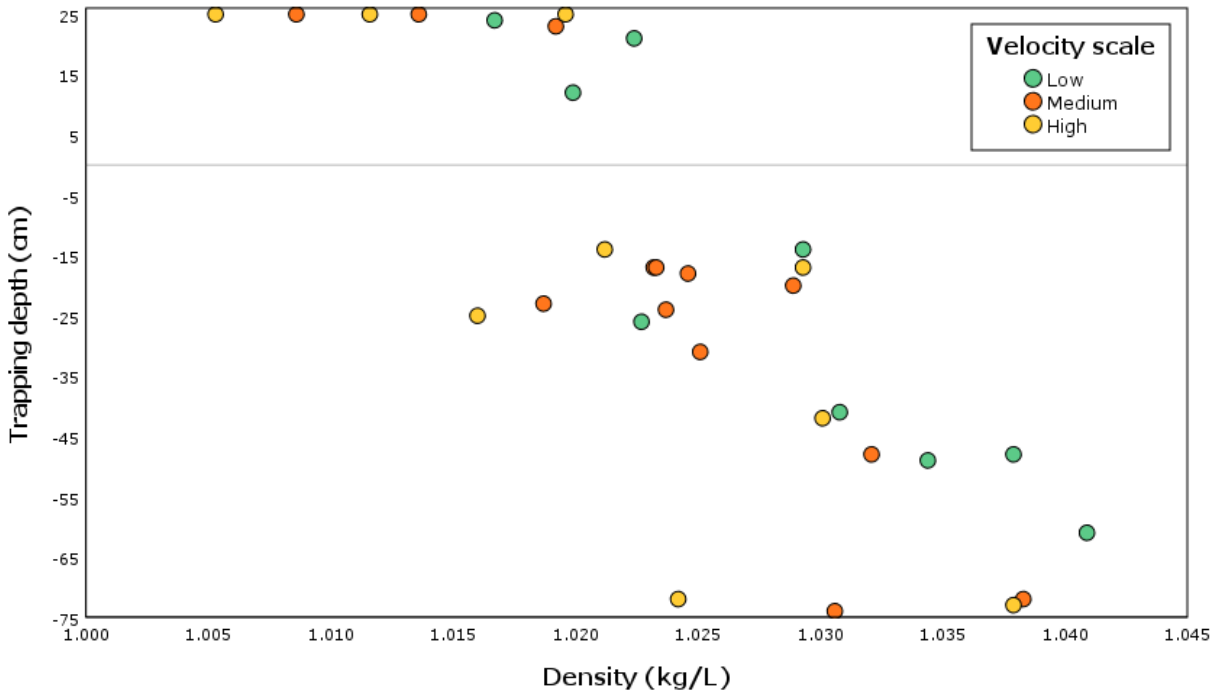

Figure 14. Trapping depth versus density of the produced water release. The release angle for these experiments were horizontal and the color of the circular dots represents the velocity of the PW release. The grey vertical line represents the depth of the release outlet in the 100 cm deep basin.

4.1.5 Experiments with gas in the PW release

Seven releases were conducted with a gas (air) flow in the discharge and the same medium temperature was used for all releases. The seven releases also had a horizontal outlet angle, the same salinity of 48 psu and is presented in Figure 15. The amount of gas used was calculated from the PW flow and was an additional percent included in the release. The colors of the dots represent the percentage of gas flow, and the size of the dots represent the velocity

of the release. All seven releases rose to or towards the surface in the basin except the one release conducted with a low velocity. This single release made a stable plume at the same depth as the nozzle outlet, while the remaining six releases had a plume trapping depth between 7 cm and the surface.

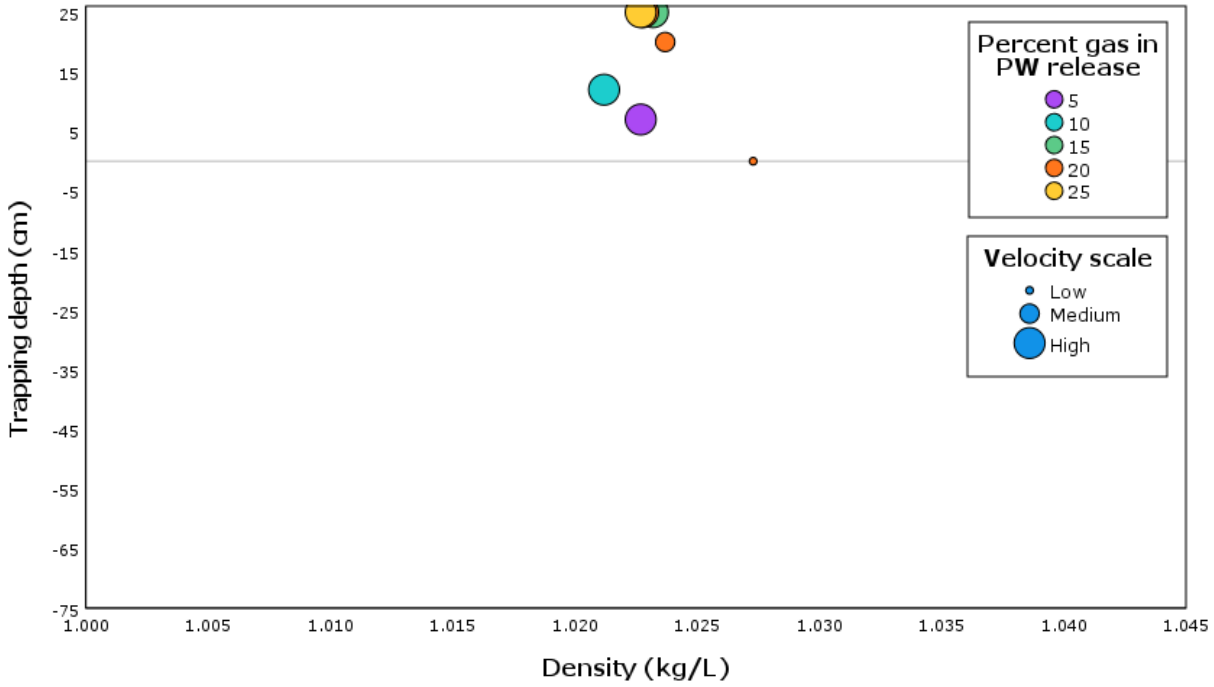

Figure 15. Trapping depth versus density of the produced water release. The release angle for these experiments were horizontal. The color in the circular dots represent the percentage of gas flow in the PW release which was calculated from the PW rate. The size of the circular dots represents the velocity of the PW release. The experiments with gas were all conducted with the same medium temperature and the same medium salinity.

Experiment 21b and 21c is shown as an orange dot in Figure 15, with a medium and high velocity and a plume depth of 20 and 25 cm, respectively. These were released with the conditions as described in the paragraph above and had a 20 % gas flow in the release. When comparing release 21b and 21c to experiment 10b and 10c, which was both released with a horizontal angle, with a salinity of 48 psu and with a medium temperature, a difference is seen. These two releases had a medium and high outlet velocity, sank to a depth of -31 and -14 cm, respectively, but was without any gas flow. This indicates that the gas bubbles had a lifting effect on the PW plume. This behavior was suggested in a study by Brandvik et al. [1] and suggests that if the gas in a PW release is sufficient, the buoyancy from the released gas could bring the plume towards or to the water surface. The rising of the plume seemed to correspond along with the increasing percentage of gas flow in the release. The purple dot,

experiment 22a with a 5 % gas flow, did not lift the plume as high as compared to the other releases that was released with an increased gas flow.

4.1.6 Experiments with oil in the PW release

The mean volume droplet size distribution was approximately 20 µm for the first 9 releases. The last three days in the lab was used to conduct PW releases containing oil droplets. A total of ten releases were conducted and is shown in Figure 16. These ten releases had the same medium temperature and the same salinity of 48 psu. The color of the dots in Figure 16 represent either only small oil droplets (d_{50} 20 µm) or small and large oil droplets (d_{50} 20 µm and d_{50} 100 µm), while the size of the dots represents the velocity. In the following Figure 17, seven experiments released with the same conditions as for the releases with oil droplets are shown. These experiments are taken from the horizontal release experiments conducted without the adding of oil droplets and is shown in Figure 17 for comparison. The dots in this figure represents the velocity of the release.

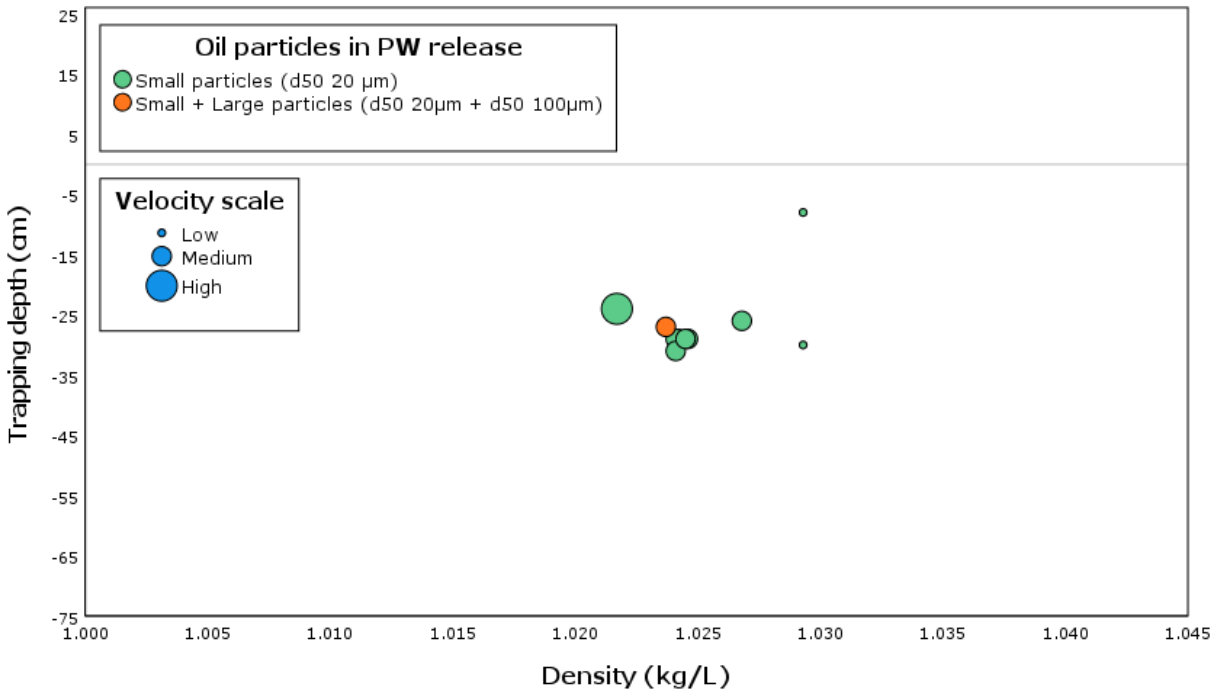

Figure 16. Trapping depth versus density of the produced water release. The release angle for these experiments were horizontal. The color in the circular dots represent the oil particles in the PW release (small oil particles/droplets, or small and large particles/droplets). The size of the circular dots represents the velocity of the PW release. The experiments with oil were all conducted with the same medium temperature and salinity on the PW.

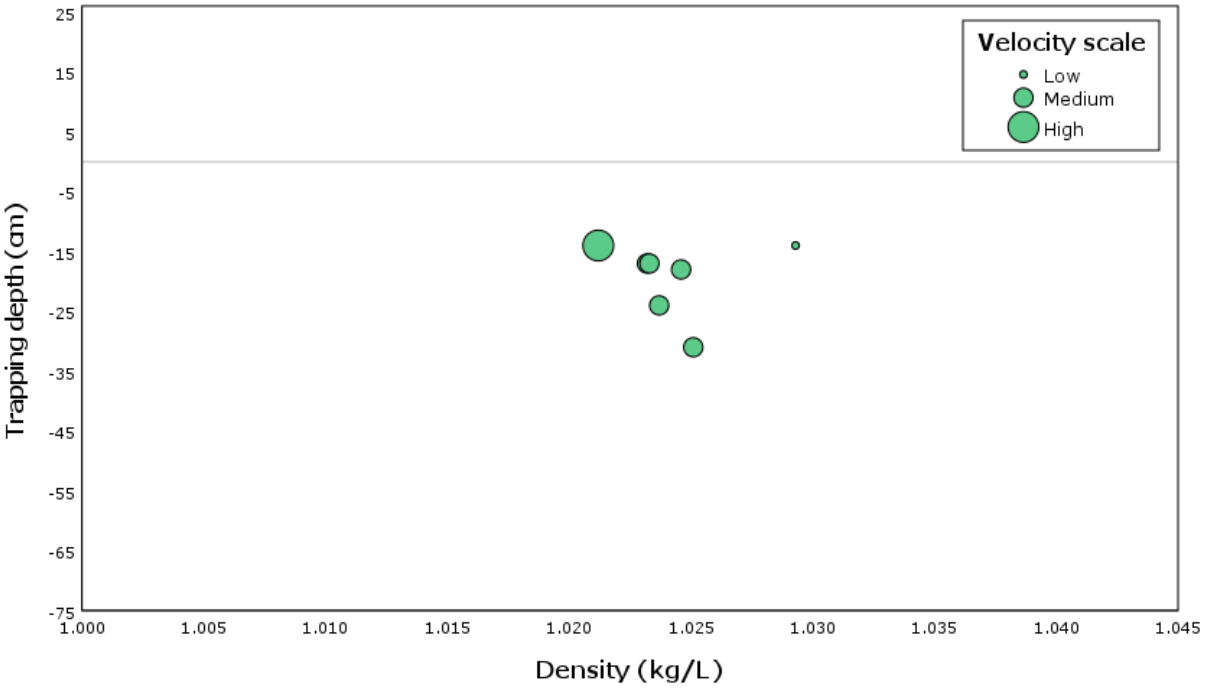

Figure 17. Trapping depth versus density of the produced water release. The release angle for these experiments were horizontal. The color in the circular dots represents the velocity of the PW release. The experiments were all conducted with the same medium temperature and the same salinity on the PW.

Based on the conducted data, the oil droplets do not seem to have an effect on the plume behavior. What would have been of interest was if the oil droplets made the plume rise or sink, but this was not seen. There was no evident difference between the plume depth when comparing the release with small and large oil droplets to the releases only containing small droplets. All the releases seemed to cluster in the same depth of -24 to -31 cm, except for one release found at a depth of -8 cm.

Also, when comparing experiments with and without added oil droplets, no variations were seen. The plume depth for the releases conducted without any added oil seem to have a plume depth higher up in the basin, and the average depth for the seven releases was 19.2 cm. The ten releases with added oil droplets had a mean depth of 26.2 cm. This mean variation can origin from uncertainties in the experiment, but do not indicate that there is a difference in the plume trapping depth of releases conducted with or without oil droplets.

4.1.7 Uncertainties from the wave basin experiment

One weakness in the experiments could be explained by how the velocity influenced the measured outlet temperature. The temperature measurement point at the nozzle outlet was not isolated and was also influenced by cooler water in the wave basin. This affected the temperatures and gave higher velocities an increased outlet temperature and is a systematic trend throughout the collected data. The varying measured outlet temperatures are shown in Table 3 for three example experiments.

Table 3. Overview of experiment 11, 14 and 17 joined by its respective measured outlet temperature.

Experiment ID (#)	**Measured outlet temperature (°C)**	**Wanted outlet temperature (°C)**
11a	36	52
11b	51	52
11c	55	52
14a	29	30
14b	38	30
14c	37	30
17a	44	70
17b	61	70
17c	67	70

Additionally, the pump that was used for the PW release experiments was operated in the lower region of its capacity. The rate that was used ranged between 0.45-1.05 L/min and it was irregularly seen that the pump delivered a fluctuating rate. This adds some uncertainty to the results and the measured velocities and rates.

4.2 Simulation in OSCAR

The work in the OSCAR model will be presented in the coming section followed by one example comparing a SAR image with an image of an oil sheen formation from the simulation. There was conducted five simulations in OSCAR based on the period 13.01.21-18.01.21 where Equinor had five actual detections by SAR satellite in the area of the Norne platform. Data and images for the five detections are available in Appendix A.6 and A.7.

4.2.1 Simulation 1

The mean volume droplet size for the first simulation was 20 µm, and the PW had an outlet temperature at 63 °C and a salinity of 48 psu. There were no surfacing plumes during the simulation in the given period that caused formation of sheens on the sea surface. No sheens were observed in the vicinity of the platform, and in the surrounding sea, no oil droplets surfaced at a later point to the extent for sheens to be formed.

4.2.2 Simulation 2

For the second simulation, when the mean volume droplet size was increased to 40 µm, there was no surfacing PW plume in the given period that resulted in the formation of oil sheens on the sea surface. This simulation also had an outlet temperature at 63 °C and a salinity of 48 psu for the PW. In the surrounding sea, outside a 1 km radius from the platform, single oil sheens were observed irregularly. The observed sheens were 0.01 mm thick, was small in size and too scattered on the sea surface for possible detection by SAR satellite and was therefore not included as a result. An example of the sheens observed in the second simulation is presented in Figure 18, which is an image from OSCAR. The sheens are seen as white squares on the left side in the figure and is surrounded by the light blue ocean. The OSCAR simulation creates still-images for every hour, and Figure 18 is an image from 13.01.21 at 14:00.

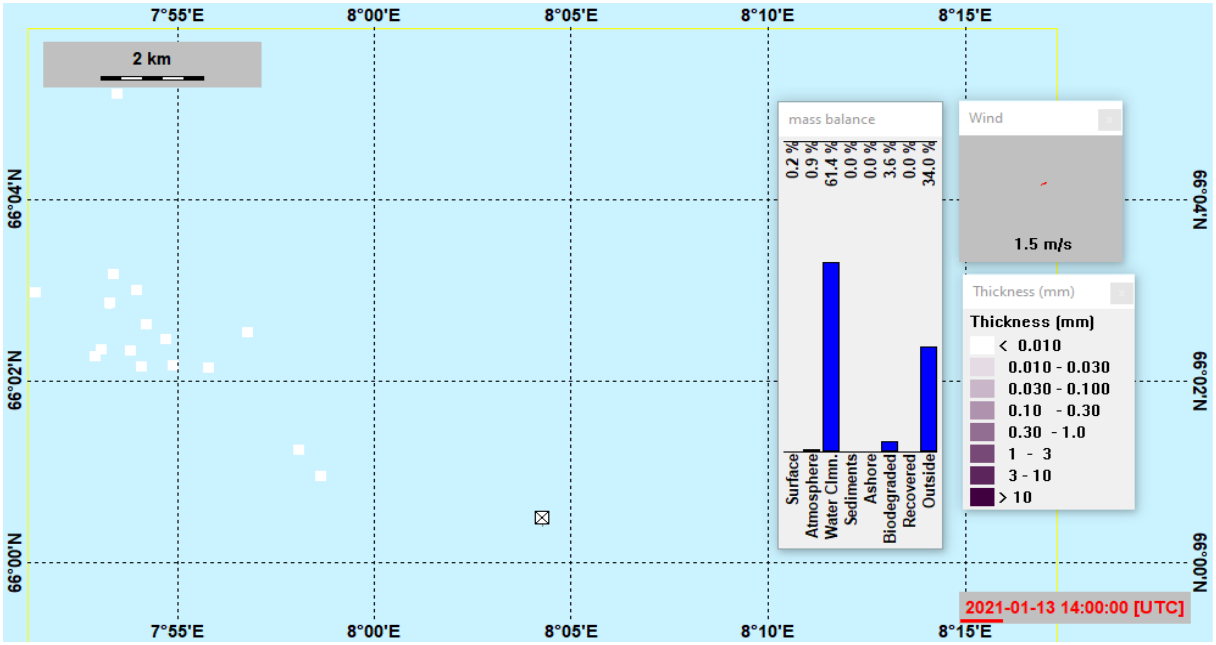

Figure 18. Image from the OSCAR simulation that show some single oil sheens shown as white squares on the left side with a mean volume droplet size of 40 µm. These sheens were seen on the 13th of January 2021 at 14:00. Each sheen cover a small area and they are too scattered from each other for possible detection by SAR satellite. The square with an "X" inside marks the release site (the Norne platform) and the sheens are located more than 2 km away from the platform.

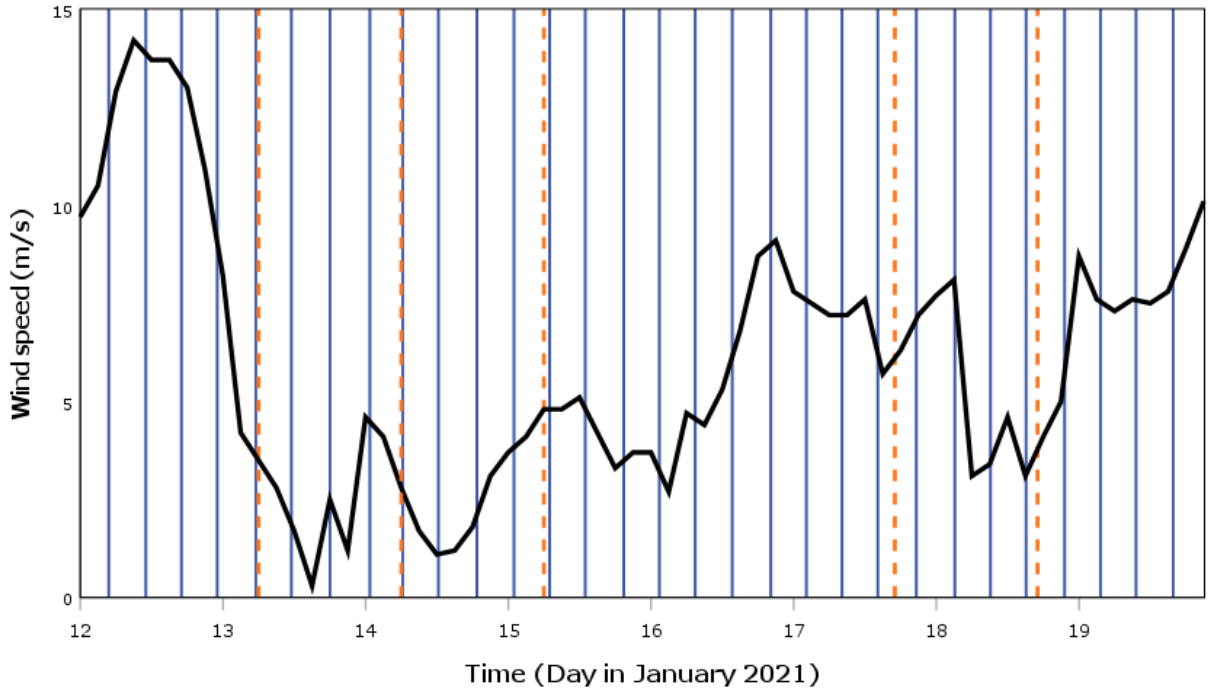

Figure 19. Wind speed from the Norwegian Metrological Institute at the Norne platform in the simulation period January 12th to 19th 2021. The wind speed is a mean value of every three hours. Vertical orange dotted lines represents the detection of surface oil slick by SAR satellite and vertical blue lines represent the regularly turning tide. No surfacing plume with formation of oil sheens was seen in OSCAR when the mean volume droplet size was 20 or 40 µm, and no vertical line is therefore seen in the figure representing the results from the first and second simulation. The two simulations had a PW temperature at 63 °C.

Figure 19 presents the five detections of oil sheens by SAR satellite for the period 13.01.21-18.01.21 and each detection is represented with a vertical orange dotted line in the figure. The black line represents the wind speed for the period 12.01.21-19.01.21 at the Norne platform. The wind speed data is from the Norwegian Metrological Institute and is an average wind speed for every three hours. The regularly shifting tide is also included in Figure 19 and is continuously represented with a vertical blue line. The tide data is available in Appendix A.4. Even with some single sheens seen in the second simulation, the same result was achieved for both simulation 1 and 2. Since no sheens were considered large enough for possible SAR detection, no vertical lines are shown in Figure 19 to represent the oil sheens from the simulation. The wind speed seen in Figure 19 was above 10 m/s on the first day, 12.01.21, which was one of the days were no oil sheens were detected by SAR satellite. This also occurred on 16.01.21 and 19.01.21 where no oil sheens were detected. The wind was about 4 m/s in the morning on January 16th, but rose to a wind speed of about 9 m/s. On January 19th, the wind stayed between 8-10 m/s. High wind speeds can create breaking waves and more turbulence in the upper water column in the ocean. The detectability by SAR satellite is also lower when the waves are high or breaking, as the radar signals might scatter. The first three detections by SAR satellite happened near the time when the tide was turning, and the currents in the ocean are lower. The fourth and fifth detection of oil on the sea surface by SAR happened in between the turning of the tide. The SAR satellite orbits the earth, so continuous surveillance in the same area is therefore not possible. The sheens that are detected are present on the sea surface as the satellite passes. The images the SAR sensor provide presents only the current situation and do not tell much about the period prior or after the sheen was detected.

As seen in Figure 2 in the Theoretical background chapter, the wind speed is on average higher during the winter in the period from September to April. The detections by SAR satellite took place in January, in a period where it is usually less detections because of higher wind speeds. A general higher wind and sea state during the winter could lead to turbulence in the upper sea column and high waves. The combination of turbulence and breaking waves is known to break up oil sheens which spreads out the oil particles in the water column. It was unusual to experience five detections in the period since the weather usually avoid sheens from surfacing and forming in this period. In a discussion with Equinor it was noted that more detections happened during summer.

From simulation 1 and 2, with a small mean volume droplet size at 20 and 40 µm, there was observed little to no oil sheens on the sea surface in the vicinity of the platform and in the surrounding sea. The small droplets are prone to the natural weathering processes happening in the ocean, especially dilution in the water column. They are also prone to be trapped in the PW plume or in the currents as their own terminal velocities for rising upwards are lower than for the PW and currents. The small droplets also contain a small volume, and several droplets is needed for a sheen to form. Conditions like wind, waves, current and tide all affect the presence of oil sheens on the sea surface. These mentioned conditions would also have to be very low for sheen formation.

4.2.3 Simulation 3

For the third simulation, the mean volume droplet size was set to 60 µm. The outlet temperature was 63 °C and the salinity 48 psu. It was observed four cases where the plume rose to the sea surface and had formation of oil sheens on the sea surface in this simulation. At what time these observations were made in OSCAR is shown in Figure 20 as vertical green dotted lines. In the same figure, the regularly tide is presented as vertical blue lines and the oil sheens detected by SAR satellite with vertical orange dotted lines. The number of single sheens seen in the surrounding area of the platform in this simulation had increased compared to simulation 1 and 2.

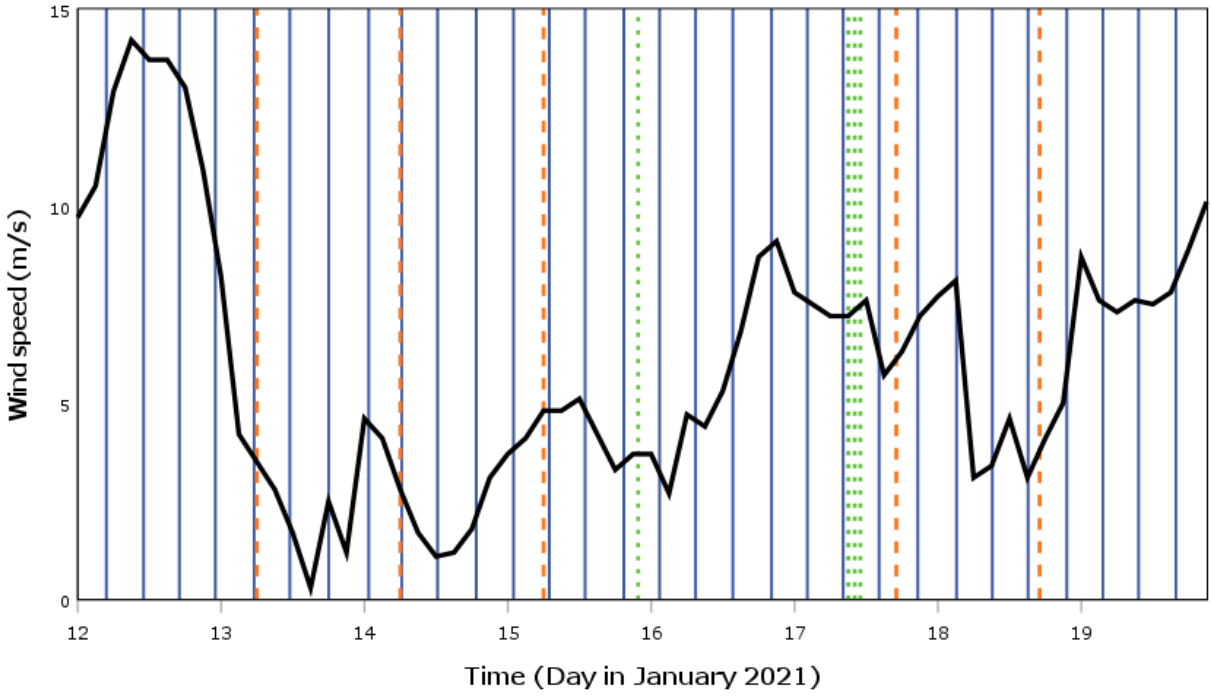

Figure 20. Wind speed from the Norwegian Metrological Institute at the Norne platform in the simulation period from January 12th to 19th 2021. The wind speed is a mean value of every three hours. Vertical blue lines represent the regularly turning tide and vertical orange dotted lines represent detection of surface oil slick by SAR satellite. Vertical green dotted lines represent a plume that rose to the surface forming oil sheens on the surface from the OSCAR simulation. Four surfacing plumes with formation of oil sheens was seen in OSCAR when the mean volume droplet size was 60 µm and the temperature of the PW was 63 °C.

4.2.4 Simulation 4

The mean volume droplet size for the fourth simulation was set to 100 µm. The release conditions were the same as for the previous simulations, with an outlet temperature at 63 °C and a salinity of 48 psu. There was observed four rising plumes that caused formation of oil sheens on the sea surface, the same amount as for simulation 3. The observed difference was the increase in number of single sheens seen on the sea surface both in the vicinity of the platform and in the surrounding sea compared to the third simulation.

There was no gas flow added to the PW release conducted in OSCAR. No buoyancy from the gas was therefore given with the absence of gas bubbles in the release. It was of interest to see formations of sheens on the sea surface that looked like the ones detected in the SAR images.

This was not achieved in the first four simulations conducted. One additional simulation was therefore done in OSCAR with a 5 °C temperature increase.

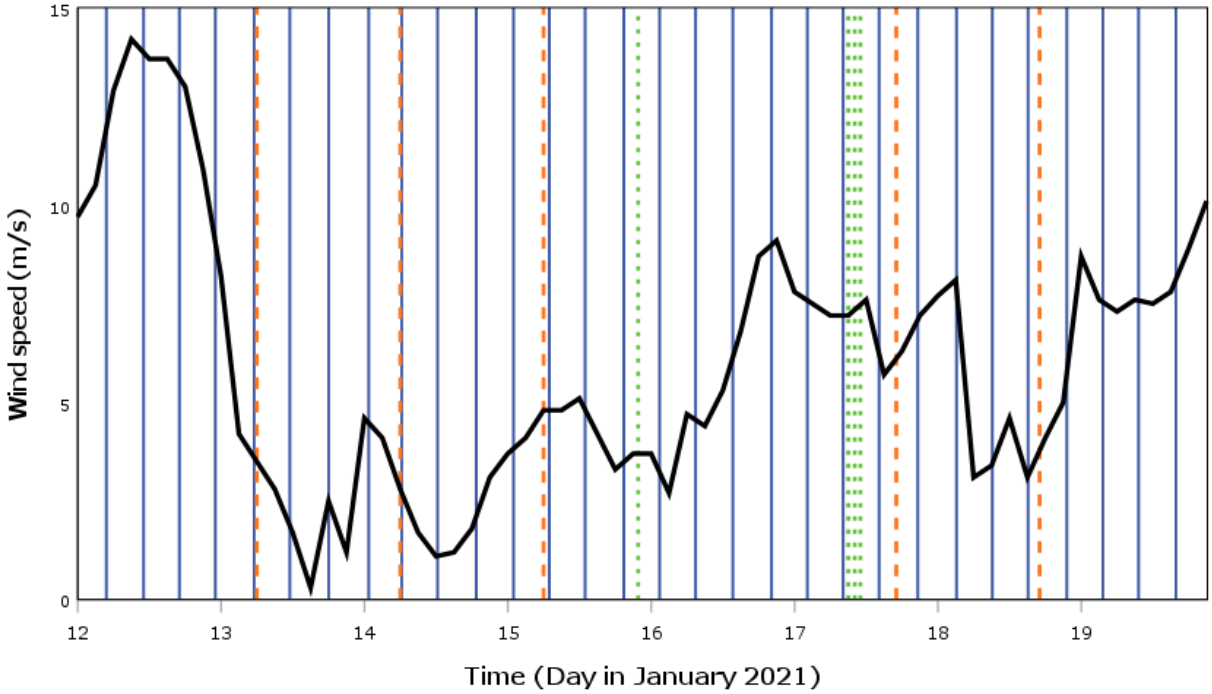

Figure 21. Wind speed from the Norwegian Metrological Institute at the Norne platform in the simulation period from January 12th to 19th 2021. The wind speed is a mean value of every three hours. Vertical blue lines represent the regularly turning tide and vertical orange dotted lines represent detection of surface oil slick by SAR satellite. Vertical green dotted lines represent a plume that rose to the surface forming oil sheens on the surface from the OSCAR simulation. Four surfacing plumes with formation of oil sheens was seen in OSCAR when the mean volume droplet size was 100 µm and the temperature of the PW was 63 °C.

4.2.5 Simulation 5

From the conducted experiments in the wave basin, it was observed that the temperature played an important role for the plume behavior in the seawater. An additional fifth simulation was therefore conducted in OSCAR with an increase in the outlet temperature to 68 °C. This was done out of interest to see if a small increase in temperature would affect the PW plume. The simulation had a mean volume droplet size of 60 µm and a salinity of 48 psu. The result from the simulation is presented in Figure 22 and had 37 cases of rising plumes that caused formation of oil sheens on the sea surface. The rising plumes with formation of oil sheens are presented as vertical green dotted lines in the figure.

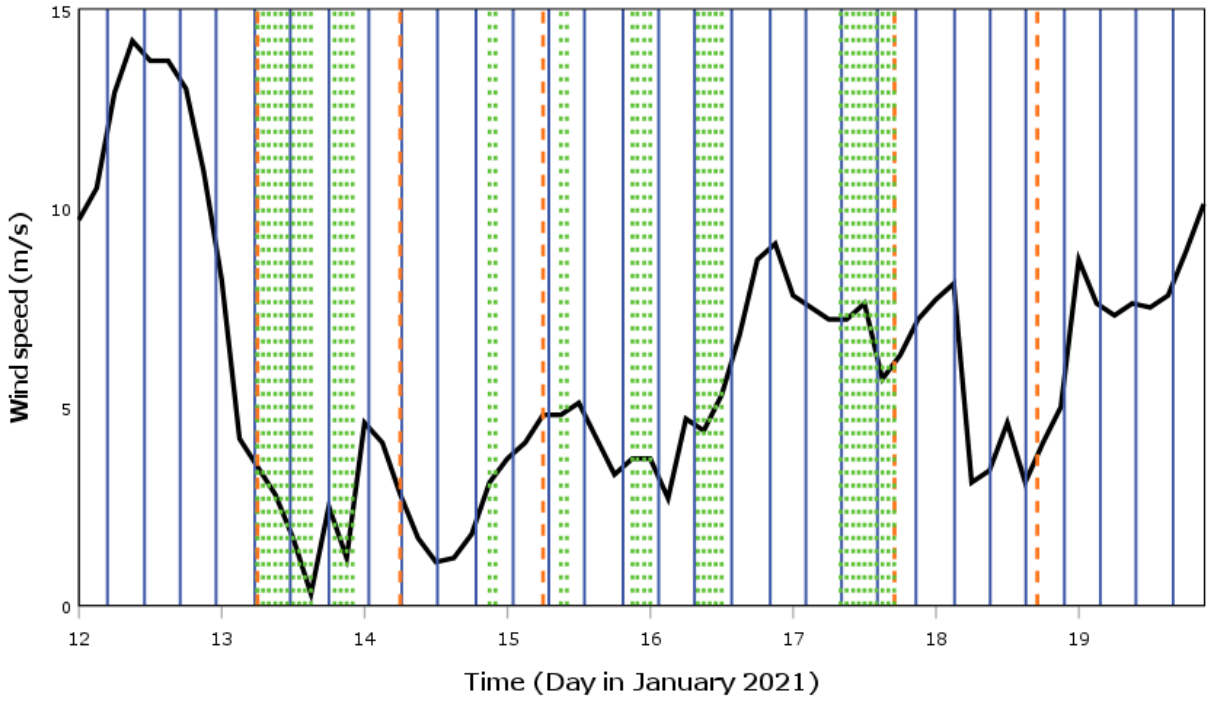

Figure 22. Wind speed from the Norwegian Metrological Institute at the Norne platform in the simulation period from January 12th to 19th 2021. The wind speed is a mean value of every three hours. Vertical blue lines represent the regularly turning tide and vertical orange dotted lines represent detection of surface oil slick by SAR satellite. Vertical green dotted lines represent a plume that rose to the surface forming oil sheens on the surface from the OSCAR simulation. 37 surfacing plumes with formation of oil sheens was seen in OSCAR when the mean volume droplet size was 60 µm and the temperature of the PW was 68 °C.

From simulation 1 and 2 in this study, the achieved results could indicate that the droplet size would have to occasionally be larger for formation of oil sheens on the sea surface that could possibly be detection by SAR satellite. As suggested in a report by Skancke, J. and Daling, P. [36] done on the Grane field, it was noted in a discussion with Equinor that one of the oil separation process steps was out of function part of the time. PW samples from the same field had a mean volume droplet size of 5 µm. The first two simulations conducted in this study had a larger mean volume droplet size but could show differences from reality as no gas flow was present in the simulated releases. When the droplet size was larger, in the range of 60-100 µm more oil sheens were frequently seen on the surface. This could indicate that the detected sheens by SAR satellite may be due to a larger droplet size in the PW release at the Norne platform.

4.2.6 SAR image compared to OSCAR simulation

In this project, the OSCAR model was used to enable comparing simulated oil slicks to SAR images. One comparison is shown in the present study and is seen in Figure 23 and Figure 24. Figure 23 is an image from OSCAR the 14.01.21 at midnight. The previous day (13.01.21) it was seen a rising plume in the simulation from 19:00 to 22:00 which resulted in the formation of oil sheens on the sea surface. At midnight, the sheens were still seen on the sea surface and is represented with white squares on the left side in the figure. The PW that was let out in the simulation had an outlet temperature at 68 °C and a salinity of 48 psu. The mean volume droplet size was 60 µm. The PW discharge was let out in a north direction in the simulation and did not change during the release. It can also be seen in Figure 23 that the wind speed at the time was 4.8 m/s, blowing in a northeast direction. The thickness of the sheens observed were 0.01 mm, but also contained a single sheen with a thickness between 0.03-0.10 mm. Further, in Figure 24, an oil sheen is seen in the SAR image outlined in black. It was detected at 06:03 in the morning and the wind speed at the time was 6.4 m/s. The inner orange circle in the figure has a radius of 700 m. The oil sheen stretches out in a northwest direction several kilometers and seems to have been drifting away from the platform. The SAR satellite sensor found that the slick covered an area of 1.36 km^2.

The two sheens seen in Figure 23 and Figure 24 are somewhat similar visually from above and stretches out in the same direction. It is known that the Norne platform rotates around a cylindrical turret, always facing the direction of the weather. This will constantly change the outlet direction of the PW discharge at Norne with a shifting weather and can therefore show some variations when compared to the simulation image where the direction of the discharge was constant let out north. This is a factor that can influence why the two sheens do not visually have the exact same shape. The sheen in Figure 23 was from the previous day, but it is possible that the sheen detected by SAR satellite was present at the sea surface a while before the satellite came by and detected it. This was only an assumption, but as mentioned earlier, the satellite is not present at all times and the image in Figure 24 only show how the condition was at that exact time and gives no indications about the situation before or after the sheen was detected.

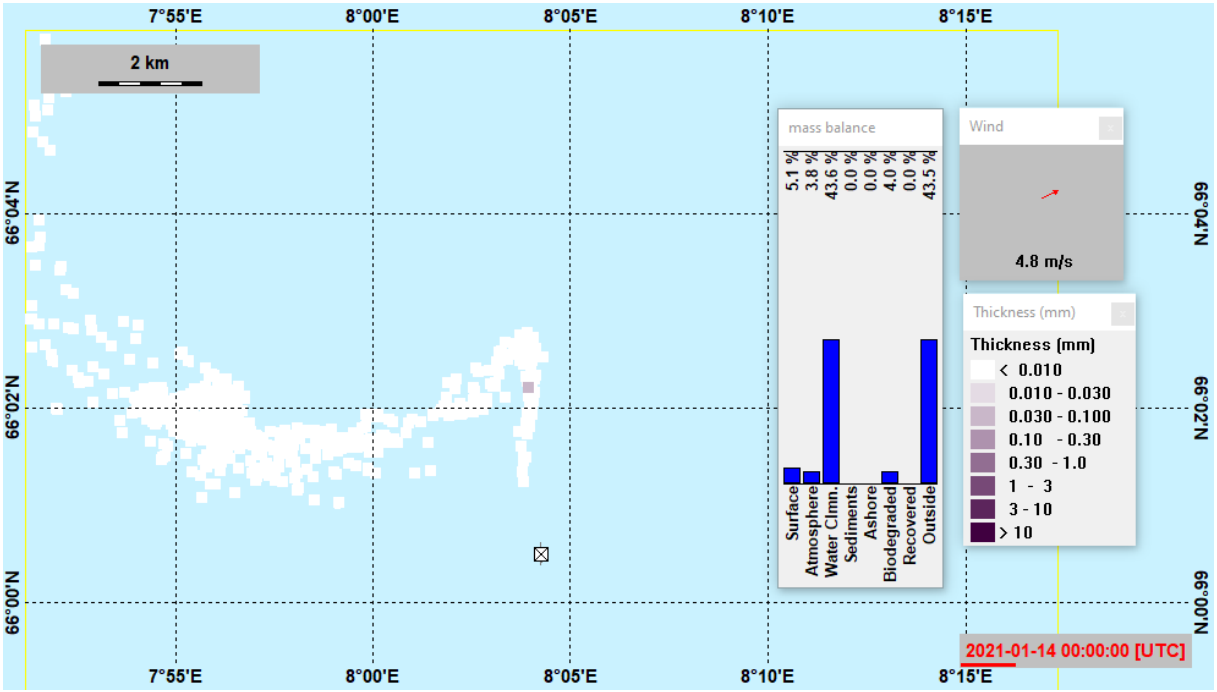

Figure 23. Image from OSCAR with visible oil sheens on the sea surface. The sheens are seen as white squares on the left side surrounded by the light blue ocean. The square with an "X" inside is the release site (the Norne platform). The simulation had an outlet temperature at 68 °C and a salinity of 48 psu. The mean volume droplet size was 60 µm for this simulation.

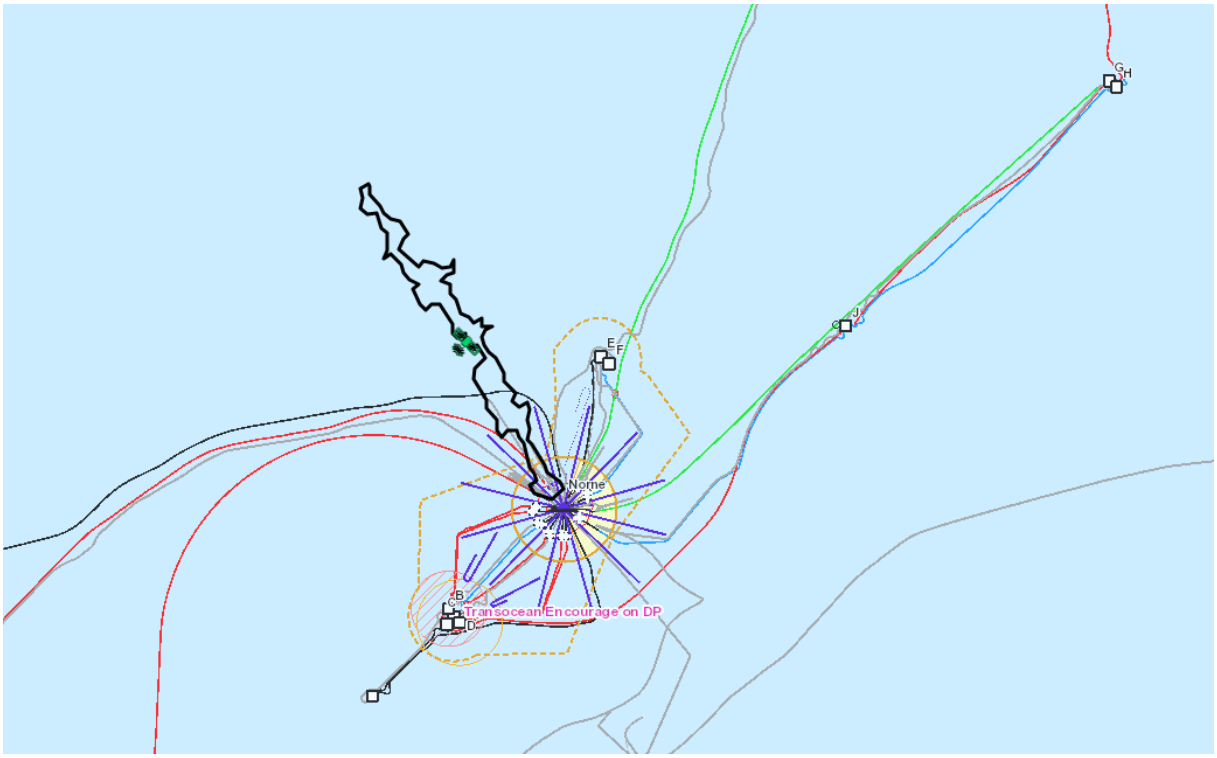

Figure 24. SAR image of the oil sheen detected 14.01.21. The oil sheen was detected 06:03 in the morning and was characterized as an oil sheen due to regular PW releases. The image is provided by Equinor.

4.2.7 Uncertainties in OSCAR

It must be mentioned that the results from the OSCAR simulations is not the only possible sequence of events. As seen in Table 4 below, the used wind data in OSCAR from the Norwegian Metrological Institute differed from the measured wind data obtained by the SAR satellite at the detection time. There was not taken any in situ measurements of the currents, winds, salinity and sea temperature at the Norne field to be used in the simulation. This could possibly give some uncertainty to the simulations.

Table 4. Comparison of wind speed detected by SAR satellite and the wind used in OSCAR at the time of satellite oil detection. The wind used in the simulation is from the Norwegian Metrological Institute (Metno). The data from Metno is rounded up or down to the nearest hour.

Date	**Time of detection**	**Wind speed (m/s)**	
		SAR satellite	**OSCAR (Metno)**
13.01.2021	06:08	3.5	3.8
14.01.2021	06:03	6.4	3.2
15.01.2021	05:54	6.1	5.0
17.01.2021	16:55	5.6	5.3
18.01.2021	16:53	No data	3.1

5. Conclusion

5.1 Wave Basin conclusion

From the conducted experiments in the wave basin, the general trend was that the denser the PW release, the deeper it sank. The angle of release played an important role and influenced how deep the plume sank. The downward angle gave the release a momentum and it was observed that more of the releases with a downward angle sank deeper compared to the releases with a horizontal outlet angle. The releases with a horizontal outlet angle were not given a momentum in the vertical direction and was much more influenced by its salinity and temperature. As an example, all the PW releases with a horizontal release angle and a salinity of 35 psu rose to or close to the surface. This behavior was not seen for the releases with a salinity of 35 psu when the outlet angle was downward, as only two releases had the same trapping depth as the nozzle outlet and the rest sank below.

Further, the inclusion of gas in the PW releases led to a rise of the plume in the wave basin. The releases conducted with gas all rose above the nozzle outlet and among these, three surfaced. It was seen that the increased amount of gas included in the release influenced the PW plume to rise higher in the basin. Additionally, the adding of oil droplets to the PW, both small and large droplets, did not seem to affect the PW release. When comparing releases conducted with the same outlet conditions, with and without oil droplets added, no change in the plume depth was seen.

5.2 OSCAR conclusion

The simulations in OSCAR were conducted with a varying mean volume droplet size in the PW release. The smallest oil droplets (mean 20-40 µm) were too small for oil sheens to form on the sea surface. This can indicate that the natural weathering processes happening when the PW was released into the ocean does not favor the formation of oil sheens on the surface when the mean volume droplet size is in the range of 20-40 µm. The currents can also play a role in why few oil sheens were seen, as the smaller droplets get caught in the currents. When the droplet size was increased to a mean of 60-100 µm, more single oil sheens were seen on the sea surface. Four cases of a plume rising to the surface was observed and caused formation of oil sheens on the sea surface. Bigger oil droplets both have a higher buoyancy

and holds a larger volume, which can be a reason for why more oil sheens were seen when the mean volume droplet size was larger. The last simulation was conducted with a 5 °C temperature increase compared to the four other simulations and resulted in higher amounts of surfacing plumes causing increased oil sheen formations on the surface in the simulation period.

The influence by temperature on the PW release was seen in both the wave basin experiments and in the simulation. It is seen from the horizontal release experiments that when there was given no momentum in the vertical direction, the density played an important role for plume behavior. It is known that temperature has a greater effect on the density of water than salinity [58]. The seen increase in oil sheen formation on the surface when comparing simulation 3 and 5 supports the fact that the temperature does influence the PW greatly.

This thesis also helps fill some of the knowledge gap regarding PW releases and its behavior once let out in the ocean.

6. Recommendations

Based on the conducted experiments in the wave basin and the simulations done in OSCAR the following recommendations are given:

1. Use of a downward release angle for PW releases from offshore installations. This can help give the PW release a momentum down into the water column and can possibly prevent the rising of the plume to the surface.
2. Attach a nozzle at the outlet opening that serves the function to minimize the oil droplet size in the PW. It is of importance to avoid the larger oil droplets in the PW for the potential formation of oil sheens. A higher outlet velocity through the nozzle can also help break up the oil droplets.
3. Use the available seawater to cool down the PW in a heat exchanger before it is released to sea. Temperature has a high influence on the plume density and its behavior. A lower temperature could possibly help decrease the amount of surfacing plumes.

Bibliography

[1] Brandvik, P. J. *et al. Detection of Surface Oil Slicks resulting from Possible Subsea Leaks*. (2020).

[2] Brekke, C. & Solberg, A. H. S. Oil spill detection by satellite remote sensing. *Remote Sens. Environ.* **95**, 1–13 (2005).

[3] Fingas, M. & Brown, C. E. Oil Spill Remote Sensing. in *Oil Spill Science and Technology: Second Edition* 305–385 (Elsevier Inc., 2017).

[4] Fingas, M. & Brown, C. E. A Review of Oil Spill Remote Sensing. *Sensors* 18 (2018).

[5] Marghany, M. Oil Spill Pollution Automatic Detection from MultiSAR Satellite Data Using Genetic Algorithm. in *Advanced Geoscience Remote Sensing* (InTech, 2014).

[6] Read, J. M. & Torrado, M. Remote Sensing. in *International Encyclopedia of Human Geography* 335–346 (Elsevier Inc., 2009).

[7] Topouzelis, K. & Singha, S. Oil Spill Detection Using Space-Borne Sentinel-1 SAR Imagery. in *Oil Spill Science and Technology: Second Edition* 387–402 (Elsevier Inc., 2017).

[8] Wahl, T., Skøelv, Å. & Andersen, J. H. S. Practical Use of ERS-1 SAR Images. *Pollut. Monit.* 3 (1994).

[9] Fakhru'l-Razi, A. *et al.* Review of technologies for oil and gas produced water treatment. *Journal of Hazardous Materials* vol. 170 530–551 (2009).

[10] Trapnes, H. H. Characterisation of gas-liquid interfaces related to offshore produced water treatment. (Norwegian University of Science and Technology, 2013).

[11] Alamooti, A. M. & Malekabadi, F. K. An Introduction to Enhanced Oil Recovery. in *Fundamentals of Enhanced Oil and Gas Recovery from Conventional and Unconventional Reservoirs* 1–40 (Elsevier Inc., 2018).

[12] Formation water | Oilfield Glossary. https://www.glossary.oilfield.slb.com/en/Terms/f/formation_water.aspx.

[13] Convention | OSPAR Commission. https://www.ospar.org/convention.

[14] Speight, J. G. & El-Gendy, N. S. Introduction to Petroleum Biotechnology. in *Introduction to Petroleum Biotechnology* 69–101 (Elsevier, 2018).

[15] Geraudie, P., Nahrgang, J., Forget-Leray, J., Minier, C. & Camus, L. In vivo effects of environmental concentrations of produced water on the reproductive function of polar cod (Boreogadus saida). in *Journal of Toxicology and Environmental Health - Part A: Current Issues* vol. 77 557–573 (Taylor and Francis Inc., 2014).

[16] Alammar, A., Park, S. H., Williams, C. J., Derby, B. & Szekely, G. Oil-in-water separation with graphene-based nanocomposite membranes for produced water treatment. *J. Memb. Sci.* **603**, 118007 (2020).

[17] Xu, J. *et al.* Polyoxadiazole hollow fibers for produced water treatment by direct contact membrane distillation. *Desalination* **432**, 32–39 (2018).

[18] Al-Ghouti, M. A., Al-Kaabi, M. A., Ashfaq, M. Y. & Da'na, D. A. Produced water characteristics, treatment and reuse: A review. *Journal of Water Process Engineering* vol. 28 222–239 (2019).

[19] Fingas, M. & Brown, C. Review of oil spill remote sensing. *Marine Pollution Bulletin* vol. 83 9–23 (2014).

[20] P&ID Symbols (Complete List & PDF) - Projectmaterials. https://blog.projectmaterials.com/instrumentation/pid-symbols/.

[21] The meso-scale laboratory at SINTEF SeaLab - SINTEF. https://www.SINTEF.no/en/all-laboratories/the-meso-scale-laboratory-at-SINTEF-sealab/.

[22] Van Lopik, J. H., Hartog, N., Zaadnoordijk, W. J., Cirkel, D. G. & Raoof, A. Salinization in a stratified aquifer induced by heat transfer from well casings. *Adv. Water Resour.* **86**, 32–45 (2015).Chouder, A., Silvestre, S., Taghezouit, B. & Karatepe, E. Monitoring, modelling and simulation of PV systems using LabVIEW. *Sol. Energy* **91**, 337–349 (2013).

[23] Nortek AS. *The Comprehensive Manual for Velocimeters*. https://www.nortekgroup.com/assets/software/N3015-030-Comprehensive-Manual-Velocimeters_1118.pdf (2018).

[24] Migliaccio, M., Nunziata, F. & Buono, A. SAR polarimetry for sea oil slick observation. *International Journal of Remote Sensing* vol. 36 3243–3273 (2015).

[25] Satellite Imagery, SAR and Optical - KSAT - Kongsberg Satellite Services. https://www.ksat.no/earth-observation/satellite-imagery--processing/satellite-imagery-sar-and-optical/.

[26] Faksness, L. G. & Brandvik, P. J. Distribution of water soluble components from Arctic marine oil spills - A combined laboratory and field study. *Cold Reg. Sci. Technol.* **54**, 97–105 (2008).

[27] Faksness, L. G., Brandvik, P. J. & Sydnes, L. K. Composition of the water accommodated fractions as a function of exposure times and temperatures. *Mar. Pollut. Bull.* **56**, 1746–1754 (2008).

[28] Nahrgang, J. *et al.* Early life stages of an arctic keystone species (Boreogadus saida) show high sensitivity to a water-soluble fraction of crude oil. *Environ. Pollut.* **218**, 605–614 (2016).

[29] Bender, M. L. *et al.* Effects of chronic dietary petroleum exposure on reproductive development in polar cod (Boreogadus saida). *Aquat. Toxicol.* **180**, 196–208 (2016).

[30] Nahrgang, J. *et al.* Growth and metabolism of adult polar cod (Boreogadus saida) in response to dietary crude oil. *Ecotoxicol. Environ. Saf.* (2019).

[31] Christiansen, J. S., Karamushko, L. I. & Nahrgang, J. Sub-lethal levels of waterborne petroleum may depress routine metabolism in polar cod Boreogadus saida (Lepechin, 1774). *Polar Biol.* **33**, 1049–1055 (2010).

[32] Hop, H., Trudeau, V. L. & Graham, M. Spawning energetics of Arctic cod (*Boreogadus saida*) in relation to seasonal development of the ovary and plasma sex steroid levels. *Can. J. Fish. Aquat. Sci.* **52**, 541–550 (1995).

[33] Steffensen, I. & Karstad, P. I. Norne field development - fast track from discovery to production. in *1995 SPE Int Tech Conf* vol. 48 296–339 (OnePetro, 1995).

[34] Norne - equinor.com. https://www.equinor.com/en/what-we-do/norwegian-continental-shelf-platforms/norne.html.

[35] Discharges to the sea - Norwegianpetroleum.no. https://www.norskpetroleum.no/en/environment-and-technology/discharges-to-the-sea/.

[36] Skancke, J. & Daling, P. *Oil film thickness and water column concentrations resulting from produced water discharge at the Grane/Grand field*. (2019).

[37] Sharqawy, M. H., Lienhard V, J. H. & Zubair, S. M. Thermophysical properties of seawater: A review of existing correlations and data. *Desalin. Water Treat.* **16**, 354–380 (2010).

[38] Isdale, JD., Morris, R. Physical properties of seawater solutions: density. *Desalinisation.* **10**(4), 329-339 (1972).

[39] Millero, FJ., Poisson, A. International one-atmosphere equation of state of seawater. *Deep-Sea Res.* **28A**(6), 625-629 (1981).

[40] Activity per sea area - Norwegianpetroleum.no. https://www.norskpetroleum.no/en/developments-and-operations/activity-per-sea-area/.

[41] Norwegian Sea | North Atlantic Ocean | Britannica. https://www.britannica.com/place/Norwegian-Sea.

[42] International Council for the Exploration of the Sea. *Norwegian Sea ecoregion-Ecosystem overview* (2019).

[43] US Department of Commerce, NOAA. Tides and Water Levels, What Causes Tides, NOS Education Offering.

[44] Nordgård, E. L. Model Compounds for Heavy Crude Oil Components and Tetrameric Acids Characterization and Interfacial Behaviour. (NTNU, 2009).

[45] Azizian, S. & Khosravi, M. Advanced oil spill decontamination techniques. in *Interface Science and Technology* vol. 30 283–332 (Elsevier B.V., 2019).

[46] Toor, J. S. & Sikka, S. C. Developmental and reproductive disorders-Role of endocrine disruptors in testicular toxicity. in *Reproductive and Developmental Toxicology* 1111–1121 (Elsevier, 2017).

[47] Myrstad, M. *Oil spill forensics - Identification of possible sources for oil spills found along the coastline of mid-Norway - An experimental study combining GC-MS analysis and multivariate statistics.* (NTNU, 2016).

[48] Brandvik, P. J. *et al. Experimental Oil Release in Broken Ice-A Large-Scale Field Verification of Results From Laboratory Studies of Oil Weathering and Ignitability of Weathered Oil Spills*. SINTEF Materials and Chemistry (2010).

[49] Hansen, S. K. Leaching of surfactants as a function of oil droplet size and surfactant properties. An approach using mass spectrometry and multivariate data analysis. (NTNU, 2017).

[50] Repsol Norge AS. *Årsrapport til Miljødirektoratet for Varg*. https://www.norskoljeoggass.no/contentassets/858441a2af864132b23c5237836ffb1e/varg.pdf (2016).

[51] Brandvik, P. J. & Daling, P. S. *Weathering of oil spills at sea and use of numerical oil weathering models*. KJ3050 Marine Organic Environmental Chemistry Lecture compendium.

[52] Brandvik, P. J. & Daling, P. S. *Crude oil composition, properties and laboratory methods to characterise crude oils*. KJ3050 Marine Organic Environmental Chemistry Lecture compendium.

[53] United States Geological Survey. Water Density. https://www.usgs.gov/special-topic/water-science-school/science/water-density?qt-science_center_objects=0#qt-science_center_objects.

[54] Science Learning Hub - Pokapū Akoranga Pūtaiao. Ocean density. https://www.sciencelearn.org.nz/resources/687-ocean-density (2010).

[55] SINTEF Ocean/Environmental Technology. The OSCAR model. https://www.SINTEF.no/globalassets/upload/materialer_kjemi/faktaark/environment/oscar-fact.pdf (2017).

[56] Kartverket. Rørvik. https://kartverket.no/til-sjos/se-havniva/resultat?id=9000017.

[57] van Akan, H. M. *The Oceanic Thermohaline Circulation: An Introduction*. (Springer Netherlands, 2007).

[58] Bergman, J. Density of Ocean Water. *National Earth Science Theachers Association (NESTA)* https://www.windows2universe.org/earth/Water/density.html (2001).

[59] Halim, N. S. A. *et al.* Recent Development on Electrospun Nanofiber Membrane for Produced Water Treatment: A review. *Journal of Environmental Chemical Engineering* vol. 9 104613 (2021).

[60] Judd, S. *et al.* The size and performance of offshore produced water oil-removal technologies for reinjection. *Sep. Purif. Technol.* **134**, 241–246 (2014).

[61] O'Hara, P. D. & Morandin, L. A. Effects of sheens associated with offshore oil and gas development on the feather microstructure of pelagic seabirds. *Mar. Pollut. Bull.* **60**, 672–678 (2010).

[62] Beyer, J., Goksøyr, A., Hjermann, D. Ø. & Klungsøyr, J. Environmental effects of offshore produced water discharges: A review focused on the Norwegian continental shelf. *Marine Environmental Research* vol. 162 105155 (2020).

[63] Brandvik, P. J., Johansen, Ø., Leirvik, F., Farooq, U. & Daling, P. S. Droplet breakup in subsurface oil releases - Part 1: Experimental study of droplet breakup and effectiveness of dispersant injection. *Mar. Pollut. Bull.* **73**, 319–326 (2013).

[64] Johansen, Ø., Brandvik, P. J. & Farooq, U. Droplet breakup in subsea oil releases - Part 2: Predictions of droplet size distributions with and without injection of chemical dispersants. *Mar. Pollut. Bull.* **73**, 327–335 (2013).

[65] Sørheim, K. R., Bakken, O. & Johnsen, M. *Drivis crude oil - Properties and behaviour at sea*. SINTEF Ocean Environmental Technology (2017).

[66] Fanneløp, T. K. & Sjøen, K. Hydrodynamics of underwater blowouts. *Aerosp. Sci. Meet.* (1980).

[67] Dunnebier, D. A. E. Experimental and modeling study of subsea releases of oil and gas. (NTNU, 2015).

[68] Reed, M. *et al.* MEMW Users Manual (Marine Environmental Modelling Workbench). 221 (2006).

[69] Johansen, Ø. Development and verification of deep-water blowout models. in *Marine Pollution Bulletin* vol. 47 360–368 (Elsevier Ltd, 2003).

[70] Johansen, Ø. DeepBlow - a Lagrangian Plume Model for Deep Water Blowouts. *Spill Sci. Technol. Bull.* **6**, 103–111 (2000).

[71] Yapa, P. D., Zheng, L. & Chen, F. A model for deepwater oil/gas blowouts. in *Marine Pollution Bulletin* vol. 43 234–241 (2001).

[72] Dissanayake, A. L., Gros, J. & Socolofsky, S. A. Integral models for bubble, droplet, and multiphase plume dynamics in stratification and crossflow. *Environ. Fluid Mech.* **18**, 1167–1202 (2018).

A.1 Experimental data from produced water releases

Experimental data that was conducted form the indoor PW releases in the wave basin at SINTEF Sealab is shown in Table A. 1.

Table A. 1. Experimental data from the PW releases conducted in the wave basin. The table continues over multiple pages.

Date (d.m.y)	Experiment (#)	Temperature (°C)	Salinity (psu)	Density (kg/L)	Rate PW (L/min)	Rate Gas (L/min)	Velocity PW (m/s)	Nozzle alignement (°)	Trapping depth (cm)
10.11.2020	1a	38	48	1.0289	0.45		0.60	45	-54
10.11.2020	1b	45	48	1.0259	0.77		1.02	45	-34
10.11.2020	1c	50	48	1.0237	1.02		1.35	45	-60
11.11.2020	2a	39	35						
11.11.2020	2b	45	35		0.76				
11.11.2020	2c	51	35		1.04				
12.11.2020	3a	36	60	1.0387	0.44		0.58	45	-68
12.11.2020	3b	42	60	1.0362	0.75		0.99	45	-67
12.11.2020	3c	48	60	1.0335	1.04		1.38	45	-45
13.11.2020	4a	25	48	1.0335	0.45		0.60	45	0
13.11.2020	4b	30	48	1.0319	0.75		0.99	45	-49
13.11.2020	4c	37	48	1.0293	1.03		1.37	45	-49
16.11.2020	5a	27	35	1.0230	0.45		0.60	45	0
16.11.2020	5b	30	35	1.0220	0.78		1.03	45	-18
16.11.2020	5c	36	35	1.0199	1.09		1.45	45	-33
17.11.2020	6a	36	60	1.0387	0.43		0.57	45	-55

17.11.2020	6b	40	60	1.0370	0.76		1.01	45	-65
17.11.2020	6c	46	60	1.0344	1.05		1.39	45	-65
18.11.2020	7a	46	48	1.0255	0.44		0.58	45	-58
18.11.2020	7b	58	48	1.0197	0.75		0.99	45	-76
18.11.2020	7c	64	48	1.0165	1.04		1.38	45	-60
19.11.2020	8a	45	35	1.0163	0.45		0.60	45	-9
19.11.2020	8b	56	35	1.0111	0.75		0.99	45	-26
19.11.2020	8c	64	35	1.0070	1.03		1.37	45	-40
20.11.2020	9a	26	60	1.0423	0.44		0.58	45	-47
20.11.2020	9b	55	60	1.0301	0.78		1.03	45	-62
20.11.2020	9c	66	60	1.0242	1.06		1.41	45	-76
23.11.2020	10a	37	48	1.0293	0.45		0.60	0	-14
23.11.2020	10b	47	48	1.0251	0.73		0.97	0	-31
23.11.2020	10c	55	48	1.0212	1.02		1.35	0	-14
24.11.2020	11a	36	35	1.0199	0.46		0.61	0	12
24.11.2020	11b	51	35	1.0136	0.75		0.99	0	25
24.11.2020	11c	55	35	1.0116	1.05		1.39	0	25
25.11.2020	12a	38	60	1.0379	0.43		0.57	0	-48
25.11.2020	12b	51	60	1.0321	0.74		0.98	0	-48
25.11.2020	12c	55	60	1.0301	1.05		1.39	0	-42
26.11.2020	13a	33	48	1.0308	0.46		0.61	0	-41

26.11.2020	13b	38	48	1.0289	0.74		0.98	0	-20
26.11.2020	13c	37	48	1.0293	1.04		1.38	0	-17
27.11.2020	14a	29	35	1.0224	0.45		0.60	0	21
27.11.2020	14b	38	35	1.0192	0.74		0.98	0	23
27.11.2020	14c	37	35	1.0196	1.03		1.37	0	25
30.11.2020	15a	30	60	1.0409	0.44		0.58	0	-61
30.11.2020	15b	37	60	1.0383	0.75		0.99	0	-72
30.11.2020	15c	38	60	1.0379	1.03		1.37	0	-73
01.12.2020	16a	52	48	1.0227	0.44		0.58	0	-26
01.12.2020	16b	60	48	1.0187	0.74		0.98	0	-23
01.12.2020	16c	65	48	1.0160	1.05		1.39	0	-25
02.12.2020	17a	44	35	1.0167	0.45		0.60	0	24
02.12.2020	17b	61	35	1.0086	0.76		1.01	0	24
02.12.2020	17c	67	35	1.0053	1.05		1.39	0	25
03.12.2020	18a	46	60	1.0344	0.45		0.60	0	-49
03.12.2020	18b	54	60	1.0306	0.76		1.01	0	-74
03.12.2020	18c	66	60	1.0242	1.04		1.38	0	-72
04.12.2020	19a	48	48	1.0246	0.75		0.99	0	-18
04.12.2020	19b	51	48	1.0232	0.75		0.99	0	-17
04.12.2020	19c	51	48	1.0232	0.76		1.01	0	-17
04.12.2020	19d	50	48	1.0237	0.74		0.98	0	-24

07.12.2020	20a	48	48	1.0246	0.74		0.98	45	-59
07.12.2020	20b	51	48	1.0232	0.76		1.01	45	-62
07.12.2020	20c	51	48	1.0232	0.76		1.01	45	-63
07.12.2020	20d	47	48	1.0251	0.75		0.99	45	-60
10.12.2020	21a	42	48	1.0273	0.45	0.09	0.60	0	0
10.12.2020	21b	50	48	1.0237	0.78	0.15	1.03	0	20
10.12.2020	21c	52	48	1.0227	1.08	0.21	1.43	0	25
11.12.2020	22a	52	48	1.0227	1.04	0.08	1.38	0	7
11.12.2020	22b	55	48	1.0212	1.04	0.11	1.38	0	12
11.12.2020	22c	51	48	1.0232	1.09	0.16	1.45	0	25
11.12.2020	22d	52	48	1.0227	1.03	0.25	1.37	0	25
16.12.2020	23a	49	48	1.0241	0.75		0.99	0	-29
16.12.2020	23b	49	48	1.0241	0.77		1.02	0	-29
16.12.2020	23c	48	48	1.0246	0.76		1.01	0	-29
16.12.2020	23d	49	48	1.0241	0.77		1.02	0	-31
17.12.2020	24a	37	48	1.0293	0.47		0.62	0	-30
17.12.2020	24b	48	48	1.0246	0.76		1.01	0	-29
17.12.2020	24c	54	48	1.0217	1.04		1.38	0	-24
18.12.2020	25a	37	48	1.0293	0.48		0.64	0	-8
18.12.2020	25b	43	48	1.0268	0.77		1.02	0	-26
18.12.2020	25c	50	48	1.0237	0.78		1.03	0	-27

A.2 Jetting water data from the Norne field

Data for jetting water releases was provided by Equinor for the period 04.12.2020-25.02.2021 and is shown in Table A. 2.

Table A. 2. Overview of the jetting water activity at the Norne platform in the period 04.12.2020 - 25.02.2021. The table continues over multiple pages.

Sample time	Analysis date	Data entry point	Sample point	Input value	Parameter
25.02.2021 00:00	25.02.2021	Norne FPSO - Jettevann	Coaleser	15	Oljeindeks [mg/l]
25.02.2021 00:00	25.02.2021	Norne FPSO - Jettevann	Coaleser	1000	Vannmengde [m3]
25.02.2021 00:00	28.02.2021	Norne FPSO - Jettevann	Avgassingstank	421	Vannmengde [m3]
25.02.2021 00:00	25.02.2021	Norne FPSO - Jettevann	Coaleser	15	Olje [kg]
25.02.2021 00:00	28.02.2021	Norne FPSO - Jettevann	Avgassingstank	15	Oljeindeks [mg/l]
25.02.2021 00:00	28.02.2021	Norne FPSO - Jettevann	Avgassingstank	6.315	Olje [kg]
14.02.2021 00:00	14.02.2021	Norne FPSO - Jettevann	Testseparator	20	Oljeindeks [mg/l]
14.02.2021 00:00	14.02.2021	Norne FPSO - Jettevann	Testseparator	20	Olje [kg]
14.02.2021 00:00	14.02.2021	Norne FPSO - Jettevann	Testseparator	1000	Vannmengde [m3]
29.01.2021 00:00	29.01.2021	Norne FPSO - Jettevann	Coaleser	6	Olje [kg]
29.01.2021 00:00	29.01.2021	Norne FPSO - Jettevann	Avgassingstank	2.1	Olje [kg]
29.01.2021 00:00	29.01.2021	Norne FPSO - Jettevann	Avgassingstank	100	Vannmengde [m3]
29.01.2021 00:00	29.01.2021	Norne FPSO - Jettevann	Coaleser	250	Vannmengde [m3]
29.01.2021 00:00	29.01.2021	Norne FPSO - Jettevann	Coaleser	24	Oljeindeks [mg/l]
29.01.2021 00:00	29.01.2021	Norne FPSO - Jettevann	Avgassingstank	21	Oljeindeks [mg/l]
26.01.2021 00:00	26.01.2021	Norne FPSO - Jettevann	Sandsyklon - test	123	Oljeindeks [mg/l]
26.01.2021 00:00	26.01.2021	Norne FPSO - Jettevann	Sandsykloner - inlet	547	Oljeindeks [mg/l]
20.01.2021 00:00	20.01.2021	Norne FPSO - Jettevann	Inlet-separator	19	Oljeindeks [mg/l]
20.01.2021 00:00	20.01.2021	Norne FPSO - Jettevann	Testseparator	100	Oljeindeks [mg/l]

20.01.2021 00:00	20.01.2021	Norne FPSO - Jettevann	Inlet-separator	450	Vannmengde [m3]
20.01.2021 00:00	20.01.2021	Norne FPSO - Jettevann	Testseparator	450	Vannmengde [m3]
20.01.2021 00:00	20.01.2021	Norne FPSO - Jettevann	Testseparator	45	Olje [kg]
20.01.2021 00:00	20.01.2021	Norne FPSO - Jettevann	Inlet-separator	8.55	Olje [kg]
29.12.2020 00:00	29.12.2020	Norne FPSO - Jettevann	Sandsyklon - test	51	Oljeindeks [mg/l]
29.12.2020 00:00	29.12.2020	Norne FPSO - Jettevann	Sandsykloner - inlet	271	Oljeindeks [mg/l]
24.12.2020 02:00	24.12.2020	Norne FPSO - Jettevann	Avgassingstank	300	Vannmengde [m3]
24.12.2020 02:00	24.12.2020	Norne FPSO - Jettevann	Avgassingstank	26	Oljeindeks [mg/l]
24.12.2020 02:00	24.12.2020	Norne FPSO - Jettevann	Avgassingstank	7.8	Olje [kg]
13.12.2020 00:00	13.12.2020	Norne FPSO - Jettevann	Testseparator	8.25	Olje [kg]
13.12.2020 00:00	13.12.2020	Norne FPSO - Jettevann	Testseparator	550	Vannmengde [m3]
13.12.2020 00:00	13.12.2020	Norne FPSO - Jettevann	Testseparator	15	Oljeindeks [mg/l]
11.12.2020 00:00	11.12.2020	Norne FPSO - Jettevann	Inlet-separator	16	Oljeindeks [mg/l]
11.12.2020 00:00	11.12.2020	Norne FPSO - Jettevann	Inlet-separator	390	Vannmengde [m3]
11.12.2020 00:00	11.12.2020	Norne FPSO - Jettevann	Inlet-separator	6.24	Olje [kg]
04.12.2020 02:00	05.12.2020	Norne FPSO - Jettevann	Avgassingstank	400	Vannmengde [m3]
04.12.2020 02:00	05.12.2020	Norne FPSO - Jettevann	Avgassingstank	16	Oljeindeks [mg/l]
04.12.2020 02:00	05.12.2020	Norne FPSO - Jettevann	Avgassingstank	6.4	Olje [kg]
04.12.2020 00:00	06.12.2020	Norne FPSO - Jettevann	Sandsykloner - inlet	644	Oljeindeks [mg/l]
04.12.2020 00:00	06.12.2020	Norne FPSO - Jettevann	Sandsyklon - test	166	Oljeindeks [mg/l]

A.3 Produced water data from the Norne field

Data was provided by Equinor for the produced water releases at the Norne field in the period 01.12.2020 – 28.02.2021. The data is shown is Table A. 3 and include the oil index (mg/L), amount of water released (m^3) and weight of oil in the release (kg). There is a total of 93 samples and the mean oil index for the given period is mg/L.

Table A. 3. Overview of the produced water releases at the Norne platform in the period 01.12.2020 – 28.02.2021. The table continues over multiple pages.

Sample time	Analysis date	Data entry point	Sample point	Input value	Parameter
28.02.2021 00:00	01.03.2021	Norne FPSO - Utslippsvann	Avgassingstank - overbord	13	Oljeindeks [mg/l]
28.02.2021 00:00	01.03.2021	Norne FPSO - Utslippsvann	Avgassingstank - overbord	23611	Vannmengde [m3]
28.02.2021 00:00	01.03.2021	Norne FPSO - Utslippsvann	Avgassingstank - overbord	306.943	Olje [kg]
27.02.2021 00:00	28.02.2021	Norne FPSO - Utslippsvann	Avgassingstank - overbord	186.756	Olje [kg]
27.02.2021 00:00	28.02.2021	Norne FPSO - Utslippsvann	Avgassingstank - overbord	7.9	Oljeindeks [mg/l]
27.02.2021 00:00	28.02.2021	Norne FPSO - Utslippsvann	Avgassingstank - overbord	23640	Vannmengde [m3]
26.02.2021 00:00	27.02.2021	Norne FPSO - Utslippsvann	Avgassingstank - overbord	20915	Vannmengde [m3]
26.02.2021 00:00	27.02.2021	Norne FPSO - Utslippsvann	Avgassingstank - overbord	8.5	Oljeindeks [mg/l]
26.02.2021 00:00	27.02.2021	Norne FPSO - Utslippsvann	Avgassingstank - overbord	177.7775	Olje [kg]
25.02.2021 00:00	26.02.2021	Norne FPSO - Utslippsvann	Avgassingstank - overbord	161.5068	Olje [kg]
25.02.2021 00:00	26.02.2021	Norne FPSO - Utslippsvann	Avgassingstank - overbord	7.8	Oljeindeks [mg/l]
25.02.2021 00:00	26.02.2021	Norne FPSO - Utslippsvann	Avgassingstank - overbord	20706	Vannmengde [m3]
24.02.2021 00:00	25.02.2021	Norne FPSO - Utslippsvann	Avgassingstank - overbord	23269	Vannmengde [m3]
24.02.2021 00:00	25.02.2021	Norne FPSO - Utslippsvann	Avgassingstank - overbord	255.959	Olje [kg]
24.02.2021 00:00	25.02.2021	Norne FPSO - Utslippsvann	Avgassingstank - overbord	11	Oljeindeks [mg/l]
23.02.2021 00:00	24.02.2021	Norne FPSO - Utslippsvann	Avgassingstank - overbord	257.565	Olje [kg]
23.02.2021 00:00	24.02.2021	Norne FPSO - Utslippsvann	Avgassingstank - overbord	11	Oljeindeks [mg/l]
23.02.2021 00:00	24.02.2021	Norne FPSO - Utslippsvann	Avgassingstank - overbord	23415	Vannmengde [m3]
22.02.2021 00:00	23.02.2021	Norne FPSO - Utslippsvann	Avgassingstank - overbord	22316	Vannmengde [m3]

22.02.2021 00:00	23.02.2021	Norne FPSO - Utslippsvann	Avgassingstank - overbord	13	Oljeindeks [mg/l]
22.02.2021 00:00	23.02.2021	Norne FPSO - Utslippsvann	Avgassingstank - overbord	290.108	Olje [kg]
21.02.2021 00:00	22.02.2021	Norne FPSO - Utslippsvann	Avgassingstank - overbord	270.324	Olje [kg]
21.02.2021 00:00	22.02.2021	Norne FPSO - Utslippsvann	Avgassingstank - overbord	12	Oljeindeks [mg/l]
21.02.2021 00:00	22.02.2021	Norne FPSO - Utslippsvann	Avgassingstank - overbord	22527	Vannmengde [m3]
20.02.2021 00:00	21.02.2021	Norne FPSO - Utslippsvann	Avgassingstank - overbord	10	Oljeindeks [mg/l]
20.02.2021 00:00	21.02.2021	Norne FPSO - Utslippsvann	Avgassingstank - overbord	22122	Vannmengde [m3]
20.02.2021 00:00	21.02.2021	Norne FPSO - Utslippsvann	Avgassingstank - overbord	221.22	Olje [kg]
19.02.2021 00:00	20.02.2021	Norne FPSO - Utslippsvann	Avgassingstank - overbord	247.192	Olje [kg]
19.02.2021 00:00	20.02.2021	Norne FPSO - Utslippsvann	Avgassingstank - overbord	22472	Vannmengde [m3]
19.02.2021 00:00	20.02.2021	Norne FPSO - Utslippsvann	Avgassingstank - overbord	11	Oljeindeks [mg/l]
18.02.2021 00:00	19.02.2021	Norne FPSO - Utslippsvann	Avgassingstank - overbord	6.4	Oljeindeks [mg/l]
18.02.2021 00:00	19.02.2021	Norne FPSO - Utslippsvann	Avgassingstank - overbord	22498	Vannmengde [m3]
18.02.2021 00:00	19.02.2021	Norne FPSO - Utslippsvann	Avgassingstank - overbord	143.9872	Olje [kg]
17.02.2021 00:00	18.02.2021	Norne FPSO - Utslippsvann	Avgassingstank - overbord	4.7	Oljeindeks [mg/l]
17.02.2021 00:00	18.02.2021	Norne FPSO - Utslippsvann	Avgassingstank - overbord	20674	Vannmengde [m3]
17.02.2021 00:00	18.02.2021	Norne FPSO - Utslippsvann	Avgassingstank - overbord	97.1678	Olje [kg]
16.02.2021 00:00	17.02.2021	Norne FPSO - Utslippsvann	Avgassingstank - overbord	20702	Vannmengde [m3]
16.02.2021 00:00	17.02.2021	Norne FPSO - Utslippsvann	Avgassingstank - overbord	4.9	Oljeindeks [mg/l]
16.02.2021 00:00	17.02.2021	Norne FPSO - Utslippsvann	Avgassingstank - overbord	101.4398	Olje [kg]
15.02.2021 00:00	16.02.2021	Norne FPSO - Utslippsvann	Avgassingstank - overbord	9.2	Oljeindeks [mg/l]

15.02.2021 00:00	16.02.2021	Norne FPSO - Utslippsvann	Avgassingstank - overbord	211.6368	Olje [kg]
15.02.2021 00:00	16.02.2021	Norne FPSO - Utslippsvann	Avgassingstank - overbord	23004	Vannmengde [m3]
14.02.2021 00:00	15.02.2021	Norne FPSO - Utslippsvann	Avgassingstank - overbord	23416	Vannmengde [m3]
14.02.2021 00:00	15.02.2021	Norne FPSO - Utslippsvann	Avgassingstank - overbord	12	Oljeindeks [mg/l]
14.02.2021 00:00	15.02.2021	Norne FPSO - Utslippsvann	Avgassingstank - overbord	280.992	Olje [kg]
13.02.2021 00:00	14.02.2021	Norne FPSO - Utslippsvann	Avgassingstank - overbord	217.096	Olje [kg]
13.02.2021 00:00	14.02.2021	Norne FPSO - Utslippsvann	Avgassingstank - overbord	19736	Vannmengde [m3]
13.02.2021 00:00	14.02.2021	Norne FPSO - Utslippsvann	Avgassingstank - overbord	11	Oljeindeks [mg/l]
12.02.2021 00:00	13.02.2021	Norne FPSO - Utslippsvann	Avgassingstank - overbord	8.8	Oljeindeks [mg/l]
12.02.2021 00:00	13.02.2021	Norne FPSO - Utslippsvann	Avgassingstank - overbord	17589	Vannmengde [m3]
12.02.2021 00:00	13.02.2021	Norne FPSO - Utslippsvann	Avgassingstank - overbord	154.7832	Olje [kg]
11.02.2021 00:00	12.02.2021	Norne FPSO - Utslippsvann	Avgassingstank - overbord	150.8283	Olje [kg]
11.02.2021 00:00	12.02.2021	Norne FPSO - Utslippsvann	Avgassingstank - overbord	16947	Vannmengde [m3]
11.02.2021 00:00	12.02.2021	Norne FPSO - Utslippsvann	Avgassingstank - overbord	8.9	Oljeindeks [mg/l]
10.02.2021 00:00	11.02.2021	Norne FPSO - Utslippsvann	Avgassingstank - overbord	26	Oljeindeks [mg/l]
10.02.2021 00:00	11.02.2021	Norne FPSO - Utslippsvann	Avgassingstank - overbord	20339	Vannmengde [m3]
10.02.2021 00:00	11.02.2021	Norne FPSO - Utslippsvann	Avgassingstank - overbord	528.814	Olje [kg]
09.02.2021 00:00	10.02.2021	Norne FPSO - Utslippsvann	Avgassingstank - overbord	167.2456	Olje [kg]
09.02.2021 00:00	10.02.2021	Norne FPSO - Utslippsvann	Avgassingstank - overbord	7.6	Oljeindeks [mg/l]
09.02.2021 00:00	10.02.2021	Norne FPSO - Utslippsvann	Avgassingstank - overbord	22006	Vannmengde [m3]
08.02.2021 00:00	09.02.2021	Norne FPSO - Utslippsvann	Avgassingstank - overbord	7.1	Oljeindeks [mg/l]

08.02.2021 00:00	09.02.2021	Norne FPSO - Utslippsvann	Avgassingstank - overbord	154.5102	Olje [kg]
08.02.2021 00:00	09.02.2021	Norne FPSO - Utslippsvann	Avgassingstank - overbord	21762	Vannmengde [m3]
07.02.2021 00:00	08.02.2021	Norne FPSO - Utslippsvann	Avgassingstank - overbord	21680	Vannmengde [m3]
07.02.2021 00:00	08.02.2021	Norne FPSO - Utslippsvann	Avgassingstank - overbord	164.768	Olje [kg]
07.02.2021 00:00	08.02.2021	Norne FPSO - Utslippsvann	Avgassingstank - overbord	7.6	Oljeindeks [mg/l]
06.02.2021 00:00	07.02.2021	Norne FPSO - Utslippsvann	Avgassingstank - overbord	7.1	Oljeindeks [mg/l]
06.02.2021 00:00	07.02.2021	Norne FPSO - Utslippsvann	Avgassingstank - overbord	21116	Vannmengde [m3]
06.02.2021 00:00	07.02.2021	Norne FPSO - Utslippsvann	Avgassingstank - overbord	149.9236	Olje [kg]
05.02.2021 00:00	06.02.2021	Norne FPSO - Utslippsvann	Avgassingstank - overbord	130.1008	Olje [kg]
05.02.2021 00:00	06.02.2021	Norne FPSO - Utslippsvann	Avgassingstank - overbord	20984	Vannmengde [m3]
05.02.2021 00:00	06.02.2021	Norne FPSO - Utslippsvann	Avgassingstank - overbord	6.2	Oljeindeks [mg/l]
04.02.2021 00:00	05.02.2021	Norne FPSO - Utslippsvann	Avgassingstank - overbord	7.6	Oljeindeks [mg/l]
04.02.2021 00:00	05.02.2021	Norne FPSO - Utslippsvann	Avgassingstank - overbord	156.3396	Olje [kg]
04.02.2021 00:00	05.02.2021	Norne FPSO - Utslippsvann	Avgassingstank - overbord	20571	Vannmengde [m3]
03.02.2021 00:00	04.02.2021	Norne FPSO - Utslippsvann	Avgassingstank - overbord	20991	Vannmengde [m3]
03.02.2021 00:00	04.02.2021	Norne FPSO - Utslippsvann	Avgassingstank - overbord	7.7	Oljeindeks [mg/l]
03.02.2021 00:00	04.02.2021	Norne FPSO - Utslippsvann	Avgassingstank - overbord	161.6307	Olje [kg]
02.02.2021 00:00	03.02.2021	Norne FPSO - Utslippsvann	Avgassingstank - overbord	178.4419	Olje [kg]
02.02.2021 00:00	03.02.2021	Norne FPSO - Utslippsvann	Avgassingstank - overbord	19609	Vannmengde [m3]
02.02.2021 00:00	03.02.2021	Norne FPSO - Utslippsvann	Avgassingstank - overbord	9.1	Oljeindeks [mg/l]
01.02.2021 00:00	02.02.2021	Norne FPSO - Utslippsvann	Avgassingstank - overbord	9.9	Oljeindeks [mg/l]

01.02.2021 00:00	02.02.2021	Norne FPSO - Utslippsvann	Avgassingstank - overbord	20197	Vannmengde [m3]
01.02.2021 00:00	02.02.2021	Norne FPSO - Utslippsvann	Avgassingstank - overbord	199.9503	Olje [kg]
31.01.2021 00:00	01.02.2021	Norne FPSO - Utslippsvann	Avgassingstank - overbord	14	Oljeindeks [mg/l]
31.01.2021 00:00	01.02.2021	Norne FPSO - Utslippsvann	Avgassingstank - overbord	19883	Vannmengde [m3]
31.01.2021 00:00	01.02.2021	Norne FPSO - Utslippsvann	Avgassingstank - overbord	278.362	Olje [kg]
30.01.2021 00:00	31.01.2021	Norne FPSO - Utslippsvann	Avgassingstank - overbord	8.7	Oljeindeks [mg/l]
30.01.2021 00:00	31.01.2021	Norne FPSO - Utslippsvann	Avgassingstank - overbord	19584	Vannmengde [m3]
30.01.2021 00:00	31.01.2021	Norne FPSO - Utslippsvann	Avgassingstank - overbord	170.3808	Olje [kg]
29.01.2021 00:00	30.01.2021	Norne FPSO - Utslippsvann	Avgassingstank - overbord	19634	Vannmengde [m3]
29.01.2021 00:00	30.01.2021	Norne FPSO - Utslippsvann	Avgassingstank - overbord	8.6	Oljeindeks [mg/l]
29.01.2021 00:00	30.01.2021	Norne FPSO - Utslippsvann	Avgassingstank - overbord	168.8524	Olje [kg]
28.01.2021 00:00	29.01.2021	Norne FPSO - Utslippsvann	Avgassingstank - overbord	19835	Vannmengde [m3]
28.01.2021 00:00	29.01.2021	Norne FPSO - Utslippsvann	Avgassingstank - overbord	156.6965	Olje [kg]
28.01.2021 00:00	29.01.2021	Norne FPSO - Utslippsvann	Avgassingstank - overbord	7.9	Oljeindeks [mg/l]
27.01.2021 00:00	28.01.2021	Norne FPSO - Utslippsvann	Avgassingstank - overbord	19658	Vannmengde [m3]
27.01.2021 00:00	28.01.2021	Norne FPSO - Utslippsvann	Avgassingstank - overbord	9.1	Oljeindeks [mg/l]
27.01.2021 00:00	28.01.2021	Norne FPSO - Utslippsvann	Avgassingstank - overbord	178.8878	Olje [kg]
26.01.2021 00:00	27.01.2021	Norne FPSO - Utslippsvann	Avgassingstank - overbord	10	Oljeindeks [mg/l]
26.01.2021 00:00	27.01.2021	Norne FPSO - Utslippsvann	Avgassingstank - overbord	19957	Vannmengde [m3]
26.01.2021 00:00	27.01.2021	Norne FPSO - Utslippsvann	Avgassingstank - overbord	199.57	Olje [kg]
25.01.2021 00:00	26.01.2021	Norne FPSO - Utslippsvann	Avgassingstank - overbord	253.128	Olje [kg]

25.01.2021 00:00	26.01.2021	Norne FPSO - Utslippsvann	Avgassingstank - overbord	21094	Vannmengde [m3]
25.01.2021 00:00	26.01.2021	Norne FPSO - Utslippsvann	Avgassingstank - overbord	12	Oljeindeks [mg/l]
24.01.2021 00:00	25.01.2021	Norne FPSO - Utslippsvann	Avgassingstank - overbord	21286	Vannmengde [m3]
24.01.2021 00:00	25.01.2021	Norne FPSO - Utslippsvann	Avgassingstank - overbord	9.7	Oljeindeks [mg/l]
24.01.2021 00:00	25.01.2021	Norne FPSO - Utslippsvann	Avgassingstank - overbord	206.4742	Olje [kg]
23.01.2021 00:00	24.01.2021	Norne FPSO - Utslippsvann	Avgassingstank - overbord	7.7	Oljeindeks [mg/l]
23.01.2021 00:00	24.01.2021	Norne FPSO - Utslippsvann	Avgassingstank - overbord	164.8339	Olje [kg]
23.01.2021 00:00	24.01.2021	Norne FPSO - Utslippsvann	Avgassingstank - overbord	21407	Vannmengde [m3]
22.01.2021 00:00	23.01.2021	Norne FPSO - Utslippsvann	Avgassingstank - overbord	20473	Vannmengde [m3]
22.01.2021 00:00	23.01.2021	Norne FPSO - Utslippsvann	Avgassingstank - overbord	7.4	Oljeindeks [mg/l]
22.01.2021 00:00	23.01.2021	Norne FPSO - Utslippsvann	Avgassingstank - overbord	151.5002	Olje [kg]
21.01.2021 00:00	22.01.2021	Norne FPSO - Utslippsvann	Avgassingstank - overbord	22	Oljeindeks [mg/l]
21.01.2021 00:00	22.01.2021	Norne FPSO - Utslippsvann	Avgassingstank - overbord	19466	Vannmengde [m3]
21.01.2021 00:00	22.01.2021	Norne FPSO - Utslippsvann	Avgassingstank - overbord	428.252	Olje [kg]
20.01.2021 00:00	21.01.2021	Norne FPSO - Utslippsvann	Avgassingstank - overbord	186.4584	Olje [kg]
20.01.2021 00:00	21.01.2021	Norne FPSO - Utslippsvann	Avgassingstank - overbord	9.4	Oljeindeks [mg/l]
20.01.2021 00:00	21.01.2021	Norne FPSO - Utslippsvann	Avgassingstank - overbord	19836	Vannmengde [m3]
19.01.2021 00:00	20.01.2021	Norne FPSO - Utslippsvann	Avgassingstank - overbord	19817	Vannmengde [m3]
19.01.2021 00:00	20.01.2021	Norne FPSO - Utslippsvann	Avgassingstank - overbord	6.6	Oljeindeks [mg/l]
19.01.2021 00:00	20.01.2021	Norne FPSO - Utslippsvann	Avgassingstank - overbord	130.7922	Olje [kg]
18.01.2021 00:00	19.01.2021	Norne FPSO - Utslippsvann	Avgassingstank - overbord	157.752	Olje [kg]

18.01.2021 00:00	19.01.2021	Norne FPSO - Utslippsvann	Avgassingstank - overbord	19719	Vannmengde [m3]
18.01.2021 00:00	19.01.2021	Norne FPSO - Utslippsvann	Avgassingstank - overbord	8	Oljeindeks [mg/l]
17.01.2021 00:00	18.01.2021	Norne FPSO - Utslippsvann	Avgassingstank - overbord	19924	Vannmengde [m3]
17.01.2021 00:00	18.01.2021	Norne FPSO - Utslippsvann	Avgassingstank - overbord	19	Oljeindeks [mg/l]
17.01.2021 00:00	18.01.2021	Norne FPSO - Utslippsvann	Avgassingstank - overbord	378.556	Olje [kg]
16.01.2021 00:00	17.01.2021	Norne FPSO - Utslippsvann	Avgassingstank - overbord	340.391	Olje [kg]
16.01.2021 00:00	17.01.2021	Norne FPSO - Utslippsvann	Avgassingstank - overbord	20023	Vannmengde [m3]
16.01.2021 00:00	17.01.2021	Norne FPSO - Utslippsvann	Avgassingstank - overbord	17	Oljeindeks [mg/l]
15.01.2021 00:00	16.01.2021	Norne FPSO - Utslippsvann	Avgassingstank - overbord	9.6	Oljeindeks [mg/l]
15.01.2021 00:00	16.01.2021	Norne FPSO - Utslippsvann	Avgassingstank - overbord	20009	Vannmengde [m3]
15.01.2021 00:00	16.01.2021	Norne FPSO - Utslippsvann	Avgassingstank - overbord	192.0864	Olje [kg]
14.01.2021 00:00	15.01.2021	Norne FPSO - Utslippsvann	Avgassingstank - overbord	241.044	Olje [kg]
14.01.2021 00:00	15.01.2021	Norne FPSO - Utslippsvann	Avgassingstank - overbord	12	Oljeindeks [mg/l]
14.01.2021 00:00	15.01.2021	Norne FPSO - Utslippsvann	Avgassingstank - overbord	20087	Vannmengde [m3]
13.01.2021 00:00	14.01.2021	Norne FPSO - Utslippsvann	Avgassingstank - overbord	20318	Vannmengde [m3]
13.01.2021 00:00	14.01.2021	Norne FPSO - Utslippsvann	Avgassingstank - overbord	168.6394	Olje [kg]
13.01.2021 00:00	14.01.2021	Norne FPSO - Utslippsvann	Avgassingstank - overbord	8.3	Oljeindeks [mg/l]
12.01.2021 00:00	13.01.2021	Norne FPSO - Utslippsvann	Avgassingstank - overbord	237.7188	Olje [kg]
12.01.2021 00:00	13.01.2021	Norne FPSO - Utslippsvann	Avgassingstank - overbord	24012	Vannmengde [m3]
12.01.2021 00:00	13.01.2021	Norne FPSO - Utslippsvann	Avgassingstank - overbord	9.9	Oljeindeks [mg/l]
11.01.2021 00:00	12.01.2021	Norne FPSO - Utslippsvann	Avgassingstank - overbord	14	Oljeindeks [mg/l]

11.01.2021 00:00	12.01.2021	Norne FPSO - Utslippsvann	Avgassingstank - overbord	24526	Vannmengde [m3]
11.01.2021 00:00	12.01.2021	Norne FPSO - Utslippsvann	Avgassingstank - overbord	343.364	Olje [kg]
10.01.2021 08:55	10.01.2021	Norne FPSO - Utslippsvann	Avgassingtank spot prøve	6.5	Oljeindeks [mg/l]
10.01.2021 00:00	11.01.2021	Norne FPSO - Utslippsvann	Avgassingstank - overbord	450.566	Olje [kg]
10.01.2021 00:00	11.01.2021	Norne FPSO - Utslippsvann	Avgassingstank - overbord	23714	Vannmengde [m3]
10.01.2021 00:00	11.01.2021	Norne FPSO - Utslippsvann	Avgassingstank - overbord	19	Oljeindeks [mg/l]
09.01.2021 16:00	09.01.2021	Norne FPSO - Utslippsvann	Avgassingtank spot prøve	68	Oljeindeks [mg/l]
09.01.2021 02:00	09.01.2021	Norne FPSO - Utslippsvann	Avgassingtank spot prøve	11	Oljeindeks [mg/l]
09.01.2021 00:00	10.01.2021	Norne FPSO - Utslippsvann	Avgassingstank - overbord	676.872	Olje [kg]
09.01.2021 00:00	10.01.2021	Norne FPSO - Utslippsvann	Avgassingstank - overbord	28	Oljeindeks [mg/l]
09.01.2021 00:00	10.01.2021	Norne FPSO - Utslippsvann	Avgassingstank - overbord	24174	Vannmengde [m3]
08.01.2021 00:00	09.01.2021	Norne FPSO - Utslippsvann	Avgassingstank - overbord	16354	Vannmengde [m3]
08.01.2021 00:00	09.01.2021	Norne FPSO - Utslippsvann	Avgassingstank - overbord	1308.32	Olje [kg]
08.01.2021 00:00	09.01.2021	Norne FPSO - Utslippsvann	Avgassingstank - overbord	80	Oljeindeks [mg/l]
07.01.2021 15:10	07.01.2021	Norne FPSO - Utslippsvann	Avgassingtank spot prøve	34	Oljeindeks [mg/l]
07.01.2021 00:00	08.01.2021	Norne FPSO - Utslippsvann	Avgassingstank - overbord	21	Oljeindeks [mg/l]
07.01.2021 00:00	08.01.2021	Norne FPSO - Utslippsvann	Avgassingstank - overbord	500.976	Olje [kg]
07.01.2021 00:00	08.01.2021	Norne FPSO - Utslippsvann	Avgassingstank - overbord	23856	Vannmengde [m3]
06.01.2021 00:00	07.01.2021	Norne FPSO - Utslippsvann	Avgassingstank - overbord	495.558	Olje [kg]
06.01.2021 00:00	07.01.2021	Norne FPSO - Utslippsvann	Avgassingstank - overbord	21	Oljeindeks [mg/l]
06.01.2021 00:00	07.01.2021	Norne FPSO - Utslippsvann	Avgassingstank - overbord	23598	Vannmengde [m3]

05.01.2021 00:00	06.01.2021	Norne FPSO - Utslippsvann	Avgassingstank - overbord	11	Oljeindeks [mg/l]
05.01.2021 00:00	06.01.2021	Norne FPSO - Utslippsvann	Avgassingstank - overbord	255.376	Olje [kg]
05.01.2021 00:00	06.01.2021	Norne FPSO - Utslippsvann	Avgassingstank - overbord	23216	Vannmengde [m3]
04.01.2021 00:00	05.01.2021	Norne FPSO - Utslippsvann	Avgassingstank - overbord	330.555	Olje [kg]
04.01.2021 00:00	05.01.2021	Norne FPSO - Utslippsvann	Avgassingstank - overbord	22037	Vannmengde [m3]
04.01.2021 00:00	05.01.2021	Norne FPSO - Utslippsvann	Avgassingstank - overbord	15	Oljeindeks [mg/l]
03.01.2021 00:00	04.01.2021	Norne FPSO - Utslippsvann	Avgassingstank - overbord	9.6	Oljeindeks [mg/l]
03.01.2021 00:00	04.01.2021	Norne FPSO - Utslippsvann	Avgassingstank - overbord	205.9584	Olje [kg]
03.01.2021 00:00	04.01.2021	Norne FPSO - Utslippsvann	Avgassingstank - overbord	21454	Vannmengde [m3]
02.01.2021 00:00	03.01.2021	Norne FPSO - Utslippsvann	Avgassingstank - overbord	21395	Vannmengde [m3]
02.01.2021 00:00	03.01.2021	Norne FPSO - Utslippsvann	Avgassingstank - overbord	256.74	Olje [kg]
02.01.2021 00:00	03.01.2021	Norne FPSO - Utslippsvann	Avgassingstank - overbord	12	Oljeindeks [mg/l]
01.01.2021 00:00	02.01.2021	Norne FPSO - Utslippsvann	Avgassingstank - overbord	160.7476	Olje [kg]
01.01.2021 00:00	02.01.2021	Norne FPSO - Utslippsvann	Avgassingstank - overbord	21151	Vannmengde [m3]
01.01.2021 00:00	02.01.2021	Norne FPSO - Utslippsvann	Avgassingstank - overbord	7.6	Oljeindeks [mg/l]
31.12.2020 00:00	01.01.2021	Norne FPSO - Utslippsvann	Avgassingstank - overbord	21536	Vannmengde [m3]
31.12.2020 00:00	01.01.2021	Norne FPSO - Utslippsvann	Avgassingstank - overbord	211.0528	Olje [kg]
31.12.2020 00:00	01.01.2021	Norne FPSO - Utslippsvann	Avgassingstank - overbord	9.8	Oljeindeks [mg/l]
30.12.2020 00:00	31.12.2020	Norne FPSO - Utslippsvann	Avgassingstank - overbord	23060	Vannmengde [m3]
30.12.2020 00:00	31.12.2020	Norne FPSO - Utslippsvann	Avgassingstank - overbord	9.1	Oljeindeks [mg/l]
30.12.2020 00:00	31.12.2020	Norne FPSO - Utslippsvann	Avgassingstank - overbord	209.846	Olje [kg]

29.12.2020 00:00	30.12.2020	Norne FPSO - Utslippsvann	Avgassingstank - overbord	179.528	Olje [kg]
29.12.2020 00:00	30.12.2020	Norne FPSO - Utslippsvann	Avgassingstank - overbord	22441	Vannmengde [m3]
29.12.2020 00:00	30.12.2020	Norne FPSO - Utslippsvann	Avgassingstank - overbord	8	Oljeindeks [mg/l]
28.12.2020 00:00	29.12.2020	Norne FPSO - Utslippsvann	Avgassingstank - overbord	12	Oljeindeks [mg/l]
28.12.2020 00:00	29.12.2020	Norne FPSO - Utslippsvann	Avgassingstank - overbord	22439	Vannmengde [m3]
28.12.2020 00:00	29.12.2020	Norne FPSO - Utslippsvann	Avgassingstank - overbord	269.268	Olje [kg]
27.12.2020 00:00	28.12.2020	Norne FPSO - Utslippsvann	Avgassingstank - overbord	234.432	Olje [kg]
27.12.2020 00:00	28.12.2020	Norne FPSO - Utslippsvann	Avgassingstank - overbord	21312	Vannmengde [m3]
27.12.2020 00:00	28.12.2020	Norne FPSO - Utslippsvann	Avgassingstank - overbord	11	Oljeindeks [mg/l]
26.12.2020 00:00	27.12.2020	Norne FPSO - Utslippsvann	Avgassingstank - overbord	18	Oljeindeks [mg/l]
26.12.2020 00:00	27.12.2020	Norne FPSO - Utslippsvann	Avgassingstank - overbord	20901	Vannmengde [m3]
26.12.2020 00:00	27.12.2020	Norne FPSO - Utslippsvann	Avgassingstank - overbord	376.218	Olje [kg]
25.12.2020 00:00	26.12.2020	Norne FPSO - Utslippsvann	Avgassingstank - overbord	260.136	Olje [kg]
25.12.2020 00:00	26.12.2020	Norne FPSO - Utslippsvann	Avgassingstank - overbord	21678	Vannmengde [m3]
25.12.2020 00:00	26.12.2020	Norne FPSO - Utslippsvann	Avgassingstank - overbord	12	Oljeindeks [mg/l]
24.12.2020 00:00	25.12.2020	Norne FPSO - Utslippsvann	Avgassingstank - overbord	9.6	Oljeindeks [mg/l]
24.12.2020 00:00	25.12.2020	Norne FPSO - Utslippsvann	Avgassingstank - overbord	186.3168	Olje [kg]
24.12.2020 00:00	25.12.2020	Norne FPSO - Utslippsvann	Avgassingstank - overbord	19408	Vannmengde [m3]
23.12.2020 00:00	24.12.2020	Norne FPSO - Utslippsvann	Avgassingstank - overbord	19312	Vannmengde [m3]
23.12.2020 00:00	24.12.2020	Norne FPSO - Utslippsvann	Avgassingstank - overbord	289.68	Olje [kg]
23.12.2020 00:00	24.12.2020	Norne FPSO - Utslippsvann	Avgassingstank - overbord	15	Oljeindeks [mg/l]

22.12.2020 07:20	22.12.2020	Norne FPSO - Utslippsvann	Avgassingtank spot prøve	9.3	Oljeindeks [mg/l]
22.12.2020 00:00	23.12.2020	Norne FPSO - Utslippsvann	Avgassingstank - overbord	8.8	Oljeindeks [mg/l]
22.12.2020 00:00	23.12.2020	Norne FPSO - Utslippsvann	Avgassingstank - overbord	168.0272	Olje [kg]
22.12.2020 00:00	23.12.2020	Norne FPSO - Utslippsvann	Avgassingstank - overbord	19094	Vannmengde [m3]
21.12.2020 00:00	22.12.2020	Norne FPSO - Utslippsvann	Avgassingstank - overbord	289.845	Olje [kg]
21.12.2020 00:00	22.12.2020	Norne FPSO - Utslippsvann	Avgassingstank - overbord	19323	Vannmengde [m3]
21.12.2020 00:00	22.12.2020	Norne FPSO - Utslippsvann	Avgassingstank - overbord	15	Oljeindeks [mg/l]
20.12.2020 00:00	21.12.2020	Norne FPSO - Utslippsvann	Avgassingstank - overbord	19356	Vannmengde [m3]
20.12.2020 00:00	21.12.2020	Norne FPSO - Utslippsvann	Avgassingstank - overbord	13	Oljeindeks [mg/l]
20.12.2020 00:00	21.12.2020	Norne FPSO - Utslippsvann	Avgassingstank - overbord	251.628	Olje [kg]
19.12.2020 00:00	20.12.2020	Norne FPSO - Utslippsvann	Avgassingstank - overbord	16	Oljeindeks [mg/l]
19.12.2020 00:00	20.12.2020	Norne FPSO - Utslippsvann	Avgassingstank - overbord	19472	Vannmengde [m3]
19.12.2020 00:00	20.12.2020	Norne FPSO - Utslippsvann	Avgassingstank - overbord	311.552	Olje [kg]
18.12.2020 00:00	19.12.2020	Norne FPSO - Utslippsvann	Avgassingstank - overbord	18632	Vannmengde [m3]
18.12.2020 00:00	19.12.2020	Norne FPSO - Utslippsvann	Avgassingstank - overbord	21	Oljeindeks [mg/l]
18.12.2020 00:00	19.12.2020	Norne FPSO - Utslippsvann	Avgassingstank - overbord	391.272	Olje [kg]
17.12.2020 00:00	18.12.2020	Norne FPSO - Utslippsvann	Avgassingstank - overbord	17	Oljeindeks [mg/l]
17.12.2020 00:00	18.12.2020	Norne FPSO - Utslippsvann	Avgassingstank - overbord	18368	Vannmengde [m3]
17.12.2020 00:00	18.12.2020	Norne FPSO - Utslippsvann	Avgassingstank - overbord	312.256	Olje [kg]
16.12.2020 00:00	17.12.2020	Norne FPSO - Utslippsvann	Avgassingstank - overbord	406.01	Olje [kg]
16.12.2020 00:00	17.12.2020	Norne FPSO - Utslippsvann	Avgassingstank - overbord	18455	Vannmengde [m3]

16.12.2020 00:00	17.12.2020	Norne FPSO - Utslippsvann	Avgassingstank - overbord	22	Oljeindeks [mg/l]
15.12.2020 00:00	16.12.2020	Norne FPSO - Utslippsvann	Avgassingstank - overbord	24	Oljeindeks [mg/l]
15.12.2020 00:00	16.12.2020	Norne FPSO - Utslippsvann	Avgassingstank - overbord	18240	Vannmengde [m3]
15.12.2020 00:00	16.12.2020	Norne FPSO - Utslippsvann	Avgassingstank - overbord	437.76	Olje [kg]
14.12.2020 00:00	15.12.2020	Norne FPSO - Utslippsvann	Avgassingstank - overbord	18477	Vannmengde [m3]
14.12.2020 00:00	15.12.2020	Norne FPSO - Utslippsvann	Avgassingstank - overbord	17	Oljeindeks [mg/l]
14.12.2020 00:00	15.12.2020	Norne FPSO - Utslippsvann	Avgassingstank - overbord	314.109	Olje [kg]
13.12.2020 00:00	14.12.2020	Norne FPSO - Utslippsvann	Avgassingstank - overbord	18613	Vannmengde [m3]
13.12.2020 00:00	14.12.2020	Norne FPSO - Utslippsvann	Avgassingstank - overbord	11	Oljeindeks [mg/l]
13.12.2020 00:00	14.12.2020	Norne FPSO - Utslippsvann	Avgassingstank - overbord	204.743	Olje [kg]
12.12.2020 00:00	13.12.2020	Norne FPSO - Utslippsvann	Avgassingstank - overbord	18722	Vannmengde [m3]
12.12.2020 00:00	13.12.2020	Norne FPSO - Utslippsvann	Avgassingstank - overbord	11	Oljeindeks [mg/l]
12.12.2020 00:00	13.12.2020	Norne FPSO - Utslippsvann	Avgassingstank - overbord	205.942	Olje [kg]
11.12.2020 00:00	12.12.2020	Norne FPSO - Utslippsvann	Avgassingstank - overbord	18696	Vannmengde [m3]
11.12.2020 00:00	12.12.2020	Norne FPSO - Utslippsvann	Avgassingstank - overbord	9.6	Oljeindeks [mg/l]
11.12.2020 00:00	12.12.2020	Norne FPSO - Utslippsvann	Avgassingstank - overbord	179.4816	Olje [kg]
10.12.2020 00:00	11.12.2020	Norne FPSO - Utslippsvann	Avgassingstank - overbord	169.7787	Olje [kg]
10.12.2020 00:00	11.12.2020	Norne FPSO - Utslippsvann	Avgassingstank - overbord	18657	Vannmengde [m3]
10.12.2020 00:00	11.12.2020	Norne FPSO - Utslippsvann	Avgassingstank - overbord	9.1	Oljeindeks [mg/l]
09.12.2020 00:00	10.12.2020	Norne FPSO - Utslippsvann	Avgassingstank - overbord	13	Oljeindeks [mg/l]
09.12.2020 00:00	10.12.2020	Norne FPSO - Utslippsvann	Avgassingstank - overbord	241.553	Olje [kg]

09.12.2020 00:00	10.12.2020	Norne FPSO - Utslippsvann	Avgassingstank - overbord	18581	Vannmengde [m3]
08.12.2020 00:00	09.12.2020	Norne FPSO - Utslippsvann	Avgassingstank - overbord	148.84	Olje [kg]
08.12.2020 00:00	09.12.2020	Norne FPSO - Utslippsvann	Avgassingstank - overbord	8	Oljeindeks [mg/l]
08.12.2020 00:00	09.12.2020	Norne FPSO - Utslippsvann	Avgassingstank - overbord	18605	Vannmengde [m3]
07.12.2020 00:00	08.12.2020	Norne FPSO - Utslippsvann	Avgassingstank - overbord	316.176	Olje [kg]
07.12.2020 00:00	08.12.2020	Norne FPSO - Utslippsvann	Avgassingstank - overbord	19761	Vannmengde [m3]
07.12.2020 00:00	08.12.2020	Norne FPSO - Utslippsvann	Avgassingstank - overbord	16	Oljeindeks [mg/l]
06.12.2020 00:00	07.12.2020	Norne FPSO - Utslippsvann	Avgassingstank - overbord	20	Oljeindeks [mg/l]
06.12.2020 00:00	07.12.2020	Norne FPSO - Utslippsvann	Avgassingstank - overbord	19164	Vannmengde [m3]
06.12.2020 00:00	07.12.2020	Norne FPSO - Utslippsvann	Avgassingstank - overbord	383.28	Olje [kg]
05.12.2020 00:00	06.12.2020	Norne FPSO - Utslippsvann	Avgassingstank - overbord	477.048	Olje [kg]
05.12.2020 00:00	06.12.2020	Norne FPSO - Utslippsvann	Avgassingstank - overbord	24	Oljeindeks [mg/l]
05.12.2020 00:00	06.12.2020	Norne FPSO - Utslippsvann	Avgassingstank - overbord	19877	Vannmengde [m3]
04.12.2020 00:00	05.12.2020	Norne FPSO - Utslippsvann	Avgassingstank - overbord	11	Oljeindeks [mg/l]
04.12.2020 00:00	05.12.2020	Norne FPSO - Utslippsvann	Avgassingstank - overbord	19905	Vannmengde [m3]
04.12.2020 00:00	05.12.2020	Norne FPSO - Utslippsvann	Avgassingstank - overbord	218.955	Olje [kg]
03.12.2020 00:00	04.12.2020	Norne FPSO - Utslippsvann	Avgassingstank - overbord	152.1748	Olje [kg]
03.12.2020 00:00	04.12.2020	Norne FPSO - Utslippsvann	Avgassingstank - overbord	20023	Vannmengde [m3]
03.12.2020 00:00	04.12.2020	Norne FPSO - Utslippsvann	Avgassingstank - overbord	7.6	Oljeindeks [mg/l]
02.12.2020 00:00	03.12.2020	Norne FPSO - Utslippsvann	Avgassingstank - overbord	19523	Vannmengde [m3]
02.12.2020 00:00	03.12.2020	Norne FPSO - Utslippsvann	Avgassingstank - overbord	292.845	Olje [kg]

02.12.2020 00:00	03.12.2020	Norne FPSO - Utslippsvann	Avgassingstank - overbord	15	Oljeindeks [mg/l]
01.12.2020 00:00	02.12.2020	Norne FPSO - Utslippsvann	Avgassingstank - overbord	187.5426	Olje [kg]
01.12.2020 00:00	02.12.2020	Norne FPSO - Utslippsvann	Avgassingstank - overbord	19137	Vannmengde [m3]
01.12.2020 00:00	02.12.2020	Norne FPSO - Utslippsvann	Avgassingstank - overbord	9.8	Oljeindeks [mg/l]

A.4 Tide data

Data for when the tide was turning was found at the Norwegian Kartverket and was used in the simulation to better know when the sea currents were low. These data were also used when presenting the data from the OSCAR simulation. No data was available for the Norne area, and therefore the data that was used are from the location of Rørvik, which was the closest area to the Norne field with available tide data. Rørvik is located 64.8619°N and 11.2397°E and the data from Rørvik is presented in Table A. 4.

Table A. 4. Overview of the low and high tides during the simulation period from 12.01.21-19.01.21. These data are taken from kartverket.no and is for the location of Rørvik, Norway [56].

	Low tide		**High tide**		**Low tide**		**High tide**		**Low tide**	
Date	Time	cm	Time	cm	Time	cm	Time	cm	Time	cm
12.01.2021	04:42	68	10:50	268	17:14	57	23:19	258		
13.01.2021	05:29	65	11:36	276	18:01	48				
14.01.2021			00:06	261	06:13	64	12:19	280	18:46	45
15.01.2021			00:51	261	06:54	66	13:01	280	19:29	47
16.01.2021			01:33	256	07:34	70	13:42	275	20:10	54
17.01.2021			02:14	248	08:14	78	14:22	265	20:52	64
18.01.2021			02:55	238	08:53	87	15:03	253	21:34	77
19.01.2021			03:38	227	09:36	98	15:46	239	22:18	89

A.5 Current in the wave basin

The Vectrino field probe was used in this project to measure the background current that was used in the wave basin under the PW release experiments. The current was necessary for a stable plume to form because of the experienced back-flow of produced water. The Vectrino field probe took about 400-700 measurements during the 25 seconds it was running per depth. A mean velocity value was further used per depth and the data is presented in Table A.5.

The background current velocity profile for the wave basin is presented in Figure A. 1 and show how the background current behaved at various depths in the basin. For each depth, the mean value was used to present the currents velocity. Because of a narrow opening between the upper and the lower level in the basin (in the area of the nozzle outlet), some turbulence in the seawater is found in the lower part of the upper level as the opposite currents meet here. The pipeline for the PW releases enters the basin in the lower compartment and is brought to the upper part through this oblong narrow opening.

Table A. 5. The mean velocity versus depth in the wave basin is presented in the table below. The Vectrino field probe was used to conduct the data and a mean velocity value is given in cm/s.

Mean velocity (cm/s)	Depth from surface (cm)
2.39	0
2.69	10
2.39	20
1.50	30
0.72	40
0.60	50
1.18	60
1.56	70
1.85	80
-1.13	90

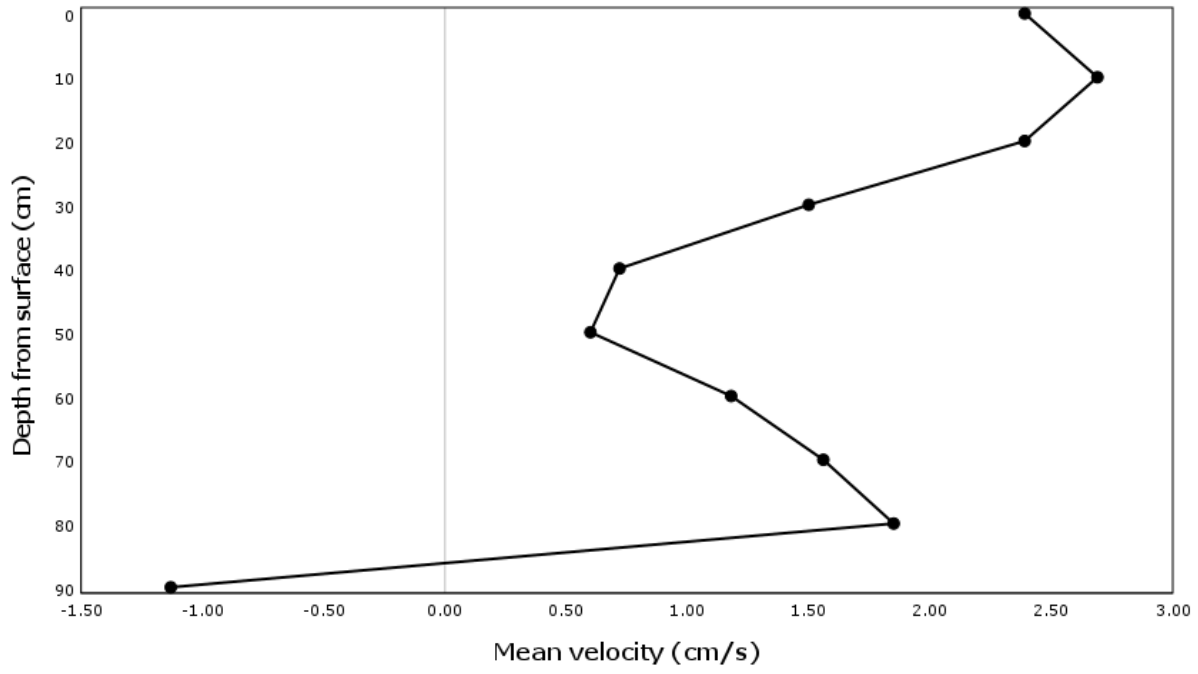

Figure A. 1. Mean velocity versus depth from surface. The velocity presented in this figure is a mean value from the collected data at each depth. The depth is given in cm from the water surface and the velocity is given in cm/s.

A.6 Satellite data provided by Equinor

Data was provided by Equinor for the period 10.12.20 -10.02.21. It had eleven detections of oil sheens on the sea surface by SAR satellite in the given period. The dates 13.01.21-18.01.21 was chosen and further used in this project. The chosen dates had detection of oil on the sea surface five out of six days. The data is given in Table A. 6 below.

Table A. 6. Overview of the data provided by Equinor over the period 10.12.20-10.02.21 with detection of oil sheen on the sea surface by SAR satellite. The table continues over multiple pages.

Date	Time	Definition	Probability	Assessment from satellite service	Comment from satellite service	Area (m2)	SAR wind speed (m/s)	Wind direction
10.12.20	05:54	Produced water	Medium. 50-80% probability of oil.	The slick is connected to an installation (Platform, rig, production vessel).	Linear detection in connection to platform. Possible produced water. Could also be a natural phenomenon.	458,439.41	3.22	239.49
12.12.20	16:55	Produced water	Medium. 50-80% probability of oil.	The slick is connected to an installation (Platform, rig, production vessel).	Possible produced water from platform.	671,677	4.22	135.71
30.12.20	16:56	Produced water	Medium. 50-80% probability of oil.	The slick is connected to an installation (Platform, rig, production vessel).	Diffuse feature connected to identified platform. Could be produced water	593,081	3.73	103.43

03.01.21	05:54	Produced water	Low. May be due to oil.	The slick is connected to an installation (Platform, rig, production vessel).	Discrete patch slick connected to platform. Shape is somewhat spread and fragmented. Could be produced water though the characteristics differs slightly from previous detections at the location.	488,712	5.65	243.08
13.01.21	06:08	Produced water	Low. May be due to oil.	The slick is connected to an installation (Platform, rig, production vessel).	Diffuse detection in connection to platform. Possible produced water.	250,196	3.52	88.7
14.01.21	06:03	Produced water	Low. May be due to oil.	The slick is connected to an installation (Platform, rig, production vessel).	Discrete slick connected to platform. Possibly produced water.	1,355,473	6.41	199.43

15.01.21	05:54	Produced water	High. More than 80% likely that wave attenuation is due to oil.	The slick is connected to an installation (Platform, rig, production vessel).	Fragmented feature connected to Norne FSPO. Probably produced water.	63,711	6.13	269.65
17.01.21	16:55	Produced water	High. More than 80% likely that wave attenuation is due to oil.	The slick is connected to an installation (Platform, rig, production vessel).	Discrete feature in connection to platform. Likely produced water.	1,418,887	5.56	157.86
18.01.21	16:53	Produced water	High. More than 80% likely that wave attenuation is due to oil.	The slick is connected to an installation (Platform, rig, production vessel).	Diffuse slick connected to platform. Possible produced water.	2,569,422	no data	no data

27.01.21	05:54	Produced water	Low. May be due to oil.	The slick is connected to an installation (Platform, rig, production vessel).	Discrete slick connected to platform. Likely produced water.	800,629	3.35	295.79
10.02.21	16:55	Spill	Low. May be due to oil.	The slick is connected to an installation (Platform, rig, production vessel).	Diffuse slick connected to platform. Likely produced water.	600,973	4.58	213.4

A.7 SAR images provided by Equinor

SAR satellite images was provided by Equinor for the period 10.12.21-10.02.21 of the detected oil on the sea surface. The oil sheens in the images are seen as the area within either the blue or black line. The yellow circle surrounding the Norne platform in the images have a radius of 700 m. The images are given in Figure A. 2 to Figure A. 12 below.

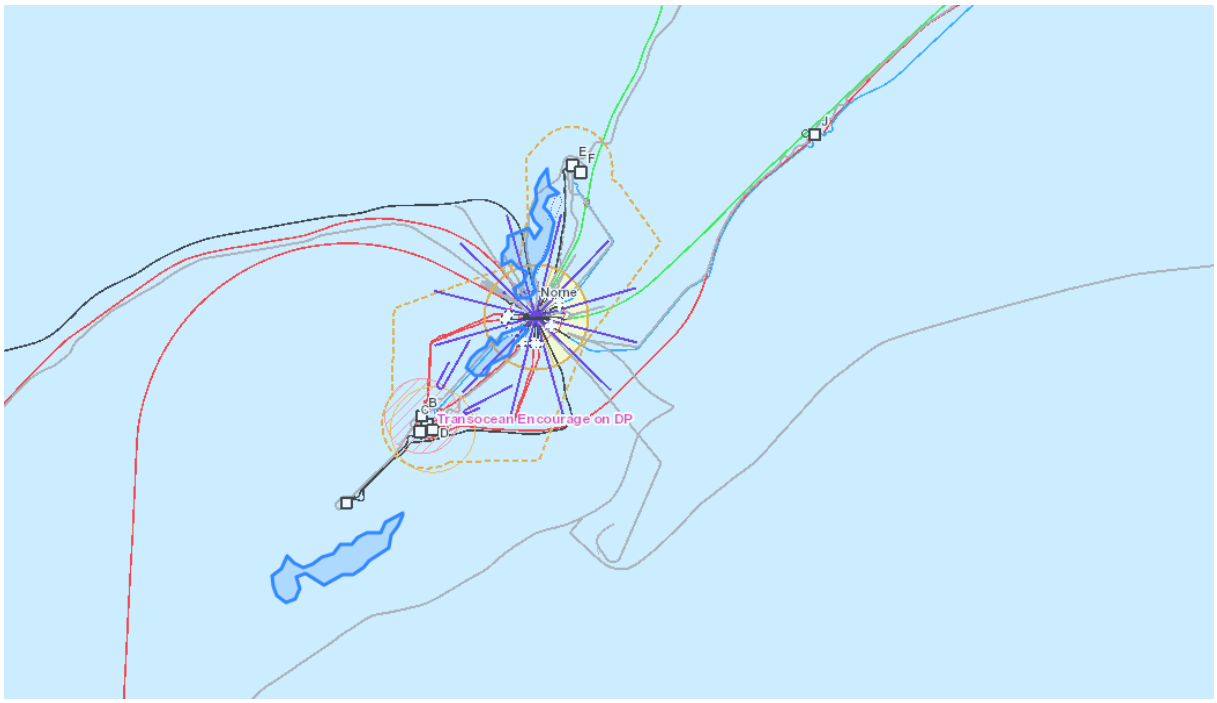

Figure A. 2. SAR image of the oil sheen detected 10.12.20.

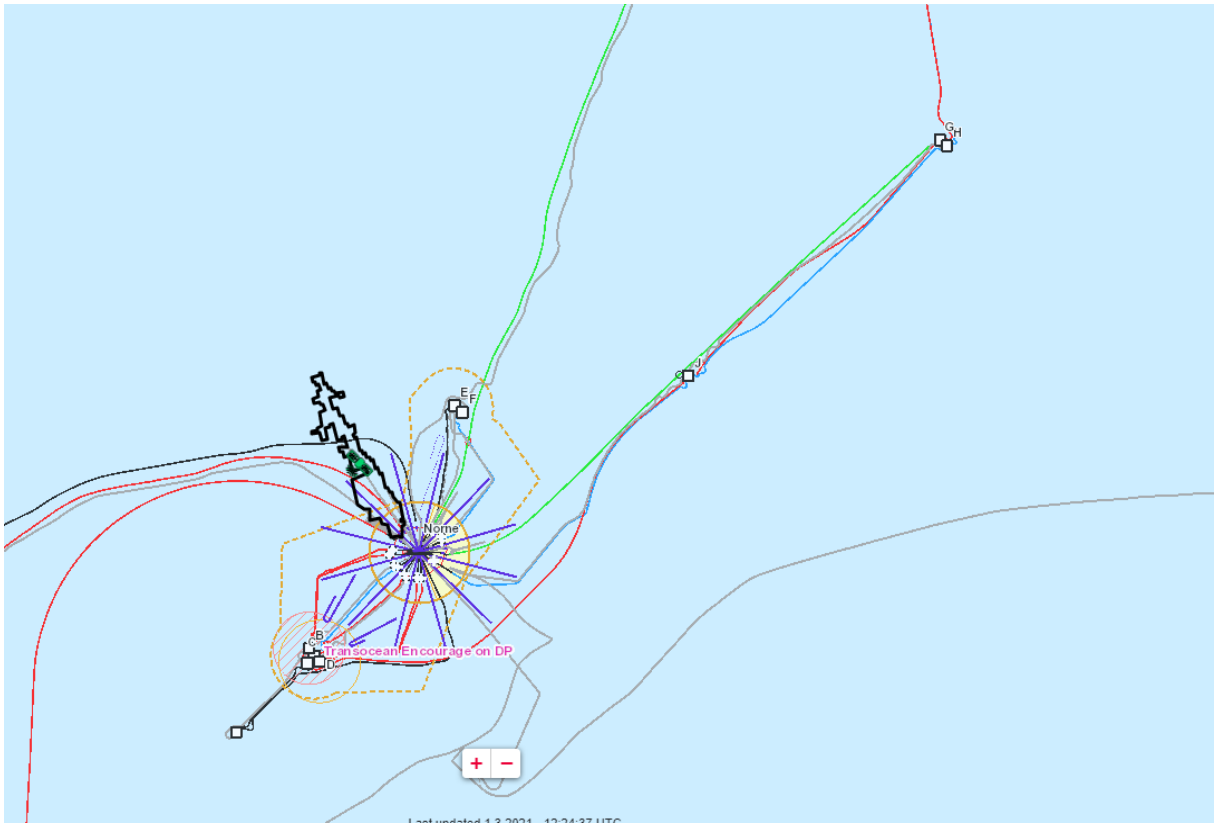

Figure A. 3. SAR image of the oil sheen detected 12.12.20.

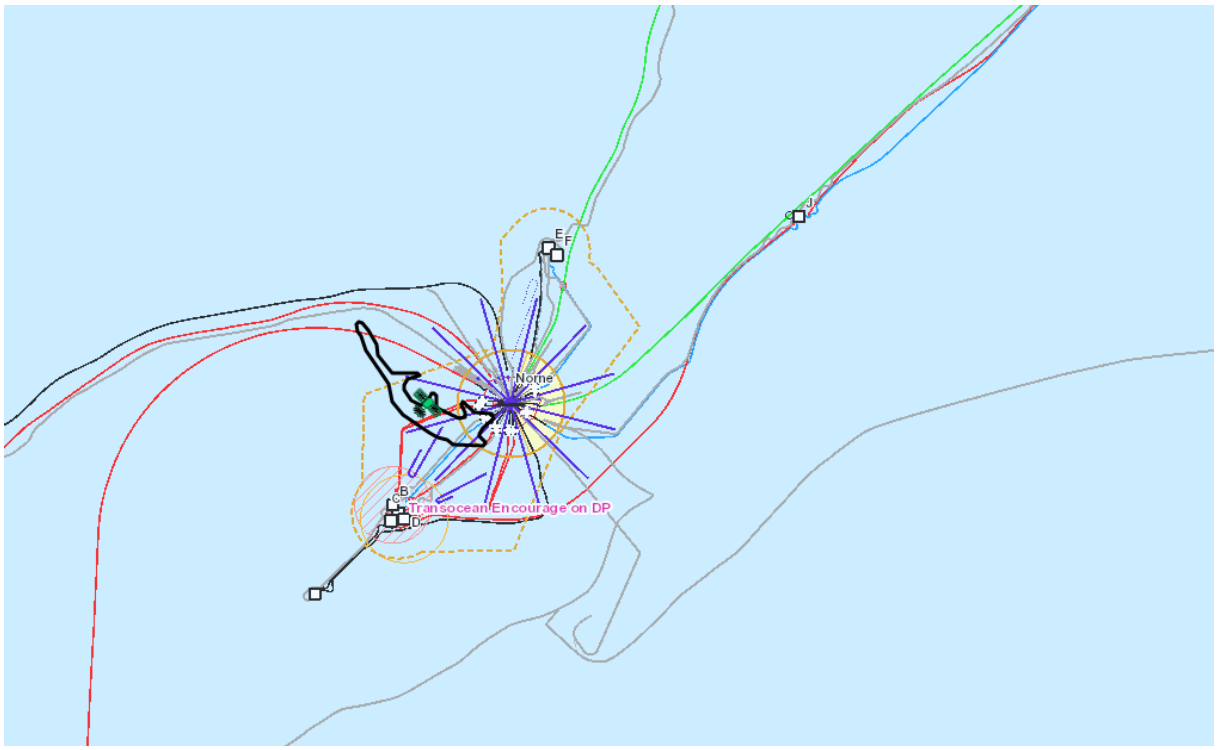

Figure A. 4. SAR image of the oil sheen detected 30.12.20.

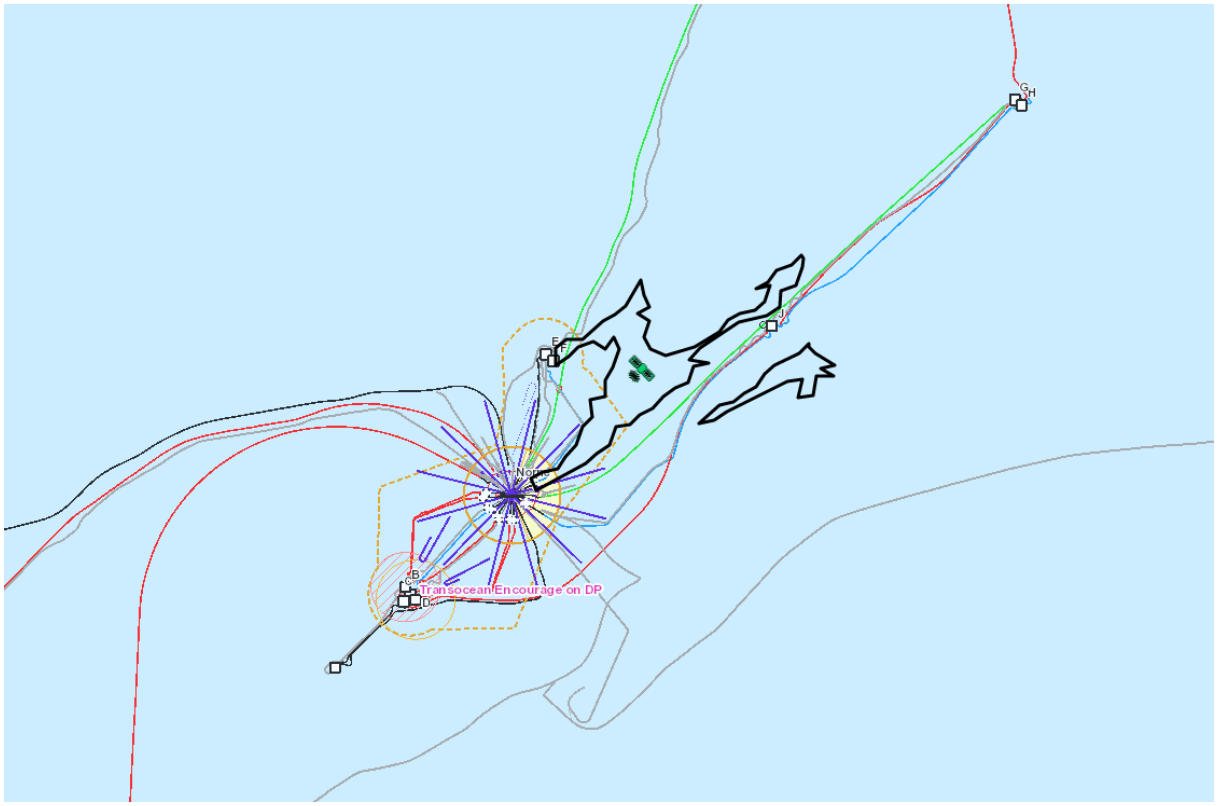

Figure A. 5. SAR image of the oil sheen detected 03.01.21.

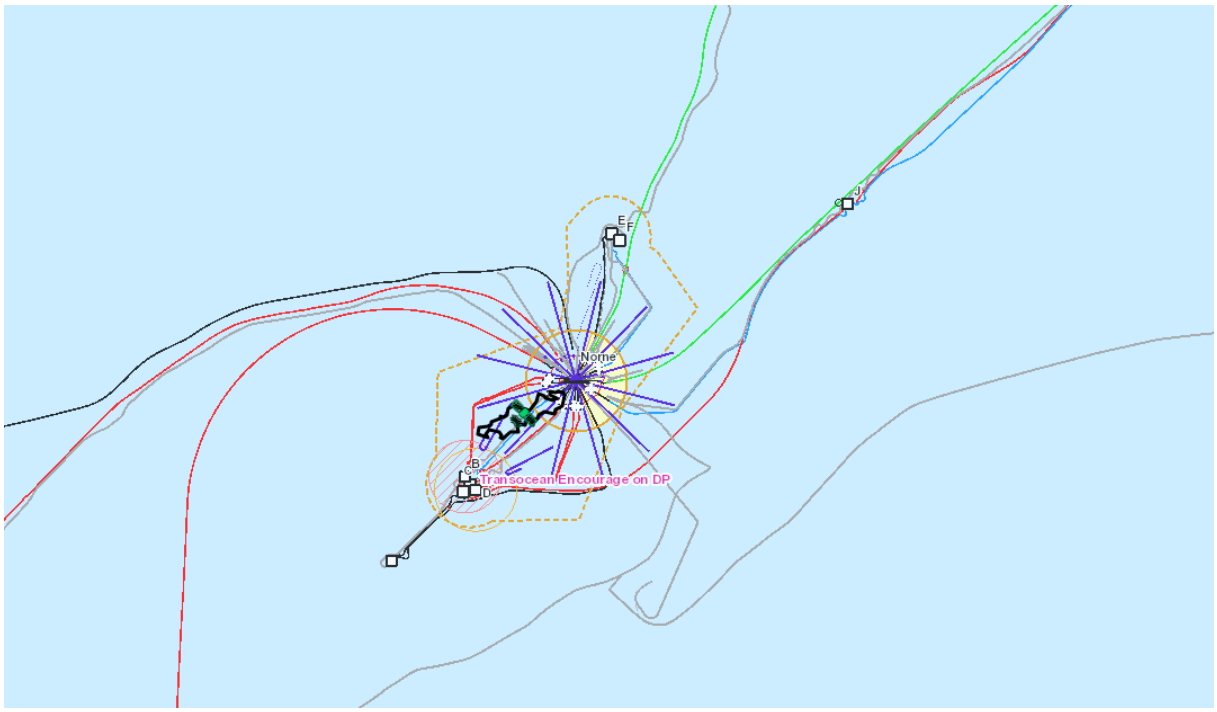

Figure A. 6. SAR image of the oil sheen detected 13.01.21.

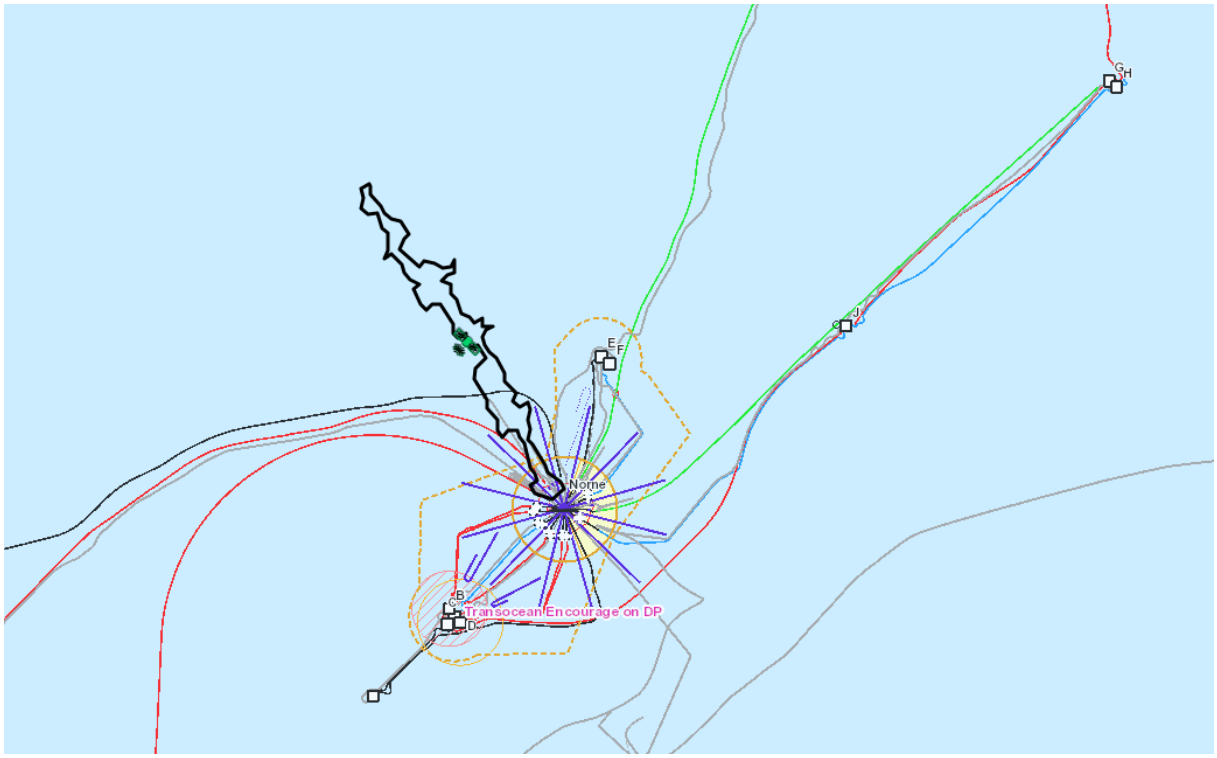

Figure A. 7. SAR image of the oil sheen detected 14.01.21.

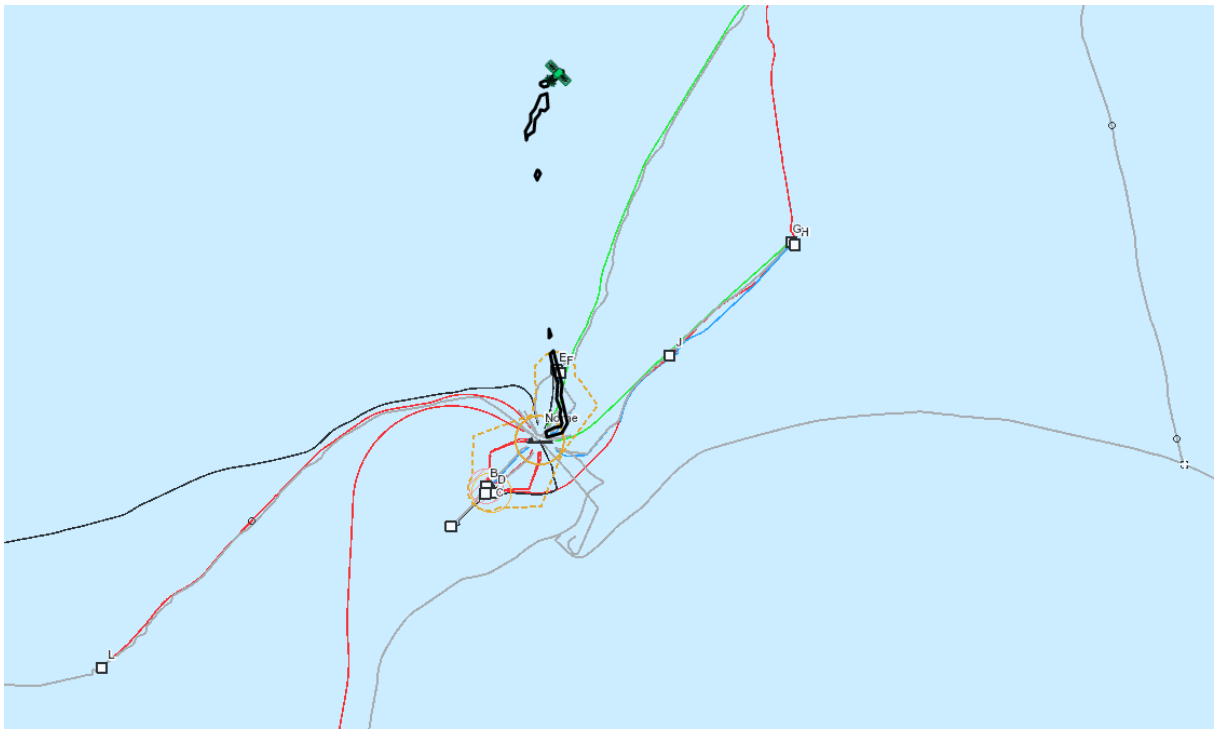

Figure A. 8. SAR image of the oil sheen detected 15.01.21.

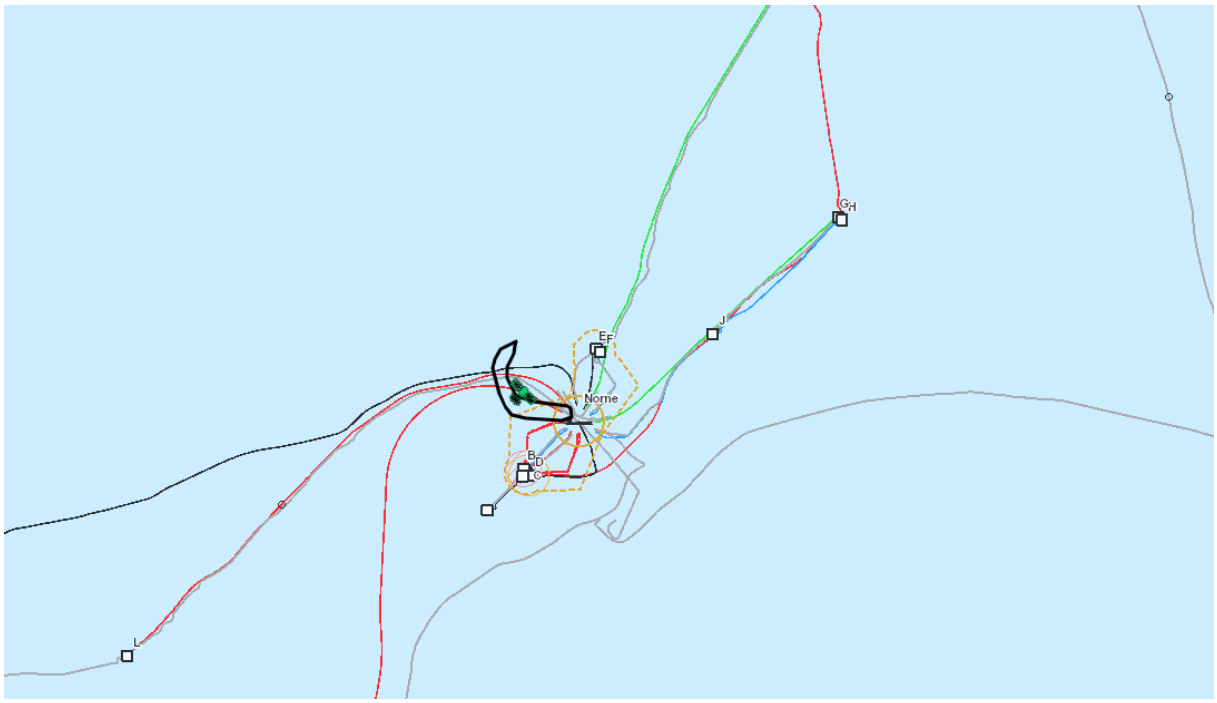

Figure A. 9. SAR image of the oil sheen detected 17.01.21.

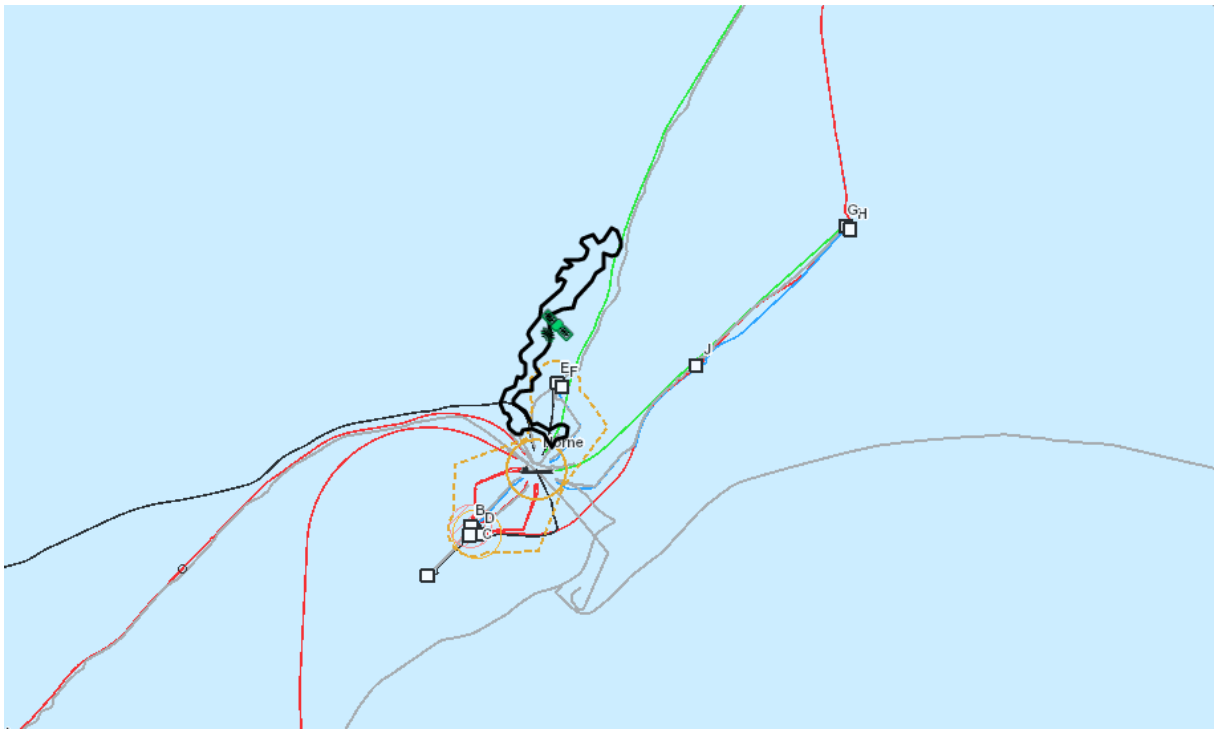

Figure A. 10. SAR image of the oil sheen detected 18.01.21.

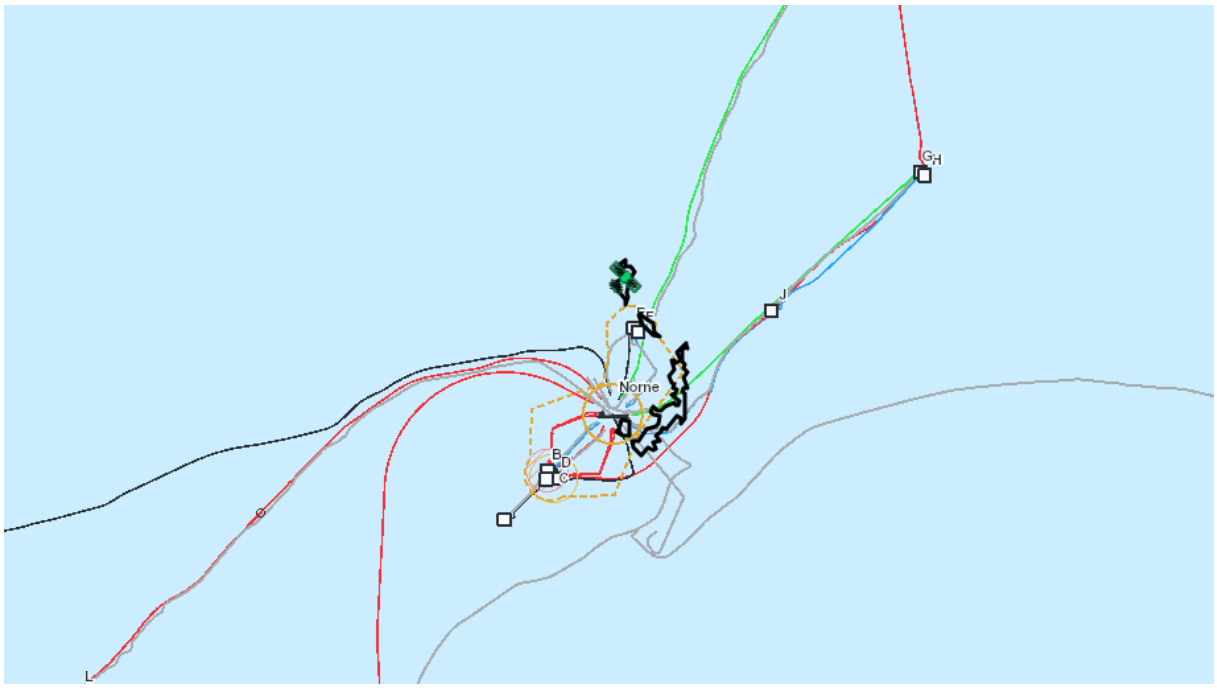

Figure A. 11. SAR image of the oil sheen detected 27.01.21.

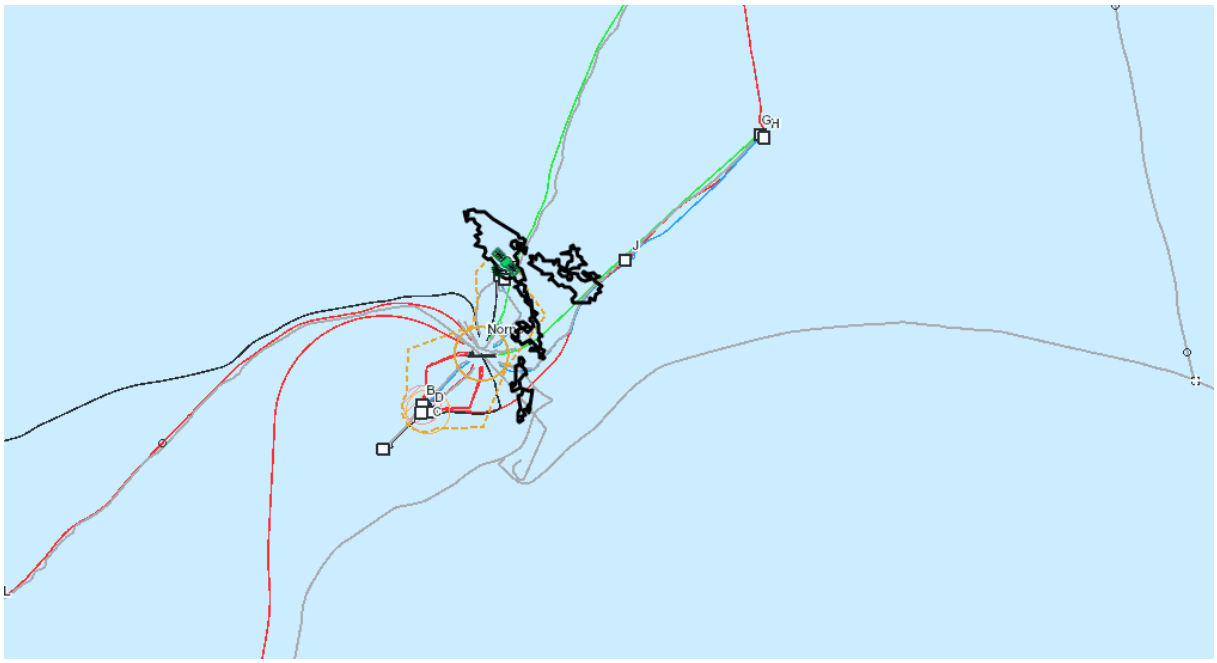

Figure A. 12. SAR image of the oil sheen detected 10.02.21.

Martin Andreas Wiken

Releases of oily produced water from offshore installations

NTNU
Kunnskap for en bedre verden